Combined Targeting of mTOR and the Microtubule in Hepatocellular Carcinoma

ZHOU, Qian

A Thesis Submitted in Partial Fulfilment
of the Requirements for the Degree of
Doctor of Philosophy
in
Medical Sciences

The Chinese University of Hong Kong
August 2011

ProQuest LLC.
789 East Eisenhower Parkway
P.O. Box 1346
Ann Arbor, MI 48106 - 1346

Abstract of thesis entitled: Combined Targeting of mTOR and the Microtubule in Hepatocellular Carcinoma

Submitted by: ZHOU, Qian

for the degree of Doctor of Philosophy in Medical Sciences

at The Chinese University of Hong Kong

Abstract

Hepatocellular carcinoma (HCC) is the fifth most common cancer worldwide and the third most common cause of cancer-related deaths. Systemic therapies are the main treatment options for HCC patients with advanced disease (~ 80% of all cases). However, only very moderate clinical responses are achieved with most of the conventional therapies. Thus, more effective therapeutic strategies are much needed. The PI3K/Akt/mTOR signaling pathway, which plays a critical role in controlling cell proliferation and survival, is aberrantly activated in ~ 45% HCC, suggesting it to be a potential target for HCC treatment. Moreover, emerging evidences indicate that activation of the PI3K/Akt/mTOR pathway may be associated with resistance to many cytotoxic chemotherapies, including microtubule targeting agents. In this study, by gene expression profiling and gene ontology analysis, "microtubule-related cellular assembly" was identified to be the major biological/functional process involved in HCC development, suggesting that microtubule is also an important therapeutic target for HCC. With these understandings, it is hypothesize in this thesis that combined targeting of a key component of the PI3K/Akt/mTOR pathway, namely the mammalian target of rapamycin (mTOR) and the microtubule would be

an effective therapeutic strategy for HCC. The objectives of the thesis are to examine the therapeutic potential of microtubule targeting, mTOR targeting, and combined targeting of the microtubule and mTOR in both *in vitro* and *in vivo* models of HCC.

Taxanes are the major chemotherapeutic agents that target the microtubule. In the first part of the thesis, the anti-tumor activity of two taxanes, paclitaxel and docetaxel (which are known to stabilize microtubules) was examined and compared with doxorubicin (a DNA intercalating agent). Across all three HCC cell lines tested, It was found that the microtubule targeting agents, taxanes, were more efficacious than doxorubicin. This supports the initial finding that microtubule assembly process is functionally important in HCC. Recent studies demonstrated that using nanoparticles for drug delivery can greatly enhance therapeutic efficacy and reduce side-effects. Therefore, the nanoparticle albumin-bound (*nab*)-paclitaxel was employed to further evaluate the therapeutic efficacy of such a delivery strategy in HCC models. In all three HCC cell lines tested, *nab*-paclitaxel was found to be the most effective agent, with an average IC_{50} value of 0.16-10.42nM, when compared to non-conjugated taxanes (paclitaxel, docetaxel) and doxorubicin. *In vitro* analysis showed that *nab*-paclitaxel was able to induce cell cycle arrest at G_2/M phase and apoptosis in HCC cells. *In vivo* study demonstrated that *nab*-paclitaxel readily inhibited the growth of HCC xenografts with lower toxicity when compared to paclitaxel, docetaxel and doxorubicin. Moreover, specific silencing of a key regulatory protein for microtubule dynamics, Stathmin 1, by siRNA significantly enhanced the effect of *nab*-paclitaxel in HCC cells, resulting in synergistic growth inhibition *in vitro*.

In the second part, the effect of mTOR inhibition, either alone or in combination

with an additional microtubule targeting agent (vinblastine) was investigated in HCC. Temsirolimus, an mTOR inhibitor, suppressed HCC cell proliferation in as early as 24 hrs with an IC_{50} of 1.27±0.06μM (Huh7), 8.77±0.76μM (HepG2), and 52.95±17.14μM (Hep3B). Vinblastine (1nM) alone caused 30-50% growth inhibition in 3 HCC cell lines. In these HCC cell lines, it was found that temsirolimus/vinblastine combination resulted in an additive to synergistic effect (when compared to single agents alone) with maximum growth inhibition of 80-90% as early as 24 hrs upon treatment. This marked growth inhibition was accompanied with cell cycle arrest at both G_1 and G_2/M phases, and PARP cleavage (a hallmark for apoptosis). Moreover, the combination specifically caused concerted down-regulation of several important anti-apoptotic and survival proteins (survivin, Bcl-2 and Mcl-1), which was not observed in single agent treatments. It was hypothesized that inhibition of these key anti-apoptotic/survival proteins may represent a novel mechanistic action of this highly effective combination approach of dual targeting of mTOR and microtubule by temsirolimus/vinblastine in HCC cells. Indeed, transient over-expression of each of these genes (survivin, Bcl-2 or Mcl-1) in HCC cells did partially rescue the growth inhibitory effect of the temsirolimus/vinblastine combination. More importantly, this novel combination significantly suppressed the growth of HCC xenografts in nude mice (when compared with single agents alone).

In the third part, the anti-tumor effect of another mTOR inhibitor everolimus in combination with microtubule targeting agents, vinblastine and patupilone (a microtubule-stabilizing agent), was investigated in HCC cells. Everolimus/vinblastine combination resulted in an additive to synergistic effect accompanied with cell cycle arrest at both G_1 and G_2/M phases, and PARP cleavage. The combination also caused concerted down-regulation of anti-apoptotic and

survival proteins (survivin, Bcl-2 and Mcl-1) as observed with the temsirolimus/vinblastine combination. However, everolimus only moderately enhanced the sensitivity of patupilone for reasons unknown.

In summary, the PI3K/Akt/mTOR pathway and the microtubule represent promising therapeutic targets for HCC treatment. The findings from this thesis offer a rationale for combining mTOR inhibitors with microtubule targeting agents for effective HCC treatment.

摘要

肝細胞癌 (HCC, Hepatocellular carcinoma) 是全世界第五大常見癌症和第三大常見癌症致死因素。對晚期肝癌（大约占 80%的病例）病人來說系統治療是主要的治療方法。但是，肝癌對大多數傳統治療都只有很低的臨床反應性。因此，更有效的治療對策是非常需要的。PI3K/Akt/mTOR 信號轉導通路在控制細胞增殖和生存中起關鍵作用,它在大約 45%的肝癌中被異常啟動，表明它是一個潛在的肝癌治療靶項。而且，新的證據表明 PI3K/Akt/mTOR 通路的啟動可能與許多細胞毒性化療藥物的耐受性相關，包括抗微管藥物。在這篇研究中，通過基因表達檢測 (gene expression profiling) 和基因本體 (gene ontology) 分析，“微管相關的細胞組裝”被發現是在肝癌發生過程中主要的生物學或功能性過程，表明微管也是一個重要的肝癌治療靶項。基於這些認識，這篇論文假設聯合抗 PI3K/Akt/mTOR 通路的一個關鍵組分，名為 mammalian target of rapamycin (mTOR) 和抗微管的靶項治療對肝癌可能是一種有效的治療對策。這篇論文的目標是檢驗抗微管，抗 mTOR，和聯合抗微管和抗 mTOR 在體外和體內肝癌模型中的治療潛力。

Taxanes 是主要的抗微管化療藥物。在論文的第一部分，兩種 taxanes，paclitaxel 和 docetaxel（已知能穩定微管）的抗腫瘤效能被進行了檢測並與 doxorubicin（一種 DNA 插入藥物）進行了比較。在三種試驗的肝癌細胞株中，研究發現了抗微管藥物，taxanes，比 doxorubicin 更有效。這支持了最初的發現微管組裝過程在肝癌中是功能性重要的。最近的研究表明用納米顆粒進行藥物運輸能夠大大加強治療效能和減少副作用。所以，納米顆粒白蛋白結合的 paclitaxel (*nab*-paclitaxel) 被用來在肝癌模型中對這種對策的治療效能進行

進一步研究。在三種試驗的肝癌細胞株中，當與非結合的 taxanes (paclitaxel, docetaxel) 和 doxorubicin 比較時，*nab*-paclitaxel 被發現是最有效的藥物，平均 IC_{50} 值 為 0.16-10.42nM。體外研究表明 *nab*-paclitaxel 在肝癌細胞中能誘導細胞週期阻滯在 G_2/M 期和細胞凋亡。體內研究顯示了 *nab*-paclitaxel 能較好地抑制異種移植腫瘤的生長，並且與 paclitaxel, docetaxel 和 doxorubicin 相比具有較低的毒性。並且，用小 RNA 幹擾特異性抑制一個微管動力學的關鍵調節性蛋白，Stathmin 1，能顯著增強 *nab*-paclitaxel 在肝癌細胞中的作用，體外導致協同性生長抑制。

在第二部分，單用 mTOR 抑制或與另一種抗微管藥物 (vinblastine) 聯合運用在肝癌中的作用被進行了研究。Temsirolimus，一種 mTOR 抑制劑，早在 24 小時能抑制肝癌細胞增殖，IC_{50} 分別是 1.27±0.06□M (Huh7), 8.77±0.76□M (HepG2) 和 52.95±17.14□M (Hep3B)。單用 vinbalstine 在三種肝癌細胞株中只導致 30-50%的生長抑制。在這些肝癌細胞株中，temsirolimus 與 vinblastine 聯合被發現能導致相加或協同的作用（當與單藥比較時），早在 24 小時達到最大生長抑制率是 80-90%。這種顯著的生長抑制伴隨著細胞週期阻滯在 G_1 和 G_2/M 期，和 PARP 剪切（一個細胞凋亡的標誌）。而且，這種聯合特異性導致了一些重要抗凋亡和生存蛋白（survivin, Bcl-2 和 Mcl-1）的一致下調，這在單藥治療中沒有觀察到。這些關鍵抗凋亡/生存蛋白的抑制被假設可能是這種在肝癌細胞中用 temsirolimus/vinblastine 進行抗 mTOR 和微管的雙重靶項高效聯合療法的新機制。確實，通過瞬時轉染在肝癌細胞中過量表達這些基因中的每一個（survivin, Bcl-2 或 Mcl-1）能部分消除這種 temsirolimus/vinblastine 聯合的生長抑制作用。更重要的是，這種新的聯合治療在裸鼠中能顯著抑制肝癌

異種移植腫瘤的生長（當與單藥比較時）。

在第三部分，另一種 mTOR 抑制劑 everolimus 與抗微管藥物，vinblastine 和 patupilone（一種微管穩定藥物），聯合運用在肝癌細胞中的抗腫瘤作用被進行了研究。Everolimus 與 vinblastine 聯合導致相加或協同的作用，並伴隨著細胞週期阻滯在 G_1 和 G_2/M 期，和 PARP 剪切。正如 temsirolimus/vinblastine 聯合所觀察到的，這種聯合也導致了抗凋亡和生存蛋白（survivin, Bcl-2 和 Mcl-1）的一致下調。然而，由於未知的原因 everolimus 只是輕微加強了 patupilone 的敏感性。

總之，PI3K/Akt/mTOR 通路和微管都表現為是肝癌前景樂觀的治療靶項。這篇論文的發現為聯合運用 mTOR 抑制劑和抗微管藥物進行有效的肝癌治療提供了依據。

Acknowledgements

First of all, I would like to express my deepest gratitude towards my supervisor Prof. Winnie Yeo for providing me the opportunity to enroll as a PhD student and making it possible for me to graduate on time at the end of my doctoral candidature in the department of clinical oncology. It is also my honor to thank my co-supervisor Prof. Vivian Lui who gave me much guidance and encouragement during the course of my PhD studies. I also want to thank Prof. Nathalie Wong, my former co-supervisor. She has given me patient guidance on the project study of Chapter 3.

I also appreciate Prof. Margaret Ng and Ms. Alice Cheng for their technical assistance on the cell cycle studies, Prof. Alfred Cheng for the kind provision of pcDNA3.1-HBx, pcDNA3.1-HBxΔ14 and pcDNA3.1-HBxΔ35 plasmids, Dr. Eugene Chin (Brown University School of Medicine, USA) for the kind provision of pcDNA3-HA vector, Dr. Arthur Ching for his technical assistance on animal studies, Dr. Queenie Wong, Mr. Wilson Leung and Ms. Priscilla Law for their technical assistance at the beginning of my PhD studies.

Heartiest thanks to my all labmates in Cancer Signaling Laboratory, Cancer Drug Testing Unit (CDTU) and other members of the Cancer Centre for their help and support during these years. Apart from great friendship, they also share numerous fruitful discussions towards my work. I would also like to show my thanks towards Ms. Gigi Lui, Ms. Candy Ho, Mr. Wai Lap Wong, Ms. Fion Sung and Ms. Winnie Tse who helped to settle many trivial clerical task for me.

Finally, I would like to thank my parents and friends for their love, support and encouragement especially during difficult times.

Publications related to thesis

1. **Zhou Q,** Ching AK, Leung WK, Szeto CY, Ho SM, Chan PK, Yuan YF, Lai PB, Yeo W, Wong N. **Novel therapeutic potential in targeting microtubules by nanoparticle albumin-bound paclitaxel in hepatocellular carcinoma.** Int J Oncol. 2011 Mar; 38(3): 721-31.
2. **Zhou Q,** Lui VW, Yeo W. **Targeting the PI3K/Akt/mTOR pathway in hepatocellular carcinoma.** Future Oncol. In revision.
3. **Zhou Q,** Lui VW, Lau CP, Cheng SH, Ng MH, Cai YJ, Yeo W. **Dual targeting of mTOR and the microtubule results in marked anti-tumor activity in hepatocellular carcinoma.** Manuscript Preparing.

Table of content

List of tables and figures

Chapter 1: Introduction

Chapter 2: Materials and Methods

Chapter 3: Novel Therapeutic Potential in Targeting the Microtubules by Nanoparticle Albumin-bound Paclitaxel in Hepatocellular Carcinoma

Chapter 5: The Role of mTOR Inhibition with Everolimus in Enhancing Chemosensitivity of Microtubule Targeting Agent Vinblastine or Patupilone in Hepatocellular Carcinoma

Chapter 7: Appendix chapter

List of Abbreviations

5-Fu	5-fluorouracil
AFP	Alfa-fetoprotein
AJCC	American Joint Committee on Cancer
AP-2	Activating protein 2
ASC	Apoptosis-associated speck-like protein
ATCC	American Type Culture Collection
Bcl-2	B cell lymphoma 2
BDL	Bile duct-ligation
BSA	Bovine serum albumin
CDKs	Cyclin-dependent kinases
COX2	Cyclooxygenase 2
DAPI	4', 6-diamidino-2-phenylindole
DLC1	Deleted in liver cancer 1
DMEM	Doubecco's Modified Eagle Medium
DMSO	Dimethyl sulfoxide
DNA	Deoxyribonucleic acid
DTT	Dithiothreitol
ECM	Extra-cellular matrix
EDTA	Ethylenediaminetetraacetic acid
EGF(R)	Epidermal growth factor (receptor)
FABP7	Fatty acid-binding protein 7
FBS	Fetal bovine serum
FDA	Food and Drug Administration
FDR	False discovery rate
FKBP12	FK506-binding protein 12
GAPDH	Glyceraldehyde 3-phosphate dehydrogenase
HA	Hemagglutinin
HBV	Hepatitis B virus
HBx	Hepatitis B virus X protein
HCC	Hepatocellular carcinoma
HCV	Hepatitis C virus
HDAC	Histone deacetylase
HEPES	4-(2-hydroxyethyl)-1-piperazineethanesulfonic acid
HGF(R)	Hepatocyte growth factor (receptor)
HIF1α	Hypoxia inducible factor 1α
hTERT	Human telomerase reverse transcriptase
IGF(R)	Insulin-like growth factor (receptor)
IPA	Ingenuity Pathway Analysis
IRS-1	Insulin receptor substrate 1
JAK	Janus-associated kinase
JCRB	Japanese Collection of Research Bioresources
JNK	c-Jun N-terminal kinase
mAB	Monoclonal antibody
MAPK	Mitogen activated protein kinase
Mcl-1	Myeloid cell leukemia sequence 1
MDR	Multi-drug resistance
MEFs	Mouse embryonic fibroblasts
MRI	Magnetic resonance imaging
MRPs	Multi-drug resistance proteins

List of Abbreviations (cont'd)

mTOR	Mammalian target of rapamycin
MTT	3-(4, 5-dimethylthiazol-2-yl)-2, 5-diphenyl tetrazolium bromide
NAFLD	Nonalcoholic fatty liver disease
NF-κB	Nuclear factor-κB
OD	Optical density
PARP	Poly-(ADP ribose) polymerase
PDGF	Platelet-derived growth factor
PDK	Phosphoinositide-dependent kinase
PDPK2	3-phosphoinositide-dependent protein kinase 2
PEI	Percutaneous ethanol injection
PH	Pleckstrin homology
PI	Propidium iodide
PI3K	Phosphatidylinositol 3-kinase
PIP2	Phosphatidylinositol 4, 5-bisphosphate
PIP3	Phosphatidylinositol (3-5)-trisphosphate
PMSF	Phenylmethyl sulfonyl fluoride
PR	Partial response
PTEN	Phosphatase and tensin homolog
RNA	Ribonucleic acid
RPMI	Roswell Park Memorial Institute medium
RTKs	Receptor tyrosine kinases
RT-PCR	Reverse transcription polymerase chain reaction
SAM	Significance Analysis of Microarray
SD	Standard deviation
SDS-PAGE	Sodium dodecyl sulphate-polyacrylamide gel electrophoresis
SEM	Standard error of mean
shRNA	Small hairpin RNA
siRNA	Small interfering RNA
SPARC	Secreted Protein Acidic and Rich in Cysteine
SSC	Sodium chloride-sodium citrate concentrate
STAT	Signal transducer and activator of transcription
STK31	Serine/threonine kinase 31
TAA	Thioacetamide
TBST	Tris-Buffered Saline Tween-20
TGFα	Transforming growth factor-α
TNFα	Tumor necrosis factor-α
TRAIL	Tumor necrosis factor-related apoptosis inducing ligand
TTP	Time to progression
US	Ultrasound
VEGF(R)	Vascular endothelial growth factor receptor

Chapter 1: Introduction

1.1 Overview of hepatocellular carcinoma

1.1.1 Epidemiology and etiology of HCC

Hepatocellular carcinoma (HCC), or liver cancer, with a mounting annual incidence of 4.9/100,000, is the third most common cause of cancer death worldwide (1). In China, there is a particularly high incidence of 40/100,000 a year (2). There is a general higher predominance of HCC in males than females (~ 3:1) (1). The disease is characterized by its aggressiveness, notoriously poor response rate to conventional therapies, as well as poor clinical outcome with dismal survival rate. In patients with unresectable HCC, the median survival is reported to be only 4-6 months (3). Cumulative evidences demonstrate that HCC is a complex disease associated with multiple etiologic and risk factors, among which, chronic infection with hepatitis viruses (e.g. hepatitis B virus and hepatitis C virus), alcoholism and aflatoxin are the most recognized causes of HCC (3-5). (Fig. 1.1)

One of the most common risk factors of HCC is chronic infection with the hepatitis B virus (HBV), accounting for 50-80% of HCC cases worldwide (6). A large scale HBV study in Chinese population showed that chronic HBV infection was associated with a 98-fold higher relative risk for HCC development (7). Hepatitis C virus (HCV) infection is the second most common cause of HCC, accounting for approximately 20% of all HCC (1). Studies suggest that there is a 20-fold increased risk for HCC in the HCV-infected population. In addition, HBV-associated HCC is more common in most parts of Asia including China, while

HCV-related HCC is more common in Japan and increasing in the US (1). Furthermore, De Mitri *et al* showed that HBV and HCV seemed to have an intrahepatic synergistic effect on HCC development (8), and co-infection with HBV and HCV may increase the risk of HCC by 3.6-fold compared with mono-infection (9).

While the presence of cirrhosis increases the risk of HCC, it is not an essential precursor to the development of HCC. In HBV-associated HCC, ~40% of patients do not have cirrhosis (10). Similarly, HCV-associated HCC can occur without cirrhosis (11). Chronic liver disease and cirrhosis due to alcohol, genetic hemochromatosis (12), primary biliary cirrhosis (13), α1-antitrypsin deficiency, aflatoxin and metabolic diseases such as diabetes and nonalcoholic fatty liver disease (NAFLD) (14) are also recognized causes for HCC development, although worldwide they each accounts for only a small fraction of all HCCs.

It is believed that a better understanding of the etiology and pathogenesis of HCC may enable identification of common molecular alterations that could potentially lead to novel therapeutic strategies.

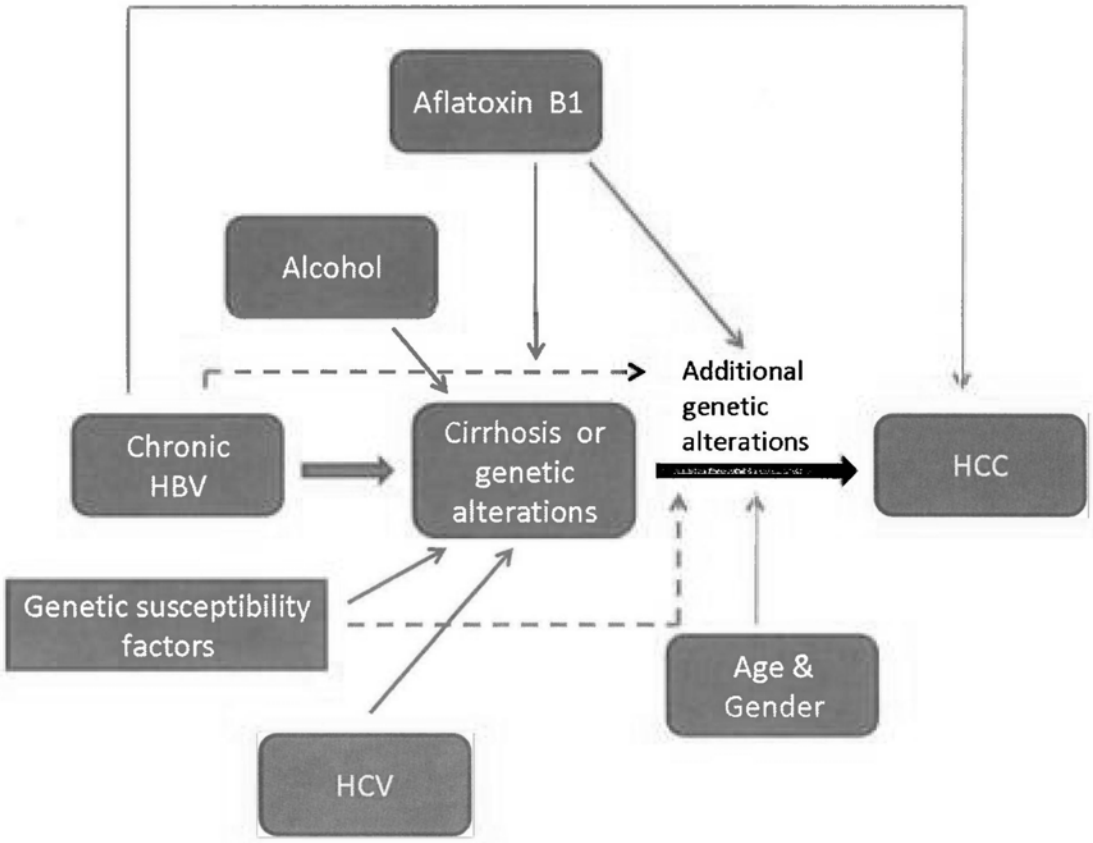

Figure 1.1 The role of host and environmental factors in the pathogenesis of HCC. The interaction between host factors, viral infection such as HBV, HCV, and environmental factors such as dietary aflatoxin and alcohol may initiate the progression of normal liver to premalignant state, such as cirrhosis. It is likely that these factors, when combined with genetic susceptibility factors, as well as age and gender will eventually lead to the development of HCC. (Modified from Herath *et al* (15).)

1.1.2 Diagnosis, current treatment, limitations and prognosis of HCC

HCC develops without much noticeable early symptoms. Often, patients already present with advanced disease at diagnosis with signs of massive tumor, obstructive jaundice due to bile duct infiltration, liver impairment as a result of tumor and co-existing chronic liver disease, or constitutional symptoms affecting the general well-being of a patient such as weight loss, chills and fever. In fact, liver dysfunction or hepatic failure is one of the most common factors that limit for aggressive therapeutic intervention for patients with advanced HCC.

The tests commonly used to diagnose HCC include serum tumor marker alfa-fetoprotein (AFP), radiographic imaging and liver biopsy. Due to its low sensitivity and low positive predictive value with co-existing cirrhosis, ultrasound (US) imaging has largely been replaced by CT scan and magnetic resonance imaging (MRI) for more accurate diagnosis.

The treatment options for HCC patients are dictated by the extent of HCC and hepatic reserve of an individual patient. The only proven cure for HCC is surgery. Liver transplantation for small tumors (single tumor <5cm, two to three tumors <3cm), offers up to 60% survival in 5 years (16). However, the severe shortage of liver donors exists in parts of Asia and this greatly limits the applicability of this treatment option for most HCC patients. Surgical resection of liver can be considered for HCC patients with small tumors and adequate liver function. In clinical practice, only 10-15% of HCC patients are candidates for surgical removal in most centres. Local ablative therapy, including percutaneous ethanol injection

(PEI), radiofrequency ablation, microwave coagulation therapy, interstitial laser therapy and laproscopic guided cryosurgery may be of some usefulness for tumors less than 5 cm (17). Loco-regional therapy with transarterial chemoembolization has been shown to improve survival over best support care in selective patients with more advanced disease that confines to the liver (18, 19). Unlike other cancers, radiation therapy is not a main stream treatment option for HCC as further liver damage may not be affordable by most patients; however, novel radiation techniques are currently under investigation.

For the majority of HCC patients, systemic chemotherapies or supportive therapies become the major treatment options. Unfortunately, most conventional cytotoxic chemotherapeutic agents show limited efficacy and have not been shown to significantly improve patient survival (20-23). Accumulating preclinical and clinical evidences indicate that HCC tumors are inherently chemotherapy-resistant for reasons not fully understood. Several previous studies demonstrated that over-expression of multi-drug resistance genes, such as MDR1 (P-gp) and the multi-drug resistance proteins (MRPs) in HCC cells may contribute to chemo-resistance (24-26). Recent studies suggested that activation of some signaling pathways may contribute to chemo-resistance in HCC. Among these, activation of the PI3K/Akt/mTOR signaling pathway has been shown to contribute to resistance to taxanes and other drugs acting on microtubules, including vincristine, colchicine, and paclitaxel (27, 28).

The recent expansion of knowledge on the molecular mechanisms in HCC has

led to the clinical use of the first molecular targeting agent for the treatment of HCC. Sorafenib is an oral multi-kinase inhibitor of the vascular endothelial growth factor (VEGF) receptor, platelet-derived growth factor (PDGF) receptor, and Raf. Based on 2 multi-centre phase III trials, sorafenib has been clinically approved by US Food and Drug Administration (FDA) for the treatment of unresectable HCC (29, 30). In the Asian study, sorafenib has been shown to prolong patient survival from 4.2 months to 6.5 months; 3.3% patients achieved a partial response (PR) and 54.0% had stable disease (30). However, the survival improvement and response rate of sorafenib is still far from satisfactory. Therefore, development of more efficacious therapeutic strategies is much needed for HCC patients.

1.1.3 Molecular mechanisms in hepatocarcinogenesis

HCC is known to exhibit numerous genetic abnormalities, including chromosomal deletions and rearrangements, aneuploidy, gene amplifications and mutations, as well as epigenetic alterations. Some of the widely reported ones include aberrations of *TP53* (31-34), β-catenin (35, 36), ErbB receptor family members (37), *c-myc* (38), *MET* and its ligand hepatocyte growth factor (*HGF*) (39, 40), *p16(INK4a)*, E-cadherin and cyclooxygenase 2 (*COX2*) (41-47).

HBV, the major etiologic factor for HCC, is known to integrate into the host genome and induce chromosome instability (48, 49). Recently, emerging evidences indicate a complex viral-host interaction, at least at the level of interfering signaling networks in liver cells, which may contribute to HBV-induced hepatocarcinogenesis.

Recent studies by Minami *et al* and Wang *et al* demonstrated that insertional mutations resulting from HBV genome integration at specific sites of the host genome can induce activation of cellular genes, including cyclin A and human telomerase reverse transcriptase (hTERT) gene, which are related to cell proliferation and survival (50, 51). Feitelson *et al* has also shown that the HBV protein, hepatitis B virus X protein (HBx), is capable of regulating cell proliferation (52). Although HBx does not bind to DNA directly, studies have demonstrated that it can co-activate the transcription of several important viral and cellular genes, thus exerting its effects on cell proliferation and apoptosis (53, 54). HBx is a transactivator that up-regulates the expression of some major proto-oncogenes such as *c-myc* and *c-jun* (55, 56) and key transcriptional factors like NF-κB and AP-2 (57, 58). HBx is also found to alter several major signaling pathways, including the JAK/STAT pathway (59), the Ras/Raf/MAPK pathway (60), p21waf1/cip1 (61), the Wnt/β-catenin signaling (62) and the PI3K/Akt/mTOR pathways (63). In fact, some of these activated pathways and factors including growth factors and angiogenic factors in HCC may serve as promising druggable targets for therapeutic development in HCC. (Table 1.1)

Table 1.1 Molecular targets for therapy in HCC

Mechanisms/pathways	Molecular targets	Agents
Growth factors	EGFR	-monoclonal antibody (e.g. cetuximab) -tyrosine kinase inhibitor (e.g. gefitinib, erlotinib, lapatinib)
	IGF-1R	-monoclonal antibody (e.g. cixutumumab, OSI-906)
	c-Met	-small molecular inhibitors (e.g. ARQ197) -tyrosine kinase inhibitors (e.g. XL184, foretinib)
Ras/Raf/MAPK pathway	Ras	-inhibitors of farnesyl transferase (tipifanib)
	Raf	-Raf kinase inhibitor (sorafenib)
	MEK	-AZD6244
PI3K/Akt/mTOR pathway	PI3K	-wortmannin, LY294002, PI-103
	Akt	-alkylphospholipid perifosine, MK2206
	mTOR	-rapamycin, everolimus, temsirolimus, AZD8055
Wnt/β-catenin pathway	Wnt	-monoclonal antibody of Wnt 1 and Wnt 2
	β-catenin	-small molecular inhibitors (e.g. ICG-001)
Chromatin remodeling	HDAC	-small molecular inhibitors (e.g. PXD101, LBH589, vorinostat)
Protein turnover	Proteasome	-bortezomib
Cell cycle regulators	CDKs	-flavopiridol
Apoptosis	Bcl-2	-small molecular inhibitors (e.g. ABT-737, ABT-263)
	TRAIL	-monoclonal antibody (e.g. mapatumumab, tigatuzumab)
Angiogenic factors	VEGF	-monoclonal antibody (bevacizumab)
	VEGFR	-tyrosine kinase inhibitors (e.g. sorafenib, brivanib, linifanib, exelinib, axitinib, foretinib, SU6688)
	PDGFR	-tyrosine kinase inihibitors (e.g. sorafenib, linifanib, axitinib, SU6688)
	Angiopoietin 2/Tie2	-tyrosine kinase inhibitors (e.g. regorafenib, XL184)
	Heparanase	-PI-88
	Vasculature	-vascular disrupting agents (e.g. Oxi4503, Combretastatin A4)

CDKs, Cyclin-dependent kinases; EGFR, epidermal growth factor receptor; HDAC, histone deacetylase; mTOR, mammalian target of rapamycin; PI3K, phosphatidylinositol 3-kinase; PDGFR, platelet-derived growth factor receptor;

TRAIL, tumor necrosis factor-related apoptosis inducing ligand; VEGF(R), vascular endothelial growth factor (receptor). (Modified from Pang *et al*, Llovet *et al* and Tanaka *et al* (64-66).)

1.2 The PI3K/Akt/mTOR pathway in HCC

1.2.1 The PI3K/Akt/mTOR pathway

The phosphoinositide 3-kinases (PI3Ks), which are divided into three classes (Class IA, Class IB, Class II and Class III), are important kinases regulating cell survival, proliferation and differentiation (67-69). Class IA is the most widely studied and it has three catalytic subunits (p110α, β, δ). In response to growth factors stimulation and the subsequent activation of receptor tyrosine kinases (RTKs), PI3K is recruited to the membrane by direct or indirect interaction with the activated receptors. The activated PI3K generates the second messenger phosphatidylinositol (3-5)-trisphosphate (PIP3) from phosphatidylinositol 4, 5-bisphosphate (PIP2) by phosphorylating inositols on the lipid membrane. Then the serine-threonine kinase Akt is recruited to the membrane via binding to PIP3, resulting in its phosphorylation by phosphoinositide-dependent kinases (PDKs) (70). Once activated, Akt activates downstream signaling effectors to regulate cell survival, proliferation, cell cycle progression, migration, and angiogenesis. Akt then induces the activation (phosphorylation) of mammalian target of rapamycin complex 1 (mTORC1), a serine/threonine kinase. The mTOR protein, in turn, regulates its downstream effectors, p70S6 kinase and translational repressor protein 4E-BP1 by phosphorylation. It is known that both of the two proteins regulate the translation of several important proliferative and angiogenic factors, such as c-myc, cyclin D1, HIF1α, and VEGF (71, 72). While PI3K/Akt/mTOR signaling is known to be activated by various growth factors and cytokines, this pathway can also be

negatively regulated by PTEN (phosphatase and tensin homolog deleted on chromosome 10), a well-known tumor suppressor, which dephosphorylates PIP3. (Fig. 1.2)

Comprehensive cancer genomic analyses have recently revealed that components of the PI3K pathway are frequently mutated or altered in many human malignancies (73-76), including HCC. Some of the mechanisms of PI3K/Akt/mTOR dysregulation are summarized below:

1. Gain-of-function mutation or amplification of PIK3CA, the p110α catalytic subunit (74).
2. Amplification or increased activity/expression of PIK3CB, the p110β catalytic subunit (77, 78).
3. Loss-of-function of PTEN through gene deletion, mutation, or epigenetic silencing (79-82).
4. Amplification or mutation of the Akt isoforms (Akt1, Akt2 and Akt3) (83-85).
5. Upstream activation through RTK signaling, e.g., the epidermal growth factor receptor (EGFR) family or insulin-like growth factor 1 receptor (IGF1-R).

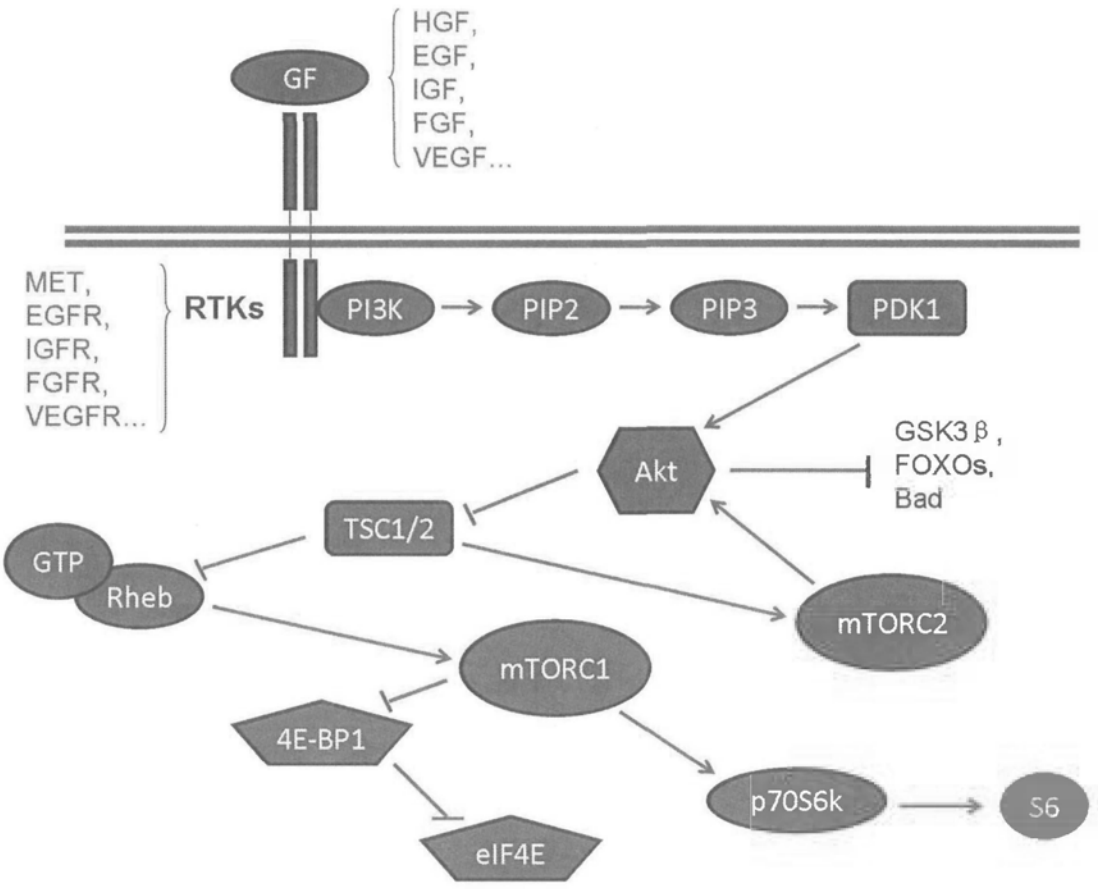

Figure 1.2 The PI3K/Akt/mTOR pathway. Receptor tyrosine kinases (RTKs) stimulate Class I PI3K activity. PI3K generates PIP3 from PIP2. PIP3 recruits Akt and PDK1 to the membrane where Akt is phosphorylated on Thr308 by PDK1. Full Akt activation requires Ser473 phosphorylation, which is effected by mTORC2. Once activated, Akt phosphorylates and inactivates several substrates, including GSK3β, FOXO transcription factors, and Bad. Active Akt inhibits TSC2 activity through direct phosphorylation. TSC2 is a GAP that functions in association with TSC1 to inactivate the small G protein Rheb. Akt-driven TSC1/TSC2 complex inactivation allows Rheb to accumulate in a GTP bound state. Rheb-GTP then up-regulates, through a mechanism not yet fully elucidated, the protein kinase activity of mTORC1. mTORC1 phosphorylates the downstream effectors p70S6k

and 4E-BP1 which are critical for translation. Ribosomal S6 protein is a downstream effector of p70S6k. TSC1/2 complex is required to activate mTORC2. Arrows indicate activating events, whereas perpendicular lines highlight inhibitory events. (Modified from Martelli *et al* (86).)

1.2.2 PI3K/Akt/mTOR pathway activation in HCC

Cumulative evidences indicate that abnormal activation of the PI3K/Akt/mTOR signaling pathway frequently occurs in HCC. Sahin *et al* showed that phosphorylation of mTOR and the expression of its downstream effector, p70S6k, are up-regulated in 45% of HCC (87). Villanueva *et al* demonstrated that S6 was over-activated in 50% of the HCC cases (88). Similarly, mTOR is found to be activated in about 40% of HCC (89). Interestingly, a recent study by Zhou *et al* demonstrated that the PI3K/Akt/mTOR pathway is more significantly activated in high-grade HCC tumors and is associated with the poor prognosis in HCC patients (90). They demonstrated that Akt and S6 phosphorylation, by immunohistochemistry, were strongly associated with poor prognosis and poor overall survival (90). By analysis 528 HCC cases using Cox multi-factor analysis, they further demonstrated that tumor differentiation (P=0.006), vascular invasion (P=0.028), TNM stage (P=0.005), p-Akt (P=0.021), PTEN (P=0.003), and p-S6 (P=0.002) were independent prognostic factors for HCC (90). All these evidences indicate that activation of PI3K/Akt/mTOR pathway may functionally contribute to HCC progression.

The cellular mechanisms underlying such a wide-spread activation of the PI3K/Akt/mTOR pathway in HCC is not fully understood. However, activation by upstream receptor kinases is believed to be one key mechanism. These may include over-expression of c-Met, EGFR and IGF1-R. c-Met has been found to be over-expressed in 83% of HCC (39, 91). The oncogenic role of c-Met signaling in

HCC development has been confirmed *in vivo*, whereby mice transgenic for the c-Met ligand, HGF (one of the most potent hepatocyte mitogens), leads to carcinogenesis of HCC (92). Similarly, EGFR was found to be over-expressed in 68% of HCC and EGFR expression was up-regulated more frequently in HCC cases with advanced stage and poor differentiation ($P<0.05$) (37, 39). In addition, studies have demonstrated that activation of IGF1-R in HCC was significantly associated with mTOR signaling ($P=0.035$) (88, 93).

Hepatitis virus infections also contribute to the activation of the PI3K pathway in HCC. The HBx protein can activate PI3K/Akt/mTOR cascade, thus blocking apoptosis through a p53-independent manner. Unlike other DNA tumor viruses which block apoptosis by inactivating p53, HBx blocks apoptosis through a HBx-PI3K-Akt-Bad pathway and by inactivating caspase 3 activity that is at least partially p53-independent in HCC cells (63). HCV has also been reported to increase the expression of N-Ras in HCC cells, which then activate the PI3K pathway. When Huh7 cells were infected with HCV *in vitro*, there was a 6-fold increase in N-Ras expression and a 4-fold increase in Akt phosphorylation, indicating a direct role of HCV in PI3K pathway activation in HCC (94). In addition, the PI3K pathway has been shown to be possibly involved in the development of cirrhosis. Neef *et al* showed that in rats with established liver cirrhosis (induced by bile duct-ligation (BDL) or thioacetamide (TAA) injections), treatment with an mTOR inhibitor, rapamycin, led to significant reduction of fibrogenesis, with improved liver function and prolonged survival (95). These emerging evidences, together with the widely

observed clinical activation of this pathway in HCC tumors, indicate the importance of PI3K/Akt/mTOR pathway in HCC carcinogenesis and possibly progression.

Genomic alteration of the PI3K pathway, as revealed by recent genome sequencing efforts in HCC, also indicates its involvement in HCC. Somatic loss of PTEN by gene mutation or deletion is found to occur in 5% of HCC (from http://www.sanger.ac.uk/genetics/CGP/cosmic/), which may contribute to Akt activation in HCC. Besides PTEN mutations, mutations of *PIK3CA,* the PI3K catalytic subunit α-isoform gene encoding p110α, are also found in 6% of HCC (from http://www.sanger.ac.uk/genetics/CGP/cosmic/). All the reported mutations in *PIK3CA* in HCC are somatic missense mutations (i.e. mutations resulting in change in codon for amino acid) clustered in two 'hotspot' regions in exons 9 and 20, which encompass the helical and kinase domains of p110α respectively. Two of the most frequent *PIK3CA* mutations, E545K and H1047R, have been shown to increase PIP3 levels, which can activate Akt signaling and induce cellular transformation (67, 96-98).

All these evidences suggest multiple events inducing the activation of the PI3K/Akt/mTOR pathway in HCC development.

1.2.3 Targeting PI3K/Akt/mTOR pathway in HCC

As aberrant activation of the PI3K signaling pathway has been shown to contribute to cancer cell proliferation, survival and angiogenesis in various human malignancies, enormous efforts have been focused on the development of inhibitory

agents targeting PI3K and key components of the pathway, (Fig. 1.3) some of these have been tested in HCC models, while others are currently undergoing clinical assessment. (Table 1.2)

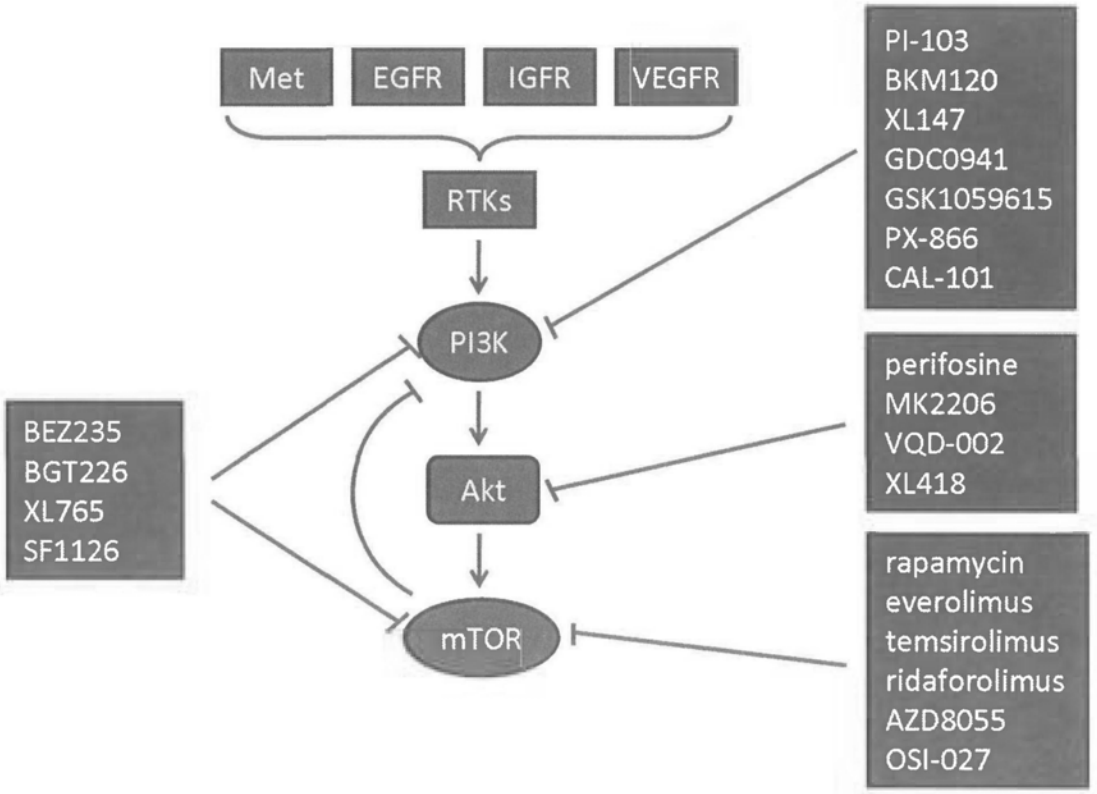

Figure 1.3 Inhibitors in clinical development that target the PI3K/Akt/mTOR pathway. EGFR, epidermal growth factor receptor; IGFR, insulin-like growth factor receptor; VEGFR, vascular endothelial growth factor receptor. Rapamycin (sirolimus; Rapamune®), everolimus (RAD001; Afinitor®), temsirolimus (CCI-779; Torisel®), ridaforolimus (AP23573; MK-8669). (Modified from Liu *et al* (99).)

Table 1.2 Summary of drugs targeting the PI3K pathway in preclinical and clinical models of HCC.

Agent	Target	Phase	NCI ID	Outcome	References
PI3K inhibitors					
Wortmannin	Pan-PI3K	preclinical	-	IC_{50} in μM range, not favorable for clinical use because of toxicity	(100)
LY294002	Pan-PI3K	preclinical	-	IC_{50} in μM range, not favorable for clinical use because of toxicity	(100)
PI-103	Class IA PI3K	preclinical	-	marked growth inhibition *in vitro*	(101)
Akt inihibitors					
Perifosine (Keryx)	Akt	Phase II	-	3% PR, 47% SD >12 weeks, TTP 14 weeks	(102)
MK2206 (Merck)	Akt	Phase II	NCT01239355	ongoing	(103)
mTOR inhibitors					
Rapamycin (Wyeth)	mTORC1	Phase I	NCT00467194	11% SD for 3 months, TTP 3 months	(104)
Everolimus (Novartis)	mTORC1	Phase II/III	NCT00390195 NCT00516165 NCT01005159 NCT01009801 NCT01035229	44% disease control rate, TTP 3.9 months	(105)
Temsirolimus (Wyeth)	mTORC1	Phase I/II	NCT01008917 NCT01010126 NCT01079767 NCT01251458 NCT01281943	43% SD when combined with sorafenib	(106)
AZD8055 (AstraZeneca)	mTORC1/2	Phase I/II	NCT00999882	ongoing	
BEZ235 (Novartis)	Class I PI3K and mTOR	preclinical	-	suppression of tumor cell proliferation at low nM concentration	(107)

PR, partial response; SD, stable disease; TTP, time to progression. Information of clinical trials extracted from http://clinicaltrials.gov/.

1.2.3.1 Targeting PI3K

As mentioned above, there are three classes of PI3Ks. Class IA is the most widely studied and it has three catalytic subunits (p110α, β, δ). Wortmannin and LY294002 are two well-known, first-generation pan-PI3K inhibitors. Wortmannin, a furanosteroid metabolite of the fungi *Talaromyces (Penicillium) wortmannii*, is a specific, irreversible inhibitor of PI3K. It displays similar potency for inhibiting the activity of class I, II, and III PI3K members *in vitro*. LY294002 was the first synthetic small molecule that reversibly inhibits the PI3K family members. Unfortunately, both of these preclinical tool compounds have IC_{50} in the micromolar range, and show little or no preferential selectivity for individual PI3K isoforms. Further, when wortmannin or LY294002 was administered to animals, unfavorable pharmacokinetic properties and considerable toxicities have been reported (108-110). Body weight loss, dry skin and even death were observed, thus limiting their use in clinical setting. Nevertheless, preclinical studies of these broad-spectrum PI3K inhibitors have greatly contributed to the understanding of the biological importance of PI3K signaling and provided crucial information for the development of novel PI3K inhibitors.

Since p110α is the main isoform responsible for most of the downstream signal transduction events upon RTK activation, some PI3K inhibitors with p110α isoform selectivity have been reported recently (111, 112). PI-103, a p110α-specific inhibitor, was shown to have potent inhibitory activity on PI3K signaling as it is able to inhibit both p110α and mTOR in glioma cells (113). Recently, Ladu *et al* showed that low

dose of PI-103 (0.5 μmol/L) was able to result in marked suppression of HCC cell growth *in vitro* (101). Although there is no *in vivo* or clinical study on these p110α-specific inhibitors yet, these encouraging data support their potential therapeutic value for HCC treatment in the future.

A recent expansion in the pipeline development of PI3K-targeting agents results in a large number of PI3K inhibitors entering into clinical trials (Fig. 1.3). A phase I study showed that the administration of CAL-101, a selective inhibitor of p110δ (another isoform of Class I PI3Ks), resulted in partial responses or stable diseases in patients with hematologic malignancies (114). PX-866, a pan-PI3K inhibitor, has demonstrated a mild side-effect profile with disease stabilization reported in 25% of the patients with solid tumors, including squamous cell skin cancer and melanoma (115). Another pan-PI3K inhibitor, GDC0941 has also been shown to result in disease stabilization in sarcoma, ovarian cancer and endometrial cancer patients (116). However, none of these studies included HCC patients.

1.2.3.2 Targeting Akt

Akt is one of the most crucial downstream effectors of the RTK-PI3K pathway, and is therefore another attractive therapeutic target for anti-cancer therapy. It includes three isoforms, Akt1, Akt2 and Akt3. Several pan-Akt inhibitors have been developed, which can be grouped into various classes, including lipid-based phosphatidylinositol analogues, ATP-competitive inhibitors, and allosteric inhibitors. Perifosine, one of the agents that is most advanced in clinical development, is a

lipid-based phosphatidylinositol analogue that binds to the pleckstrin homology domain of Akt, which prevents Akt from binding to PIP3 and subsequent membrane translocation (117). It has been tested in a phase I trial to treat solid tumors and lymphoma. In this study by Van *et al*, one partial response (sarcoma) and several patients with stable disease (renal cancer, colon cancer) had been observed (118). A phase II trial of this compound has been conducted in HCC (102). Of the 42 HCC patients treated, one patient achieved a partial response (3%) and 15 (47%) had stable disease for more than 12 weeks, with an encouraging median time to progression (TTP) of 14 weeks (102).

To address a major issue regarding the potential benefits of isoform specificity, a number of allosteric Akt inhibitors have recently been identified through systematic screening of compound libraries and application of an iterative analogue library synthesis approach. Akti-1/2, a naphthyridinone allosteric dual inhibitor of Akt1 and Akt2, has potent anti-tumor activity in tumor xenograft models, and its analogue MK2206 is in a phase I trial for patients with locally advanced or metastatic solid tumors (119). Further, a recent study by Chen *et al* showed that the combination of sorafenib and MK2206 was able to overcome sorafenib resistance in HCC cells at clinical achievable concentration (103), implicating the potential use of PI3K/Akt/mTOR inhibitors for circumventing sorafenib resistance in HCC patients. MK2206 is currently tested in a phase II study in advanced HCC (from http://www.clinicaltrials.gov/). Several other Akt inhibitors such as XL418 and VQD-002 have shown significant anti-tumor effects in preclinical studies and are

currently in phase I clinical trials in hematologic malignancies and non-small-cell lung cancer (from http://www.clinicaltrials.gov/). Thus far, the potential therapeutic efficacy of these Akt inhibitors is not determined in HCC.

1.2.3.3 Targeting mTOR

mTOR exists in two different complexes, mTORC1 and mTORC2. mTOR inhibitors that were developed earlier are specific mTORC1 targeting agents. Rapamycin (also known as sirolimus) (Rapamune®; Wyeth) is a prototype inhibitor of mTORC1. It is a bacterially derived natural compound with antifungal activity (120). It was subsequently found to have immunosuppressive (121) and, more recently, anti-neoplastic properties (122-125). Rapamycin associates with its intracellular receptor, FK506-binding protein 12 (FKBP12), which then binds directly to mTORC1 and suppresses mTOR-mediated phosphorylation of its downstream substrates, p70S6k and 4E-BP1 (122, 125). However, rapamycin is insoluble in aqueous solution and was given low priority for clinical development. Only one phase I trial using rapamycin in combination with bevacizumab is being tested in HCC patients (from http://clinicaltrials.gov/). Recently, structural analogues of rapamycin such as temsirolimus (CCI-779/Torisel®; Wyeth) and everolimus (RAD001/Afinitor®; Novartis) have been developed. These rapamycin analogues inhibit mTOR through the same mechanism as rapamycin, but have better pharmacological properties for clinical use in cancer therapy. Several clinical trials using mTOR inhibitors in patients with various cancers have been reported (122).

Results from recent clinical studies with temsirolimus and everolimus used as single agents showed that these drugs significantly improved survival in patients with advanced renal cell carcinoma. They have led to the approval of these compounds for treating this aggressive cancer (122, 126). In HCC, a phase I/II study of everolimus was conducted in 28 patients with advanced HCC and modest anti-tumor activity was observed including a TTP of 3.9 months and disease control rate of 44% (105). These encouraging results lead to the initiation of the EVOLVE (EVerOlimus for LiVer cancer Evaluation) clinical trial program; this is a global, randomized, double-blind and placebo-controlled phase III study to evaluate the efficacy of everolimus in HCC patients. The EVOLVE study aims to compare the clinical outcome of the patients given best supportive care with continuous everolimus treatment versus placebo in the second line setting. Targeted patients are those who have advanced HCC whose disease have progressed on sorafenib therapy, or who are unable to tolerate sorafenib therapy. In addition, there are phase I/II studies of temsirolimus as novel therapeutic treatment for HCC patients (from http://clinicaltrials.gov/). Other studies are testing temsirolimus in phase I/II setting by combining with sorafenib, bevacizumab or pegylated liposomal doxorubicin (106) (from http://clinicaltrials.gov/).

Since mTOR inhibitors have both immunosuppressive and anti-tumor effects, in patients undergoing liver transplantation, these agents have the potential to simultaneously protect against rejection and HCC recurrence. Campsen *et al* reported that among 688 patients who underwent liver transplant, those who

received rapamycin had 50% less rejection compared to controls (127). Levy *et al* also reported that everolimus could reduce the rejection rate in recipients of liver transplantation (128). In liver transplant patients, the use of mTOR inhibitors have been associated with side-effects, including pneumonitis, an increase in renal failure and hepatic artery thrombosis (129-131). Other small non-randomized uncontrolled pilot trials and retrospective analyses have demonstrated that rapamycin could improve the outcome for liver transplant patients with a pre-transplant diagnosis of HCC (131, 132). A controlled prospective randomized study is currently underway to further evaluate mTOR inhibitors in liver transplant patients (133) (from http://clinicaltrials.gov/).

The mTORC2 complex functions as a 3-phosphoinositide-dependent protein kinase 2 (PDPK2) and phosphorylates the C-terminus of Akt at ser473, an obligatory event for full activation of Akt (134), while mTORC1 phosphorylates the downstream effector p70S6k which then induces the degradation of insulin receptor substrate 1 (IRS-1), thus decreasing insulin-driven Akt activity (135). Inhibition of mTORC1, therefore, may result in feedback activation of Akt. Thus, it is anticipated that a kinase inhibitor of mTOR that can target both mTORC1 and mTORC2 would block the activation of the PI3K pathway more effectively than one that blocks mTORC1 only, and this could potentially overcome the problem of feedback. Recent studies by Feldman *et al* and Thoreen *et al* showed that torkinibs and torin1 — potent and selective ATP-competitive inhibitors of mTOR for both mTORC1 and mTORC2, were able to impair cell growth and proliferation more effectively than

rapamycin in mouse embryonic fibroblasts (MEFs) (136, 137). AZD8055 is a novel ATP-competitive inhibitor of mTOR kinase activity, which results in the inhibition of both mTORC1 and mTORC2 downstream substrates and thus downstream signaling (138). This inhibitor is currently tested in a multi-centre phase I/II clinical trial in patients with advanced HCC in Asia. It is anticipated that with the increasing efforts to develop new mTORC1/2 inhibitors, the issue of feedback could be overcome in the near future.

1.2.3.4 Challenges in targeting PI3K/Akt/mTOR pathway

Several potential challenges exist when targeting this pathway in cancer. The very first relates to the specificity for PI3K targeting in cancer. The two isoforms of Class I PI3Ks, namely p110α and p110β, form a complex with the p85 adaptor to bind to RTKs, and both use the same substrates and generate the same lipid products. However, p110α and p110β have very different roles in cellular signaling, growth and oncogenic transformation. Upon RTK activation, the p110α isoform is the main isoform responsible for the activation of the downstream signaling components of the PI3K pathway (139). On the other hand, p110β play an essential part in G protein-coupled receptor (GPCR) signaling in all cell types including the immune system (140). The biologic significance of the p110α isoform would suggest a preference for p110α isoform-specific inhibition, rather than p110β inhibition, as potential form of cancer treatment; such an approach may at the same time avoid toxicity to the immune system in association with p110β inhibition.

The second challenge relates to the existence of a complex mTOR feedback loop and pathway crosstalk. Some preliminary results with mTOR inhibitors in several tumor types, including advanced breast cancer and glioma, indicated a low response rate of less than 10% (122). This may be partly contributed by the undesirable mTOR feedback loop. When mTOR is activated, it can initiate a signaling cascade through p70S6k that induces upstream feedback inhibition of signaling via IGF-1 and insulin receptors, which down-regulates PI3K and Akt activity. (Fig. 1.4) Therefore, when mTOR inhibitors are used, Akt activity may be increased, which can ultimately lead to enhanced tumor growth (141). A phase I trial on glioblastoma has shown that rapamycin treatment led to Akt activation in 7 of 14 patients, presumably due to the feedback loop, which was associated with significantly shorter TTP during post-surgical rapamycin maintenance therapy (142). With such knowledge, dual PI3K-mTOR inhibitors have recently been developed to alleviate the mTOR feedback loop. BEZ235 is an imidazoquinazoline derivative that inhibits multiple Class I PI3K isoforms and mTOR kinase activity by binding to the ATP-binding pocket of PI3K (143). Preclinical data show that BEZ235 has strong anti-proliferative activity against tumor xenografts that have abnormal PI3K signaling, including loss of PTEN function or gain of function PI3K mutations (144). BEZ235 has entered phase I/II clinical trials in patients with breast cancer and endometrial cancer (from http://clinicaltrials.gov/). An *in vitro* study on HCC has demonstrated suppression of tumor cell proliferation at low nanomolar concentrations with BEZ235 (107). Other dual inhibitors, including BGT226

(Novartis), XL765 (Exelixis) and SF1126 (Semafore), are undergoing early-phase clinical testings in patients with breast cancer, non-small-cell lung cancer, and malignant gliomas (99, 145, 146), though none is planned for HCC patients.

In addition to the feedback regulation of this pathway, emerging evidences are indicating a second level of complexity associated with targeting this pathway, which is related to the crosstalk between PI3K pathway and several other important signaling pathways, including the Ras/MAPK pathway. Since RTKs, or oncogenes such as *RAS* may activate both the RAF-mitogen activated protein kinase (MAPK) and PI3K pathways, blocking the PI3K pathway could up-regulate signaling of the Ras/MAPK pathway as the two pathways are cross-inhibitory for each other (147). (Fig. 1.4) The Ras/MAPK pathway can in turn drive tumor growth thus counteracting the effect of the PI3K pathway inhibition. This latter phenomenon has recently been demonstrated by Carracedo *et al*, who reported that mTORC1 inhibition led to the activation of MAPK in a PI3K-dependent manner (148).

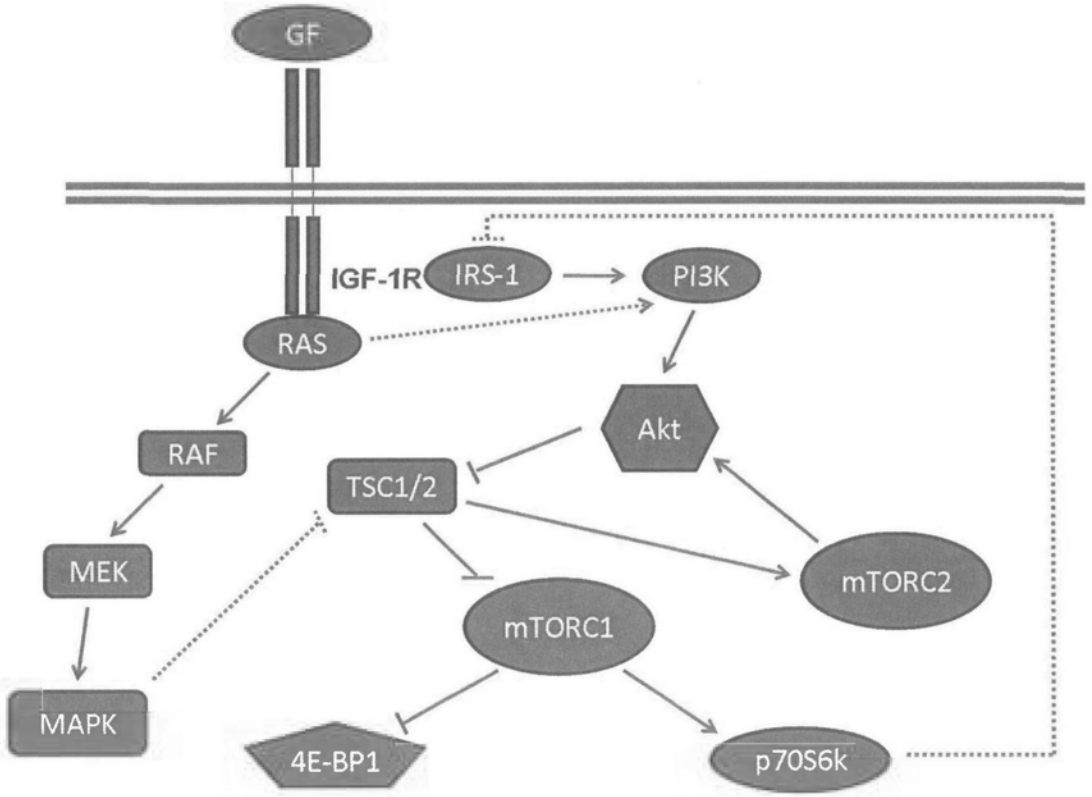

Figure 1.4 mTOR feedback loop and PI3K pathway crosstalk with Ras/MAPK pathway. IRS-1 links IGF-1R signaling to PI3K, which leads to activation of Akt and mTOR. P70S6k phosphorylates IRS-1, which destabilizes this protein and uncouples IGF-1R signaling to PI3K. Thus, mTOR activation exerts negative feedback to restrict insulin signaling. Loss of this negative feedback mechanism has been shown to occur in cells and tumors exposed to rapamycin. Growth factor mediated signaling or mutational activation of Ras oncogenes can activate both of the Ras/MAPK and PI3K pathways. MAPK may also inhibit TSC1/TSC2 complex, which then cause the activation of mTOR. IGF-1R, insulin-like growth factor 1 receptor; IRS-1, insulin receptor substrate 1. Arrows indicate activating events, whereas perpendicular lines highlight inhibitory events.

1.3 Combinatory treatment for HCC

Although specific knockout of PI3K isoforms has been shown to block oncogenic transformation driven by various activated RTKs and oncogenes (139), multiple factors revealed thus far seem to limit the clinical efficacy of PI3K/Akt/mTOR inhibitors as single agents for cancer treatment. These unanticipated factors include drug resistance, feedback regulation, and pathway crosstalk. It is believed that combination strategies may alleviate these undesired activities, thus improving the efficacy of PI3K targeting in patients. One approach will be using a combination of inhibitors against multiple signaling components of the pathway. As mentioned above, mTORC1/2 inhibitors and dual PI3K-mTOR inhibitors are attractive therapeutic options (149). The other approach will be the use of conventional chemotherapy or radiation therapy, in conjunction with PI3K targeting. Because mTOR inhibitors have been the first agents to be tested within the PI3K/Akt/mTOR pathway, here I attempt to summarize the results of previous studies on combinations of mTOR inhibitors and other compounds.

1.3.1 Combining mTOR inhibitors with chemotherapy

Recent studies demonstrated that mTOR targeting could enhance the efficacy of a broad range of cytotoxic chemotherapies, including cisplatin, doxorubicin, paclitaxel, carboplatin, dexamethasone, mitoxantrone and docetaxel, in various types of human cancers (150-153). For HCC, Tam *et al* showed that the both *in vitro* and *in vivo* suppression of HCC cell growth by cisplatin was enhanced by the addition of

everolimus (154). Similarly, an independent study by Piguet *et al* demonstrated that rapamycin was able to elicit additive anti-tumor and anti-angiogenic effects when administered together with doxorubicin in both *in vitro* and *in vivo* models of HCC (155). Bu *et al* also showed that combination of rapamycin and 5-fluorouracil (5-Fu) could induce apoptosis and cell senescence in HCC cells *in vitro* (156). These findings offer a rationale for combining mTOR inhibitors with conventional cytotoxic agents for HCC treatment.

Recently, several HCC gene expression profiling studies that aimed at identifying functional/mechanistic changes that underlie the malignant transformation of HCC have revealed that microtubule-related cellular assembly and organization is the most significant cellular event in HCC (157, 158). This important finding provides a rationale for the use of microtubule targeting in HCC.

Anti-microtubule agents are a group of compounds which bind to soluble tubulin and/or directly to the tubulin in microtubules. Most of these compounds are anti-mitotic agents that inhibit cell proliferation by acting upon the polymerization dynamics of spindle microtubules, the rapid dynamics of which are essential for proper spindle function during cell division. Anti-microtubule agents are functionally classified into two main groups. The first group, known as the microtubule-destabilizing agents, inhibits microtubule polymerization, thus results in cell cycle arrest and apoptosis. These include several *Vinca* alkaloids, such as vinblastine, vincristine, vinorelbine, vindesine and vinflunine, most of which have been used widely in clinical practice. (Table 1.3) However, studies have shown

inherent or acquired resistance of cancer cells to *Vinca* alkaloids; in HCC, this was partly contributed by the expression of multi-drug resistance gene (MDR) (159, 160). The second group is known as the microtubule-stabilizing agents. These agents stimulate microtubule polymerization, and then cause cell cycle arrest and apoptosis. The earlier compounds available in clinical practice are the taxanes, including paclitaxel and docetaxel. Newer compounds that have been developed include the epothilones and discodermolide; they also bind to the taxane site (a similar, but not identical, pharmacophore) on the β-tubulin subunit of microtubules to stabilize microtubules. (Table 1.3) Although some of these agents have demonstrated good anti-tumor activity in a number of human cancers, these chemotherapeutic agents remain to be rather ineffective for the treatment of HCC at least in the single agent setting. A phase II pharmacokinetic study of paclitaxel therapy for unresectable HCC patients did not result in any clinical response (161). Similarly, a phase II study on docetaxel showed limited efficacy with toxicity in HCC patients (162). Both paclitaxel and docetaxel treatment resulted in severe treatment-related toxicities (163, 164). Recently, nanoparticle conjugation of these compounds have been developed, which enables reducing of dose with improved pharmacodynamic profiles for clinical use (165). In clinical setting, the nanoparticle albumin-bound (*nab*)-paclitaxel has been studied in patients with advanced breast cancer, and was shown to result in a response rate of 15% in heavily pretreated patients with pre-exposure to paclitaxel (166).

Both preclinical and clinical studies demonstrate a noticeable degree of

resistance to most anti-microtubule agents for HCC treatment. Recently, two studies have suggested that the PI3K/Akt/mTOR signaling pathway may be involved in drug resistance to taxanes and other drugs acting on microtubules, including vincristine, colchicines (27, 28). VanderWeele *et al* showed that Akt activation markedly increased resistance to microtubule-directed agents, while rapamycin (an mTOR inhibitor) could inhibit Akt-mediated therapeutic resistance, indicating that the resistance phenotype is mTOR-dependent (28). These findings implicate a potential role of combining anti-microtubule agents with mTOR inhibitors for HCC treatment. In fact, such a combination strategy has already been applied in other models. Marimpietri *et al* demonstrated the combined therapeutic effects can be observed with rapamycin and vinblastine on tumor cell growth, apoptosis, and angiogenesis in neuroblastoma (167). Besides an enhanced inhibition of tumor cell growth, Campostrini *et al* also showed that such a combination was able to inhibit the proliferation of human endothelial cells, suggesting a potential anti-angiogenic activity with such combination (168). A phase I study using rapamycin and vinblastine in patients with relapsed solid tumors, including brain tumors and lymphoma, is currently underway (from http://www.clinicaltrials.gov/). Besides vinblastine, paclitaxel/mTOR inhibitor combination has been tested in advanced solid tumors recently (169-171). These include combinations of paclitaxel with rapamycin, everolimus, and ridaforolimus (AP23573; MK-8669). Shafer *et al* showed that rapamycin potentiated the growth inhibitory effects of paclitaxel on endometrial cancer cells, as indicated by induction of apoptosis and potentially

increased tubulin polymerization and acetylation (169). Another mTOR inhibitor, everolimus, was shown to result in synergistic cytotoxicity with paclitaxel in mantle cell lymphoma (170). In addition, a phase Ib study of weekly mTOR inhibitor ridaforolimus with weekly paclitaxel has shown encouraging anti-tumor activity in 29 patients with 9% partial response and 28% stable disease in solid tumors (171). To date, there has been no clinical report of such a combination strategy in HCC. However, a number of studies are currently conducted in HCC models. One study has reported that combination of rapamycin and vinblastine enhanced anti-tumor effect over either agent alone by inhibiting angiogenesis, as evident by the detection of significantly lower area of microvessels with anti-CD31 monoclonal antibody (mAB) (172).

Table 1.3 Anti-mitotic agents, their binding sites on tubulin and their stages of clinical development

Binding domain	Related agents	Therapeutic uses	Stage of clinical development	References
Vinca domain	Vinblastine	Hodgkin's disease, testicular germ-cell cancer	In clinical use	(173)
	Vincristine	Leukemia, lymphomas	In clinical use	(174, 175)
	Vinorelbine	Solid tumors, lymphomas, lung cancer	In clinical use; Phase I-III trials in progress	(176, 177)
	Vinflunine	Bladder, non-small-cell lung cancer, breast cancer	Phase III	(178)
	Cryptophycin 52	Solid tumors	Phase III finished	(179)
	Halichondrins (one of the members: Eribulin)	Breast cancer, non-small-cell lung cancer, prostate cancer, sarcoma	In clinical use; Phase I-III trials in progress	(180)
	Hemiasterlins	-	Phase I	(181)
	Dolastatins	Potential vascular-targeting agents	Phase I; Phase II completed	(182)
Taxane site	Paclitaxel	Ovarian, breast and lung tumors, Kaposi's sarcoma; trials with numerous human cancers	In clinical use; Phase I-III trials in progress	(183)
	Docetaxel	Prostate, brain and lung tumors	Phase I-III	(184)
	Epothilones	Paclitaxel-resistant tumors	Phase I-III	(185)
	Discodermolide	-	Phase I	(186)
Colchicine domain	Colchicine	Non-neoplastic diseases (gout, familial Mediterranean fever)	Failed trials because of toxicity	(187)
	Combretastatins	Potential vascular-targeting agents	Phase I/II	(188)
	2-Methoxyestradiol	-	Phase I	(189)
	Methoxybenzene-sulphonamide	Solid tumors	Phase I/II	(190)
Other microtubule binding sites	Estramustine	Prostate cancer	Phase I-III	(191)

Information of clinical trials extracted from http://clinicaltrials.gov/. (Modified from Jordan *et al* (192).)

1.3.2 Combining mTOR inhibitors with other molecular targeted therapies

The Ras/MAPK pathway is an emerging pathway to be co-targeted with the PI3K pathway. As mentioned above, while the Ras/MAPK pathway is known to be activated upon PI3K targeting in human cancers (147), recent data have also suggested that deregulation of the Ras/MAPK pathway contributes to cancer cell resistance to PI3K inhibitors (193). Therefore, interrogation of the Ras/MAPK pathway may serve as an effective approach to overcome PI3K resistance. As the Ras/MAPK pathway has already been shown to be activated in HCC (194, 195), inhibition of these two key pathways in HCC may be clinically beneficial. Recently, co-targeting of both Ras/MAPK and mTOR has been investigated in multiple cancers, including breast cancer, prostate cancer and melanoma. Results of these studies indicate that such an approach is considerably more effective than monotherapy with these agents with respect to their anti-tumor activity (196-198). Sorafenib is a Raf kinase inhibitor with demonstrated anti-tumor activities in both *in vitro* and *in vivo* models of HCC (199). It is the first molecular targeting agent approved for HCC treatment in the clinic. Combination of rapamycin and sorafenib has shown enhanced anti-tumor effect over single agents alone in an orthotopic model of HCC (200). Currently, there are three ongoing clinical trials evaluating the activity of sorafenib/mTOR targeting in advanced HCC patients using everolimus or temsirolimus (NCT01005199, NCT01008917, NCT01335074, from http://clinicaltrials.gov/).

1.3.3 Combining mTOR inhibitors with radiation

In addition to chemo-sensitization, targeted inhibition of the PI3K/Akt/mTOR pathway may also induce radio-sensitization in human cancers. Shinohara *et al* demonstrated that radiation could activate the PI3K/Akt pathway, while inhibition of PI3K or Akt sensitized tumor vasculature to radiotherapy (201). In this study, two mTOR inhibitors, rapamycin and everolimus were found to radio-sensitize the endothelial cells to radiation and resulted in increased cell apoptosis (201). This finding implicates that combination of radiotherapy and mTOR inhibitors might elicit additive/synergistic anti-tumor activity. Cumulative evidences have shown that endothelial cells are very sensitive to radiation/mTOR targeting combination. Several studies also reported the additive effect of growth inhibitory activity with the radiation/mTOR targeting (everolimus) combination in various tumor types including breast cancer, glioma, colon cancer, and pancreatic cancer; these may be attributed by the combined anti-angiogenic effects of the combination regimens (201-203). As for HCC, such a combination strategy has not been investigated; in-depth preclinical and clinical evaluation is warranted.

1.4 Aims of the present study

HCC is a global health problem of many populations. Since the understanding of the pathogenesis of HCC is still very elementary, effective approaches for HCC prevention and treatment have not been developed. The disease is resistant to most chemotherapies, and hence it is often associated with poor prognosis. By screening

for the key effectors and exploring the molecular mechanisms that are involved in HCC carcinogenesis, a better framework may be obtained as a means to develop more effective anti-tumor strategy against HCC. The PI3K/Akt/mTOR signaling pathway has been shown to be critical for HCC cell growth and survival. However, the PI3K pathway presents a promising therapeutic opportunity and a practical challenge for HCC therapy at the same time. Potential issues associated with toxicity and resistance are anticipated when targeting this pathway.

Therefore, the aims of the present study are:

1. To screen important functional changes associated with the malignant transformation of HCC.
2. To investigate the anti-tumor effect of novel microtubule targeting agent *nab*-paclitaxel on HCC *in vitro* and *in vivo*.
3. To investigate the anti-tumor effect of mTOR inhibition on HCC cells *in vitro* and *in vivo*, either alone or in combination with microtubule targeting agents.
4. To find molecular mechanisms of the highly effective combination of targeting mTOR and the microtubule in HCC cells.

Chapter 2: Materials and Methods

Materials and methods that are specific for an individual study are being described in each chapter. Those that are commonly used are listed in this chapter.

2.1 Chemicals and reagents (Table 2.1)

Chemical	Source	Cat. No.
2-Mercaptoethanol	Gibco-BRL	21985-023
3-(4,5-dimethylthiazol-2-yl)-2,5-diphenyl tetrazolium bromide (MTT)	Calbiochem	475989
(3-aminopropyl) triethoxysilane	Sigma	9324
40% Acrylamide	Bio-Rad	161-0140
Access RT-PCR System	Promega	A1250
AIM-V medium	Gibco-BRL	12055-083
Agarose	Sigma	A9539
Bovine serum albumin (BSA)	Sigma	A3350
Bromophenol blue	Sigma	B8026
Calcium chloride ($CaCl_2$)	Sigma	C1016
Dimethyl sulphoxide (DMSO)	Sigma	D8418
Doubecco's Modified Eagle Medium (DMEM)	Hyclone	SH30243.02
Ethanol, 99%	Merck	986
Ethylene diaminetera acetic acid (EDTA)	Sigma	ED-2S2
Fetal bovine serum (FBS)	Hyclone	SV30160.03
Glycerol, 99% AR Grade	Sigma	G8773
Glycine	Bio-Rad	160-0717
Hematoxylin	Sigma	010M4354
HEPES	Sigma	H7523
*Hind*III	Fermentas	ER0501
Hydrochloric acid (HCl)	Merck	9970
Hydrogen peroxide (H_2O_2)	Sigma	H6520

In-Situ Cell Death Detection Kit	Roche	11684817910
Isopropanol	Merck	9634
Ketamine	Alfasan	096245-1
Lipofectamine™ 2000 Transfection Reagent	Invitrogen	11668019
Liquid DAB+ Substrate Chromogen System	Dako	K3468
Methanol	Merck	6009
Paraffin	Fisher Scientific	T565
PBS (pH7.4)	Invitrogen	3002
Penicillin Streptomycin	Invitrogen	15140-122
Permount® Mounting Medium	Fisher Scientific	SP15-100
Poly L Lysine	Sigma	P4707
Potassium chloride	BDH	295944B
Precision Plus Protein All Blue Standards	Bio-Rad	161-0373
ProLong® Gold antifade reagent with DAPI	invitrogen	P-36931
Propidium iodide (PI)	Invitrogen	P1304MP
Protein dye	Bio-Rad	500-0006
Puromycin Dihydrochloride, Selection Anribiotic, (liquid)	Invitrogen	A1113803
RNase A	Sigma	R4642
RPMI-1640 Medium	Hyclone	SH30255.01
Sodium Carbonate (Na_2CO_3)	BDH	102405Y
Sodium Chloride (NaCl)	BDH	10241AP
Sodium Citrate	Sigma	S4641
Sodium dodecyl sulfate (SDS)	Sigma	L3771
Sodium hydrocarbonate ($NaHCO_3$)	BDH	10247V
Sodium hydroxide (NaOH)	BDH	102524X
SuperSignal West Pico Chemiluminescent Substrate	Thermo Scientific	JB119506
T4 DNA ligase	Fermentas	EL0014
Tris Base	Promega	H5135

Triton X-100	Sigma	T8787
Trypsin-EDTA	Invitrogen	25300-062
Tween 20	Sigma	P1379
*Xho*I	Fermentas	ER0691
Xylazine	Alfasan	096231-12
Xylene	Merck	8681

2.2 Cell culture

Human liver cancer cell lines HepG2, Hep3B, PLC/PRF/5, SNU398 and SK-HEP-1 were obtained from ATCC, and Huh7 was obtained from JCRB Cell Bank. HepG2, Hep3B, Huh7, PLC/PRF/5 and SK-HEP-1 were cultured in Dulbecco's modified Eagle medium (DMEM) with L-Glutamine (HycClone, Logan, Utah, USA) supplemented with 10% fetal bovine serum (Hyclone). SNU398 was cultured in RPMI-1640 medium (HycClone) supplemented with 10% fetal bovine serum. HKCI-9 previously established from our group (204) was cultured in AIM-V medium (Gibco-BRL, Grand Island, NY, USA) supplemented with 1% L-Glutamine and 10% fetal bovine serum. All cells were cultured under a humidified atmosphere of 5% CO_2 at 37˚C.

2.3 Cell viability assay

Cell viability was measured by MTT Assay. Cells plated in 96-well plates or 48-well plates were treated with drugs or siRNA transfection as indicated. For MTT assay, cells were incubated with 1mg/ml of MTT solution (Invitrogen, Carlsbad, CA, USA) for 4 hrs and the formazan product was dissolved in DMSO for OD measurement at

570nm. The percentage growth inhibition was calculated as $(OD_{vehicle}-OD_{drug})/OD_{vehicle} \times 100\%$. Cell viability was expressed as a percentage of maximum absorbance from 5 replicates in 3 independent experiments. The IC_{50} value of each drug on each cell line was determined from the dose-response curves as the drug dose at which half of the maximal growth inhibition of the cells was observed.

2.4 Flow cytometry analysis of cell cycle

Cell cycle distribution was measured after exposure to different concentrations of drugs. After 12 hrs or 16 hrs, all cells including detached cells were harvested and fixed in 70% ethanol at 4°C overnight. Fixed cells were incubated with RNase A and propidium iodide (PI) prior to flow cytometry analysis (BD FACSCalibur™, Becton Dickinson). The average value of G_0/G_1, S and G_2/M phases were calculated from 3 independent experiments.

The cell cycle can be divided in four distinct phases, G_1 phase, S phase, G_2 phase and M phase. In addition to these four phases, G_0 phase refers to both quiescent and senescent cells. PI is the most commonly used dye to quantify DNA content and aids in distinguishing different phases. Cells in G_0/G_1 phases possess normal diploid chromosomes with normal DNA content (2N), whereas cells in G_2/M phases contain exactly twice the DNA content (4N). DNA replication occurs during S phase and hence the DNA amount ranges from 2N to 4N. If there are cells undergoing apoptosis, they will appear in the sub-G_1 peak. A histogram plot of DNA content

against cell numbers shows the DNA profile that represents the cell cycle distribution of a population of cells (Fig. 2.1).

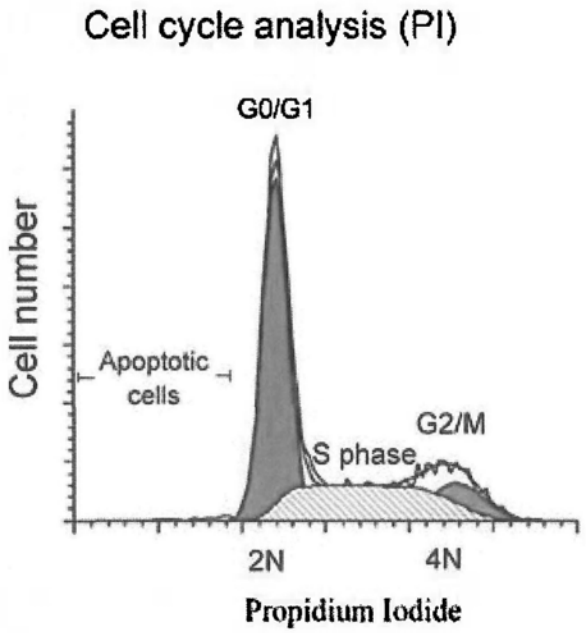

Figure 2.1 Flow cytometry analysis of cell cycle. The first peak represents G_0/G_1 phase containing cells that possess normal diploid chromosomes with normal DNA content (2N). The second peak represents G_2/M phase containing cells that possess exactly twice the DNA content (4N). The cells between the two peaks represent cells undergoing replication in S phase with DNA content ranging from 2N to 4N. Before the first peak, there may be a small peak called sub-G_1 peak, which represents apoptotic cells.

2.5 Western blot analysis

Protein lysates were obtained from cells undergoing various treatments. In short, cell pellets were lysed with lysis buffer for 30 min on ice, followed by centrifugation at 14,000 g for 10 min at 4˚C. Proteins were then quantified using the Bradford Protein Assay (Bio-Rad Laboratories, Hercules, CA, USA). Equal amounts of protein lysates (30-60μg) were separated on 6-12% SDS-PAGE and electrotransferred to nitrocellulose membrane (Bio-Rad) using a semi-dry transfer machine (Bio-Rad). Membranes were blocked by 5% non-fat milk for 1 hr at room temperature. After blocking, membranes were incubated with primary antibody at 4˚C overnight, and then washed 3 times with TBST (10 min/wash). The membranes were then incubated with peroxidase conjugated secondary antibody for 1 hr at room temperature, followed by 3 washes in TBST. Protein expression was detected using SuperSignal West Pico Chemiluminescent Substrate (Thermo Scientific, Rockford, IL, USA).

2.6 HCC xenograft models

Experimental protocols and procedures were approved by the Animal Research Ethics Committee of the Chinese University of Hong Kong. All experiments were conducted under license granted from the Department of Health, HKSAR.

Male BALB/c nude mice at 6-8 weeks old with an average body weight of about 20g were anesthetized by intraperitoneal injection (i.p.) of ketamine hydrochloride (120mg/kg) (Alfasan, Woerden, Holland) plus xylazine (6mg/kg) (Alfasan).

Anesthetized animals then received HCC cells suspended in 200µl serum free medium by subcutaneous injection below the dorsal flank.

Chapter 3: Novel Therapeutic Potential in Targeting the Microtubules by Nanoparticle Albumin-bound Paclitaxel in Hepatocellular Carcinoma

3.1 Introduction

As described in Chapter 1, there are currently very limited treatment options for patients with advamced HCC, the identification of appropriate novel chemotherapies and the development of targeting strategies are required to improve their prognosis.

Gene expression profiling has led to the discovery of vital signaling paths in human oncogenesis, and has aided the identifications of molecular targets for therapeutic developments. Using this approach, a number of potential targets, including extra-cellular matrix (ECM) related genes, osteopontin, fatty acid-binding protein 7 (FABP7) and serine/threonine kinase 31 (STK31), have been suggested as therapeutic targets for breast cancer, colorectal cancer, melanoma, glioblastoma and gastrointestinal cancer (205-209). In this study, gene expression profiling was carried out in conjunction with ontology analysis to decipher functional changes underlying the malignant transformation of HCC. A number of aberrant pathways were suggested, amongst which deregulations of microtubule-related cellular assembly has been ranked as the most significant.

Based on the annotation results obtained from Gene Ontology, the potential use of microtubule targeting drugs for their therapeutic utility was explored in HCC cells. Microtubule-stabilizing agents (taxanes) are a class of diterpenoid drugs (210) that have anti-tumor activity against a wide range of human cancers (211-213). Paclitaxel

is the most commonly used taxane, while docetaxel is a synthetic taxoid structurally similar to paclitaxel. However, both have low aqueous solubility requiring solubilization with surfactants and solvents and show severe treatment-associated toxicities in patients (163, 164). Nanoparticle albumin-bound (*nab*)-paclitaxel is a 130-nm particle formulation of paclitaxel that is devoid of any surfactant, solvent or ethanol carriers (165). *nab*-Paclitaxel has been shown to exert high anti-tumor activity, more effective intra-tumoral accumulation and less cytotoxicity than paclitaxel in preclinical animal models of multiple cancers (214, 215).

In this study, the comparative anti-tumor activity of taxane-based drugs and doxorubicin (an agent that has been most commonly studied in HCC clinical trials) was investigated in HCC cell lines and xenograft model. The efficacy of taxanes in combination with silencing of Stathmin1 (STMN1), a key regulatory protein that controls the microtubule dynamics, was also examined.

3.2 Materials and Methods

3.2.1 Expression profiling and informatics analysis

Gene expression profiling on 43 paired HCC tumors and adjacent non-tumoral liver tissues was performed according to method previously described (216). Demographic information of cases studied is shown in Table 3.1. Normal liver RNA from three individuals were pooled and used as reference control in array hybridisation (Ambion, Austin, TX; Clontech Laboratory Inc., Palo Alto, CA; and Strategene, La Jolla, CA, USA). Briefly, reverse-transcribed RNA from test sample

and normal liver pool were differentially labelled with fluorescent Cy5-dCTP or Cy3-dCTP. Labelled cDNAs were co-hybridised onto 19K cDNA arrays (Ontario Cancer Institute, Canada). The 19K cDNA microarray employed contains sequence-verified human genes and expressed sequence tag sequences mapped to National Center for Biotechnology Information's UniGene database. Hybridization took place in a dark chamber at 37°C for 16 hrs. Post-hybridization washes were carried out in 1× SCC/0.1% SDS at 50°C, 3 times at 10 min each, and gentle rinsing in 1× SSC twice for 1 to 2 min each. Hybridised signals were captured by ScanArray 5000 (Packard BioScience, UK) using emission and absorption wavelength for Cy5 and Cy3. Raw images acquired were analysed by GenePix Pro4.0 (Axon, CA, USA). Results from duplicate spots and dye swap experiments were averaged, and the normalized intensity ratio for each transcript was subjected to informatics analysis to determine the influential genes involved in the malignant HCC transformation.

A combined parametric and non-parametric analysis was performed on the microarray profiles obtained. Statistical significance (*P*-value) for each gene is calculated based on a pair-wise permutation t-test using Significant Analysis for Microarray (SAM) and paired Wilcoxon signed rank test. Correction for multiple hypotheses testing has also been carried out using Bonferonni or False Discovery Rate analysis. To establish the significance of a gene, the combined *P*-value from SAM and Wilcoxon tests was averaged, and scored for precedence by ranking. Genes that ranked top 5% percentile (at $\geq$2.0-fold median up- or down-regulation)

were selected and further subjected to functional ontology analysis by Ingenuity Pathway Analysis (IPA; http://www.ingenuity.com/).

Table 3.1 Demographic information of 43 HCC patients studied by gene expression profiling

	HCC Patients (n=43)
Gender	
Male	35 (81.4%)
Female	8 (18.6%)
Age	
Median (quartiles)	58 (50-67)
HbsAg	
Positive	40 (93.0%)
Negative	3 (7.0%)
Underlying Liver Cirrhosis	
Present	37 (86.0%)
Absent	6 (14.0%)
AJCC Staging	
Stage T1	6 (14.0%)
Stage T2	23 (53.5%)
Stage T3	10 (23.3%)
Stage T4	4 (9.3 %)
No. of Lesions at Presentation	
Single	27 (62.8%)
Multiple	16 (37.2%)

3.2.2 Drugs

Doxorubicin was purchased from EBEWE Pharma Ges (Unterach, Austria), and stored at a concentration of 2mg/ml at 4°C. Paclitaxel (Taxol®) was obtained from Bristol-Myers Squibb (Princeton, NJ, USA), and stored at a concentration of 6mg/ml in 527mg of purified Cremophor EL and 49.7% dehydrated alcohol at -20°C. Docetaxel (Taxotere®) was obtained from Aventis Pharma SA (Paris, France), and stored at a concentration of 10mg/ml in 13% w/w ethanol at 4°C. The nanoparticle albumin-bound (*nab*)-paclitaxel (*nab*-paclitaxel, Abraxane®) was obtained from Abraxis BioScience (Los Angeles, CA, USA). Each vial of *nab*-paclitaxel supplied contains 100mg of paclitaxel, stabilized in 900mg of albumin. Upon reconstitution, 20ml of PBS was added to constitute a stock concentration of 5mg/ml *nab*-paclitaxel and stored at -20°C until use.

3.2.3 Cell culture

HCC cell lines used in this study were Hep3B, SK-HEP-1, and HKCl-9. They were cultured as described in Chapter 2, section 2.2.

3.2.4 Cell viability assay

Cell viability was measured by MTT Assay as described in Chapter 2, section 2.3. Cells were plated in 96-well plates at density of 3000 cells per well. Next day, paclitaxel, docetaxel and *nab*-paclitaxel were tested at different concentrations ranging from 0 to 40μg/ml for 48 hrs, while doxorubicin tested at concentrations

ranging from 0 to 150μg/ml for 48 hrs.

3.2.5 Immunofluorescence analysis

Cells plated on sterile 18×18 mm glass cover slip were allowed to adhere for 24 hrs prior to treatment with 5ng/ml *nab*-paclitaxel or medium for another 24 hrs. Cells were then fixed in 4% paraformaldehyde and incubated with anti-β-tubulin (Zymed, Invitrogen) at 1:100 dilution at 4°C overnight. Secondary antibody Alexa-598-coupled anti-mouse immunoglobulin (Molecular Probes, Eugene, OR, USA) was applied at 1:200 dilution. Cell nuclei counterstained in DAPI (Molecular Probes) were examined under a fluorescence microscope (Nikon EFD-3, Japan). Post-capture image analysis and processing of image stacks were performed using the analySIS software.

3.2.6 Flow cytometry analysis of cell cycle

Cell cycle distribution was measured after exposure to different concentrations of *nab*-paclitaxel for 12 hrs. The experimental procedures were described in Chapter 2, section 2.4.

3.2.7 TUNEL assay

TUNEL assay was conducted according to procedures of In-Situ Cell Death Detection Kit (Roche Applied Science, Mannheim, Germany). In brief, cells treated with different concentrations of *nab*-paclitaxel were fixed and incubated with

TUNEL reaction mixture for 1 hr at 37°C. Cell nuclei counterstained in DAPI were examined by fluorescence microscope (Nikon EFD-3, Japan). Percentage apoptotic cells were calculated based on at least four randomly fields (~200 cells in total).

3.2.8 siRNA knockdown

Pre-designed siRNA sequences including STMN1 si*GENOME SMART*pool (siSTMN1) and si*CONTROL* Non-Targeting siRNA (siMock) were purchased from Dharmacon RNA Technologies (Lafayette, CO, USA). All siRNAs were introduced into HCC cell lines using Lipofectamine 2000 (Invitrogen) according to manufacturer's instructions. Briefly, cells were incubated with 100nM siRNA (siSTMN1 or siMock). Six hours after transfection, medium was replaced by complete medium. The expression of STMN1 was monitored by Western blot analysis, which indicated a repressed expression for at least 3 days. Paclitaxel and *nab*-paclitaxel at concentrations ranging from 0 to 40μg/ml were applied 1 day post-siRNA transfections. MTT assay for cell viability was carried out at 48 hrs, and the IC_{50} values calculated as described.

3.2.9 Western blot analysis

Protein lysates were extracted from cells treated with *nab*-paclitaxel for up to 48 hrs and untreated control cells. Western blot analysis was performed as described in Chapter 2, section 2.5. Primary antibodies used included anti-STMN1 (1:1000 dilution), anti-PARP (1:1000 dilution) (Cell Signaling Technology, Beverly, MA,

USA), anti-GAPDH (1:10,000 dilution) (Millipore Corporation, Bedford, MA, USA). Peroxidase conjugated secondary antibodies were applied at 1:10,000 dilution for anti-GAPDH, and 1:2000 for other primary antibodies (Santa Cruz Biotechnology, Santa Cruz, CA, USA).

3.2.10 SK-HEP-1/Luc+ xenograft model and drug study

SK-HEP-1 luciferase stable clone was prepared by transfecting SK-HEP-1 cells with firefly luciferase expression vector and selected with 500μg/ml Geneticin (Gibco-BRL) for 4 weeks. Individual colonies were screened for bioluminescence activity using the Xenogen IVIS® imager (Alameda, CA, USA). Clones with stable luminescence expression were used for *in vivo* studies.

SK-HEP-1/Luc+ xenografts were developed according to the methods described in Chapter 2, section 2.6. 5×10^6 SK-HEP-1/Luc+ cells were used for subcutaneous inoculation. Drug treatments started on day 14 after tumor cells inoculation. Mice were randomly divided into 5 groups: PBS (n=13), *nab*-paclitaxel (n=14), paclitaxel (n=9), docetaxel (n=9) and doxorubicin (n=10). More mice were used for vehicle PBS group and *nab*-pacltaxel group. Since the two groups are most important groups to be compared, larger sample sizes were applied to minimize error. Based on the suggested dose of 30mg/kg (35mmol/kg) *nab*-paclitaxel in a previous study on multiple cancers, all drugs were given by intraperitoneal injection (i.p.) every two days for five times, at a dose of 35mmol/kg (*nab*-paclitaxel: 30mg/kg, paclitaxel: 30mg/kg, docetaxel: 28mg/kg, doxorubicin: 19mg/kg) (214). Tumor growth was

monitored twice weekly by *in vivo* bioluminescent imaging and by a digital caliper measurements using the formula of [(Length × Width^2)/2] for 24 days. For *in vivo* bioluminescent imaging, 150mg/kg D-luciferin were given by intraperitoneal injection (i.p.) and 10 min after luciferin injection, mice were anesthetized by isoflurane and tumor cell viability was measured by the Xenogen IVIS® imager.

3.2.11 Statistical analysis

The data was presented as mean ± SEM. Student's t-test, Kaplan-Meier survival curves (Logrank test) and one-way ANOVA analysis were performed using Graphpad Prism 3.0 software. Differences were considered statistically significant at $P<0.05$.

3.3 Results

3.3.1 Functional ontologies involved in HCC development

To facilitate biological interpretation of Gene Ontologies in the development of HCC, genes from the microarray dataset were first ranked and selected by evidence of significant differential expression according to statistical methods. Enriched differentially expressed genes obtained from SAM and Wilcoxon signed rank test were expected to be more robust that changing thresholds alone, and were subjected to analysis for the presence of functional networks involvement using IPA. The heat map diagram (Fig. 3.1A) illustrates the pattern of clustering across patient samples and genes. IPA analysis of ~ 1,000 significant known genes (top 5% percentile

changes, Table 3.2) suggested a few significant gene ontologies, which included cellular assembly and organization, cellular function and maintenance, cell death, cell cycle, cellular composition, drug and lipid metabolism and small molecules biochemistry (Fig. 3.1B). In particular, the cellular assembly and organization category was ranked to be the most significant event, where over-representations of microtubules associated genes such as STMN1 and TUBB4 were found (Fig. 3.1C).

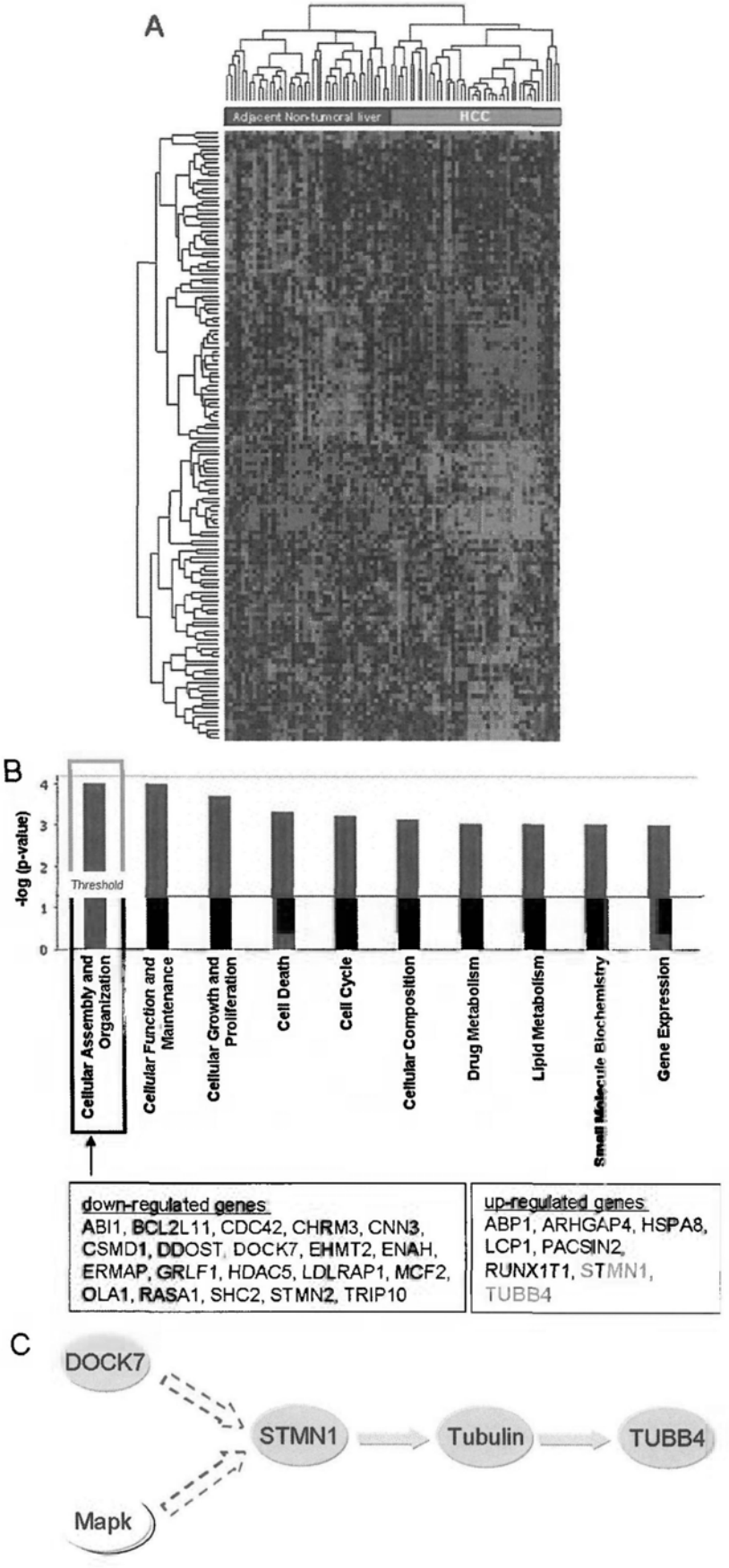

Figure 3.1 Functional ontologies involved in HCC development. A. gene

expression patterns were identified in 43 paired HCC tumors and adjacent non-tumoral livers. The top 649 genes (fold change > 2.0, see Table 3.2) are illustrated. Relative gene expression is color coded in which red represents high relative expression and green represents low relative expression in HCC tumors compared with adjacent non-tumoral livers. Patients are identified in the dendrogram across the top, whereas genes are represented by the dendrogram on the left. B. Ingenuity Pathway Analysis revealed 10 top ranked functional ontologies in HCC. The up-regulated and down-regulated genes involved in cellular assembly and organization are shown. C. The STMN1-Tubulin axis path is illustrated. Red color represents genes that are up-regulated, while green color denotes down-regulated genes.

Table 3.2 Up-regulated and down-regulated genes identified in 43 paired HCC tumors and adjacent non-tumoral livers (fold change > 2.0)

Symbol	Fold (T/TN)	Symbol	Fold (T/TN)	Symbol	Fold (T/TN)	Symbol	Fold (T/TN)
PHF3	0.012	DIP2B	0.161	CTRB1	0.219	TLK1	0.269
DDB1	0.019	JAG1	0.161	GAB2	0.219	IPW	0.269
SERTAD3	0.042	PFN2	0.163	DNALI1	0.220	NSMCE2	0.269
PSMA2	0.066	MS4A7	0.165	GAB2	0.222	WDR90	0.270
QKI	0.072	CSDC2	0.165	GEM	0.226	CIC	0.271
DYRK3	0.083	PPP1R12B	0.166	PIGM	0.228	STOML1	0.272
RNPS1	0.083	PTAR1	0.167	DOCK7	0.228	RNF169	0.273
OSTF1	0.085	ZFX	0.168	LOC220729	0.229	RAB11FIP3	0.274
EVI5L	0.091	TSHZ2	0.173	ZC3H12D	0.230	SPG7	0.274
MGAT4A	0.091	PCSK5	0.173	CMBL	0.230	NRM	0.275
RASGRF2	0.093	TM6SF1	0.173	ALDOB	0.232	DYRK4	0.275
SCRT1	0.095	CAMK2B	0.174	PGBD2	0.233	MARCH8	0.276
ACVRL1	0.096	CCDC14	0.175	ST8SIA4	0.234	CDC42	0.276
SULT1A1	0.096	REEP1	0.177	EIF1AY	0.236	IMMP2L	0.277
ZMYND8	0.099	RAMP1	0.178	YES1	0.236	BCAP31	0.278
ZNF317	0.099	DPM1	0.178	RBM38	0.236	APEX2	0.279
ANP32E	0.099	IQGAP1	0.182	STMN2	0.237	ZNF558	0.281
QSER1	0.102	ACSL1	0.183	BAP1	0.239	CNIH	0.282
TMED4	0.104	LDLRAP1	0.184	RASA1	0.240	ANKRD13D	0.282
SLC20A2	0.107	EHMT2	0.187	EPB41L3	0.240	MED19	0.283
PACS2	0.123	MAPRE2	0.187	GMFB	0.241	SVEP1	0.284
RNPEPL1	0.127	MUM1	0.188	GLUD1	0.247	CEP110	0.285
GTF2B	0.129	RPS6KB2	0.192	SERPINA3	0.247	C20orf11	0.286
DFNA5	0.131	DCK	0.192	NUP37	0.247	PKNOX2	0.287
DGCR9	0.131	ECHDC1	0.197	AP1GBP1	0.247	ZNF273	0.287
APBA2	0.132	SNX25	0.198	DIDO1	0.249	TOX	0.288
PPM1A	0.132	SLC5A9	0.198	TSPYL4	0.251	PRKAG2	0.290
AMFR	0.133	ATP6V0B	0.200	ADAMTS6	0.252	HLA-C	0.291
LIPC	0.133	ACHE	0.201	IFNAR2	0.252	VTI1B	0.291
CABLES2	0.134	SERPINB1	0.203	USP39	0.255	CSDA	0.292
MARK2	0.140	TAF11	0.203	ARHGEF3	0.255	SLA	0.293
C12orf47	0.140	CGGBP1	0.206	ELF4	0.255	ALAS2	0.294
ATP1A2	0.140	ATP1B2	0.206	DDOST	0.260	KCNE3	0.294
HSPC157	0.141	PSIP1	0.206	TMEM157	0.261	CD58	0.295
AGT	0.143	IGFBP7	0.207	TRIM24	0.261	AMD1	0.295
PGPEP1	0.147	RCL1	0.209	PLAT	0.262	WDR33	0.296
CACNA2D4	0.147	IWS1	0.210	FXR2	0.263	PTRF	0.296
PFKFB2	0.151	MMAA	0.212	MGST3	0.264	C12orf29	0.296
NBL1	0.154	TMEM176B	0.212	RET	0.265	PHF21A	0.297
ASB9	0.155	TOR2A	0.215	TMEM16D	0.267	C20orf20	0.297
BANF1	0.157	HNRPA2B1	0.218	PTPN3	0.268	PURB	0.298
C4orf18	0.157	ABI1	0.218	MLL	0.268	SGCB	0.298
VCAN	0.158	NAGLU	0.218	FOXM1	0.268	STIM2	0.300

Symbol	Fold (T/TN)	Symbol	Fold (T/TN)	Symbol	Fold (T/TN)	Symbol	Fold (T/TN)
ARL1	0.300	PC	0.339	NAP1L4	0.370	ZNF545	0.400
NEFL	0.300	RHD	0.340	S100B	0.371	PTGIS	0.400
PIN1	0.301	BCL2L11	0.341	TRIP10	0.371	GOT1	0.401
GPR162	0.301	SLC11A2	0.341	GLT25D1	0.372	SUPT6H	0.402
MLH1	0.302	PI4K2A	0.341	ACTR6	0.372	KDR	0.402
HDAC5	0.302	ME2	0.342	ZNF10	0.373	EHHADH	0.404
F5	0.303	WDR81	0.342	ALS2CR4	0.374	RHO	0.405
TCEB3	0.303	S100A4	0.344	C10orf132	0.374	TMCC1	0.406
ENO1	0.304	RXRG	0.345	TMEM56	0.375	SCGB3A2	0.406
ZNF462	0.304	PRG4	0.346	SEPT7	0.377	LRFN5	0.406
SOX10	0.304	STK4	0.346	RPS6KA3	0.378	C3orf23	0.406
CDC42SE2	0.304	TRAK2	0.347	FRMD4A	0.378	TRIM33	0.406
ESRRG	0.305	TMEM106B	0.347	ITGA8	0.378	MTCH2	0.406
SCN1A	0.306	TNS1	0.347	DDC	0.379	NFATC2IP	0.406
TRIP6	0.308	MLL3	0.350	SNX11	0.379	AKAP8L	0.409
UBE2T	0.308	KLF8	0.350	AADACL1	0.379	POLR2I	0.410
MVK	0.309	GPR146	0.350	CNIH3	0.382	RUNDC1	0.410
FMNL2	0.309	SEPT5	0.353	PPM1E	0.383	THRAP1	0.411
THOC3	0.311	CAP2	0.354	SNTA1	0.383	USP12	0.412
RKHD2	0.313	ZNF496	0.354	FCHO2	0.385	ADCY2	0.413
ENAH	0.315	CFL2	0.355	FBXW9	0.386	MARCH3	0.414
IGFBPL1	0.315	PLA1A	0.355	ART3	0.386	SLC35A4	0.414
SEMA6A	0.317	NOC3L	0.355	PCDHB4	0.386	SOBP	0.414
C9orf40	0.319	DCUN1D5	0.356	MITF	0.386	TFEB	0.414
CSGALNACT2	0.320	MAP1LC3B	0.356	ANXA5	0.387	COMMD8	0.414
BCL2L1	0.321	SPRY2	0.356	FOXJ3	0.387	UHRF2	0.414
SAFB	0.321	STAT5B	0.356	COL4A3BP	0.388	SF3A1	0.415
PTOV1	0.322	AHR	0.357	ZNF445	0.388	ITGB8	0.416
CHST12	0.323	IFT74	0.358	SH3YL1	0.388	BCR	0.416
ZNF783	0.325	MRPS10	0.359	CASP8	0.389	C16orf5	0.416
RFXDC2	0.326	C1orf96	0.359	RNASE6	0.390	CLCN4	0.416
VPS13A	0.327	TXNDC13	0.360	ADD1	0.390	BAT2D1	0.481
NEO1	0.327	SLC37A1	0.360	TRIM26	0.391	F8	0.481
KCNH2	0.327	ARHGAP15	0.361	VPS52	0.392	TBC1D15	0.482
CACNA1D	0.327	ANKRD28	0.361	HLA-C	0.392	PDE5A	0.482
CNN3	0.328	C9orf16	0.361	NPLOC4	0.392	ZIK1	0.417
FBN1	0.329	TBC1D14	0.362	NAP1L1	0.393	REEP2	0.417
CHRM3	0.331	PPP2R2D	0.363	LBH	0.393	CASQ2	0.418
FNBP4	0.332	CCT3	0.363	TRAPPC5	0.394	GOLPH3L	0.419
ERBB3	0.333	LIAS	0.365	LASS6	0.395	LYPD1	0.419
POU2F2	0.333	CDKN2AIP	0.366	LDB1	0.395	NVL	0.420
MCF2	0.335	STBD1	0.366	TSC1	0.395	PPIE	0.420
MYL4	0.336	ITGA7	0.367	LMBR1	0.396	SIAH2	0.421
CDC27	0.337	CENTA1	0.368	SLC36A1	0.397	C9orf164	0.422
C1orf51	0.337	NAV3	0.368	DPP4	0.398	SNAPC3	0.422
CBX7	0.338	CTDP1	0.369	UBE2F	0.399	ETNK1	0.422
C16orf57	0.339	RD3	0.369	SULT4A1	0.399	SCD5	0.423

Symbol	Fold (T/TN)	Symbol	Fold (T/TN)	Symbol	Fold (T/TN)	Symbol	Fold (T/TN)
FHOD1	0.424	GDAP1	0.443	SPTLC3	0.462	PDE5A	0.482
ZNF354A	0.424	POPDC2	0.443	ZNF217	0.463	Slc29a4	0.482
ELOF1	0.425	CYGB	0.445	UST	0.464	CNNM4	0.483
ZNF207	0.426	ADARB1	0.445	DLD	0.464	PLS3	0.483
SLC25A29	0.427	SPTB	0.446	PAK6	0.464	ANKRD54	0.484
PAGE4	0.427	MED8	0.446	CLASP1	0.467	KCNS1	0.484
ZNF706	0.428	SEC14L1	0.447	THEX1	0.467	SUDS3	0.485
HNRPH1	0.428	ZAK	0.447	MMP19	0.468	NOTCH4	0.486
GRLF1	0.429	UBXD4	0.447	MAP3K7IP1	0.468	DEXI	0.486
PSMD1	0.430	FCN3	0.448	IMP3	0.469	PELO	0.487
SRPR	0.431	GTPBP9	0.448	NR2F2	0.469	PPP1R2	0.487
GSDML	0.431	SPAG7	0.449	TBC1D23	0.471	GPLD1	0.489
MPND	0.431	DDAH1	0.449	ADAM12	0.472	HEATR5B	0.489
MMP2	0.432	SOD1	0.451	COQ9	0.472	PEG3	0.489
CLMN	0.432	PSMC2	0.451	NCOA3	0.475	SLC25A16	0.489
TTC21B	0.432	C18orf1	0.452	CCL2	0.475	SKIV2L2	0.490
CSMD1	0.434	USPL1	0.452	VPS4B	0.475	COL18A1	0.491
C12orf32	0.437	PPRC1	0.453	RNF34	0.475	C9orf7	0.491
PLEK	0.437	MAF	0.453	ERMAP	0.476	SNAPC3	0.494
ACOX1	0.437	ECE1	0.454	TBRG4	0.477	TMEM53	0.494
LRRC8D	0.438	PTBP1	0.454	TRIM11	0.477	LRRC8C	0.494
P11	0.438	TSSC4	0.454	VAV1	0.477	CACYBP	0.494
DAB1	0.438	VPS13B	0.456	HPCAL4	0.477	NGRN	0.494
PBX1	0.440	ATP5F1	0.457	AK1	0.478	TNRC4	0.494
SLC30A10	0.440	FSTL3	0.457	BICD1	0.479	RNF214	0.495
AMDHD1	0.440	UBFD1	0.457	DAXX	0.480	THAP10	0.495
ZNF533	0.441	CHD2	0.457	PAPPA	0.480	FRAP1	0.495
SHC2	0.442	ADD2	0.458	SPOCK1	0.480	ANGEL1	0.496
WDR7	0.442	COL11A1	0.458	SCN8A	0.480	ARMC1	0.496
SEPT3	0.442	VAV2	0.459	KTELC1	0.481	YBX1	0.497
SMARCD2	0.443	STXBP5	0.459	BAT2D1	0.481	BMP2K	0.498
NNMT	0.443	DUSP3	0.459	F8	0.481	CEP250	0.498
TMEM80	0.443	TFEB	0.460	TBC1D15	0.482	MT1G	0.499

Symbol	Fold (T/TN)	Symbol	Fold (T/TN)	Symbol	Fold (T/TN)	Symbol	Fold (T/TN)
CEP110	2.005	MT1G	2.301	SETD1A	2.793	PPHLN1	3.796
SLC11A2	2.013	ASXL2	2.315	B4GALT3	2.807	ST6GAL1	3.850
C17orf63	2.014	DYNC1I2	2.316	STMN1	2.813	ATP2B4	3.926
GABRG2	2.016	RASL12	2.316	YAF2	2.817	CDC42BPA	4.076
RAD18	2.020	RBM15B	2.326	GHDC	2.855	PPFIA4	4.274
C12orf51	2.022	SPTLC3	2.328	SNRK	2.863	FUT4	4.369
RPL41	2.025	TRIM3	2.329	TRIM21	2.883	COL5A3	4.394
ARMCX3	2.032	H2AFV	2.338	STMN1	2.893	NXPH1	4.402
RIOK3	2.037	ADD3	2.346	EGR3	2.902	RAB24	4.470
IFNAR1	2.041	SF3B1	2.351	C13orf8	2.905	TTC3	4.643
SLC29A1	2.042	ZNF294	2.386	SAE1	2.912	RHBDF1	4.775
TUBB4	2.046	FOXN2	2.400	SH3YL1	2.918	MMP11	4.816
CXCL9	2.063	CARD10	2.400	PACSIN2	2.926	SMARCA1	4.837
MRPL18	2.071	GSTO1	2.412	CSNK2B	2.945	PCDH19	5.129
ABP1	2.079	FDPS	2.413	ZNF641	2.979	MTUS1	5.332
SDK1	2.082	GARNL3	2.422	CS	2.979	KCNC2	5.855
C9orf78	2.084	CMAS	2.422	PIGQ	3.038	STK11IP	5.879
GSTM4	2.098	TACC1	2.433	KIAA1684	3.041	ZNF226	5.930
SLC13A4	2.108	SERPINA5	2.444	PLAGL1	3.069	SPP1	6.676
UBAP2L	2.126	CPNE4	2.499	ITGA3	3.071	CSK	6.752
MPST	2.167	TRIM10	2.505	H19	3.071	THOP1	7.212
ZNF621	2.168	NT5DC2	2.507	SLC25A17	3.090	CSNK2B	7.310
ZCCHC14	2.174	TLK2	2.541	TMCO6	3.141	RUNX1T1	7.457
CD79B	2.175	PNPLA6	2.542	ARHGAP4	3.151	VRK2	7.514
ZNF566	2.177	SMU1	2.546	GABBR2	3.161	RANGAP1	7.692
HSPA8	2.184	CAMK2G	2.589	EXT1	3.182	N4BP1	8.159
ATXN2	2.190	PBXIP1	2.592	C10orf137	3.220	CRAMP1L	9.027
PEX3	2.194	CANX	2.614	ZC3H12C	3.240	SCHIP1	9.132
MED10	2.197	FSTL1	2.642	GATA4	3.247	TDRD10	9.156
C4orf30	2.200	SIAH1	2.662	C11orf71	3.265	DIP2B	9.389
TSHZ2	2.200	RNF157	2.674	FGG	3.298	EEF1A1	10.221
RNF19	2.207	PFDN2	2.705	LCP1	3.325	SLC16A5	10.782
SATB1	2.210	DBNDD2	2.710	C13orf27	3.504	ME3	11.172
ZNF33B	2.211	CPEB4	2.722	PCSK9	3.507	DENND4A	11.485
SF3B1	2.230	TMEM155	2.743	ZNF613	3.507	CCNDBP1	12.494
RLF	2.231	SLC4A4	2.745	IFIT1L	3.610	GTF2H1	16.012
ZKSCAN1	2.248	CHN1	2.747	ARMCX1	3.648	TAP1	17.838
SSR1	2.257	PLS3	2.751	ZNRF1	3.669	NDUFB4	27.762
TIMM22	2.266	MDN1	2.752	STX16	3.683	ABCC10	39.991
REPS1	2.272	NOC4L	2.771	CFP	3.739		

3.3.2 Cytotoxic effect of taxanes on HCC cells

The effect of microtubule targeting drugs, paclitaxel, docetaxel and *nab*-paclitaxel was first evaluated, on HCC cell lines that displayed elevated STMN1 expressions, which would infer the presence of deregulated microtubule organization (Fig. 3.2B). A high sensitivity towards the taxane-based drugs was generally found in Hep3B, SK-HEP-1 and HKCI-9 compared to doxorubicin, a chemotherapeutic agent that is widely used for many cancers, including HCC (Fig. 3.2A). Remarkably, *nab*-paclitaxel showed the highest potency with a lowest effective dosage found in all 3 cell lines tested. The IC_{50} obtained on *nab*-paclitaxel ranged from 0.29±0.02nM to 10.42±1.37nM, which was about 44-fold to 1082-fold less than doxorubicin (IC_{50} value ranged from 105.95±10.58nM to 455.93±35.72nM) and 7-20 fold less than standard paclitaxel (IC_{50} value ranged from 3.16±0.45nM to 74.22±10.05nM) (Fig. 3.2C).

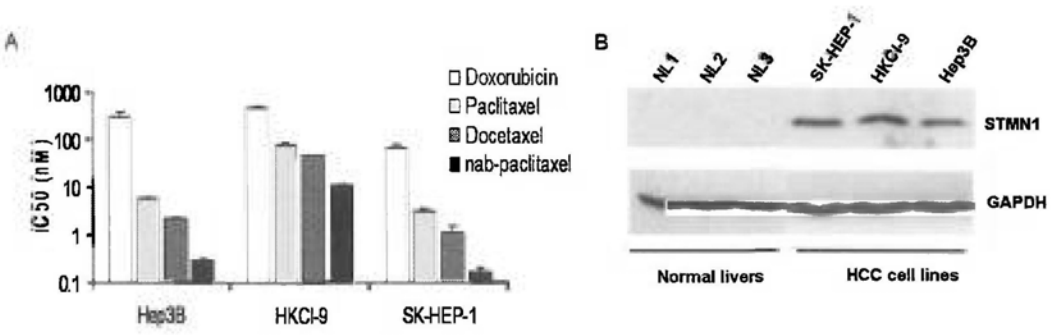

C

Drugs (IC50, nM)	Hep3B	HKCI-9	SK-HEP-1
doxorubicin	314.03±74.46	455.93±35.72	67.25±2.40
paclitaxel	5.80±0.33	74.22±10.05	3.16±0.45
docetaxel	2.10±0.20	45.00±1.54	1.11±0.14
nab-paclitaxel	0.29±0.02	10.42±1.37	0.16±0.05
Fold Change (doxorubicin vs nab-paclitaxel)	1082	44	420

Figure 3.2 Cytotoxic effects of taxanes and doxorubicin in HCC cell lines. A. Cell lines Hep3B, HKCl-9 and SK-HEP-1 were treated with increasing concentrations of doxorubicin, paclitaxel, docetaxel and *nab*-paclitaxel for 48 hrs. Effect on cell viability was investigated by MTT, and the IC_{50} values determined. Experiments were repeated three times and expressed as the mean ± SEM. B. The expression of STMN1 in normal livers and HCC cell lines was detected by western blot analysis. C. The IC_{50} value of drugs tested in HCC cell lines listed are indicated.

3.3.3 *nab*-Paclitaxel treatment induced cell cycle blockade and apoptosis

It is known that paclitaxel induces mitotic arrest through stabilizing microtubule polymerization (217, 218). A similar effect with *nab*-paclitaxel was observed, where a higher degree of microtubule polymerization was found in the treated cells (Fig. 3.3A and B). The effect of *nab*-paclitaxel on cell cycle was also studied. In both Hep3B and SK-HEP-1, flow cytometry analysis indicated that an increase in the G_2/M population was found with increasing concentrations of *nab*-paclitaxel applied, suggesting a dose-dependent cell cycle arrest ($P<0.05$; Fig. 3.4B). Flow cytometry profile also showed a sub-G_1 fraction appearing after the treatment with *nab*-paclitaxel (Fig. 3.4A). The presence of apoptotic cells were further confirmed in SK-HEP-1 and Hep3B by TUNEL analysis, which indicated the number of TUNEL positive cells corresponded to the amount of *nab*-paclitaxel used ($P<0.001$; Fig. 3.4C and D). The cleavage of nuclear protein PARP was determined by monitoring the presence of 89kDa cleaved product. PARP cleavage became evident at 12 hrs after treatment and gradually increased over 48 hrs (Fig. 3.4E).

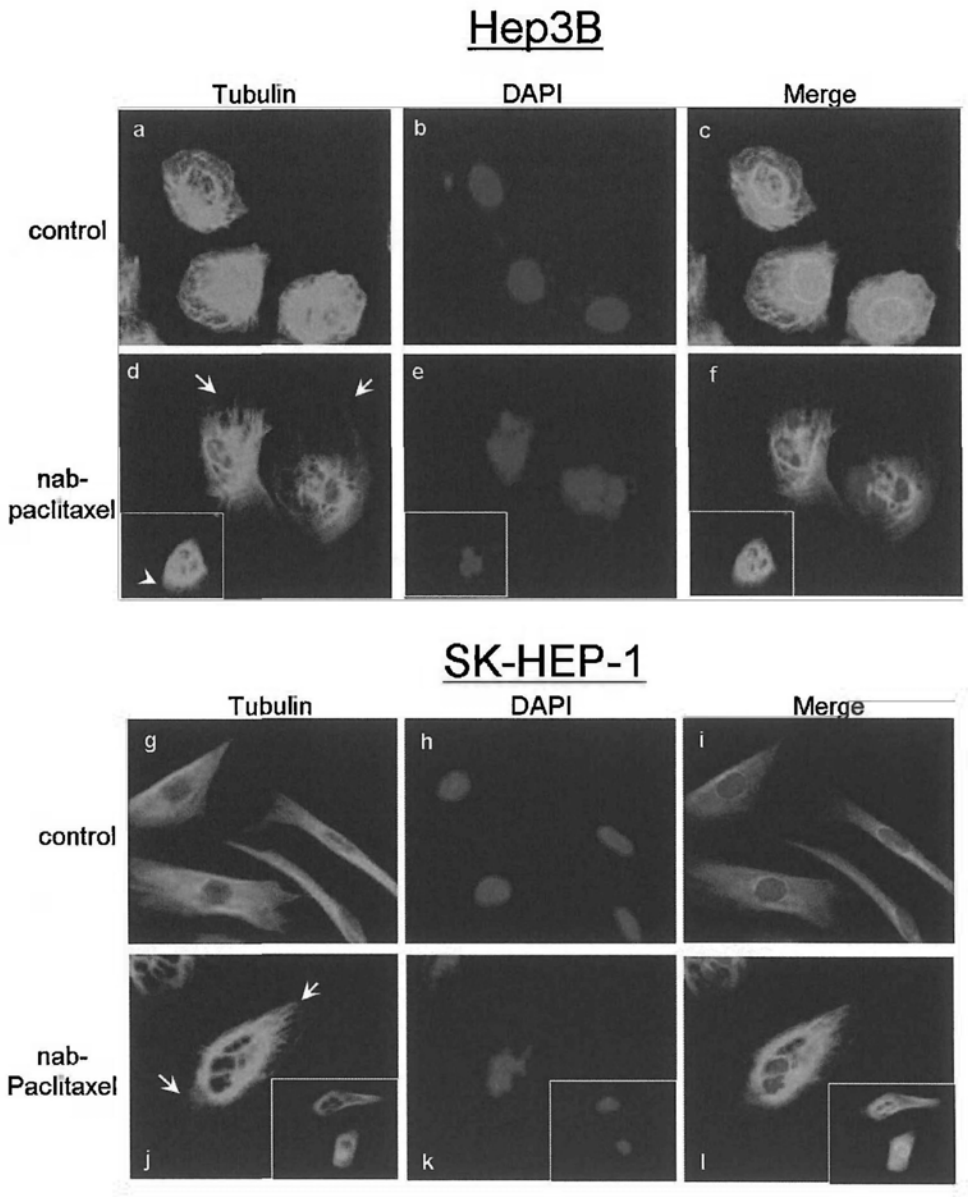

Figure 3.3 Microtubule morphology in Hep3B and SK-HEP-1 cells treated with *nab*-paclitaxel. Cells treated with 5ng/ml *nab*-paclitaxel for 24 hrs were fixed in 4% paraformaldehyde, and stained for β-tubulin (red). Nuclei were counterstained with DAPI (blue). (a to c), Hep3B control; (d to f), *nab*-paclitaxel treated Hep3B. (g to i), SK-HEP-1 control; (j to l), *nab*-paclitaxel treated SK-HEP-1. Inserts in figures (d to f) and (j to l) are captures from a different field from the same slide. *nab*-Paclitaxel treated cells showed a higher degree of microtubule polymerization (arrows). Representative images from two independent experiments are shown.

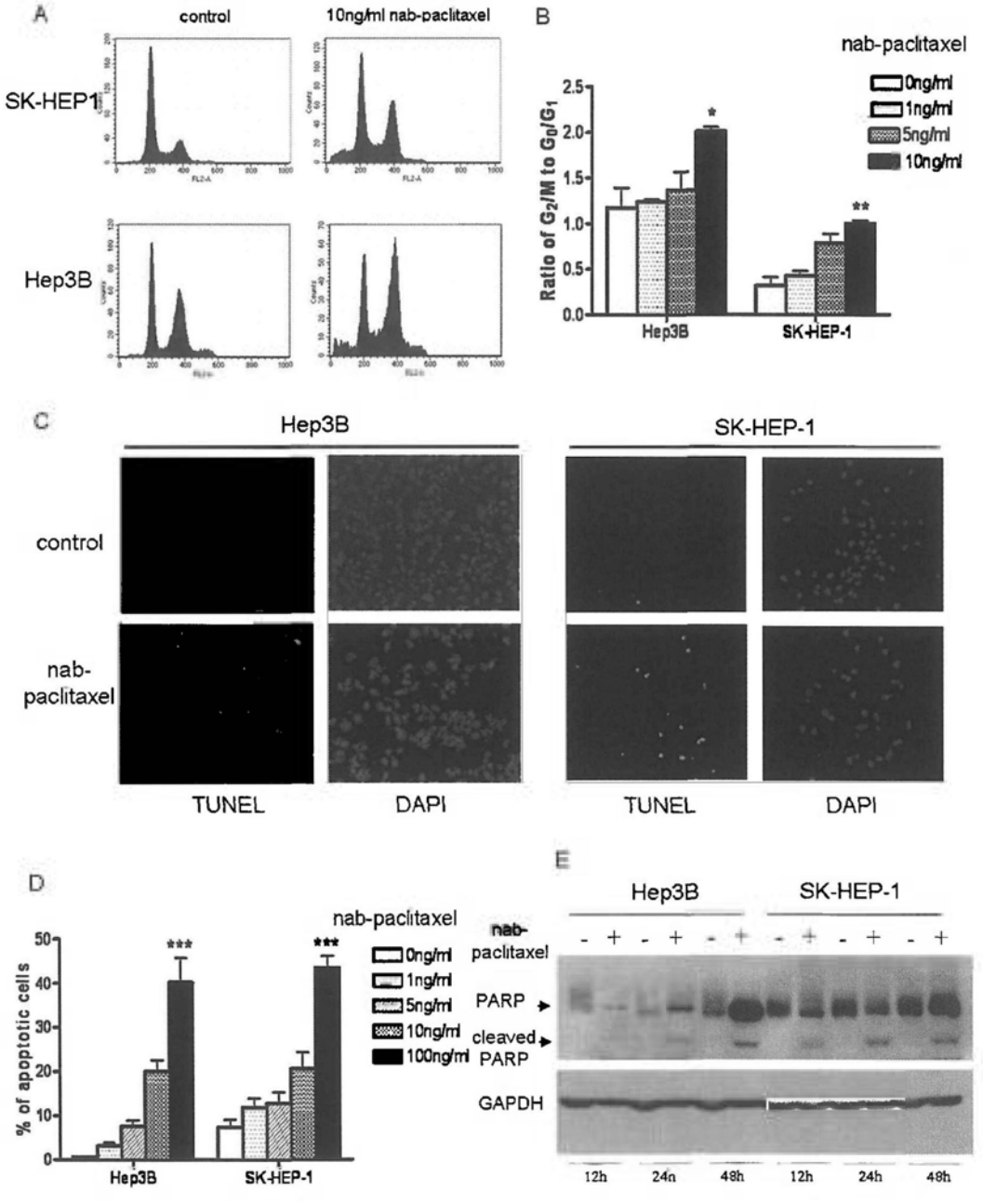

Figure 3.4 *nab*-Paclitaxel treatment induced cell cycle blockade and apoptosis.

A. Cell cycle profile of *nab*-paclitaxel treated Hep3B and SK-HEP-1. Cells treated with differing concentrations of *nab*-paclitaxel for 12 hrs were harvested, stained with PI, and analyzed by flow cytometry. B. Ratio of G_2/M to G_0/G_1 populations in Hep3B and SK-HEP-1 in response to varying concentrations of *nab*-paclitaxel (One-way ANOVA, $*P<0.05$, $**P<0.01$ vs 0ng/ml group). C. TUNEL analysis in

Hep3B and SK-HEP-1 cells showed increase number in apoptotic cells (green) after treatment of *nab*-paclitaxel at 100ng/ml for 48 hrs. Nuclei counterstained with DAPI. Images shown are representative of two independent experiments. D. Percentage of apoptotic cells increased with increasing concentrations of *nab*-paclitaxel applied (One-way ANOVA, *** $P<0.001$ vs 0ng/ml group). E. Western blot for PARP in Hep3B and SK-HEP-1 treated with *nab*-paclitaxel showed increasing amount of cleaved PARP with time.

3.3.4 Effect of *nab*-paclitaxel on *in vivo* xenograft growth

SK-HEP-1/Luc+ cells were subcutaneously inoculated into BALB/c nude mice and the anti-tumor effects of taxanes and doxorubicin *in vivo* were examined. Developed xenograft was measured for tumor size on the first day of treatment and twice weekly thereafter by IVIS imaging and caliper measurements. Using non-toxic dose of 12mmol/kg, *nab*-paclitaxel moderately inhibited the tumor growth, but other drugs showed little effect on the tumor growth (Supplementary Fig. 3.1). Therefore, the suggested dose of 35mmol/kg was used. Figure 3.5A showed the percentage change of tumor size in each treatment group with time. The control PBS group showed a gradual increase in tumor size during the study. While each treatment group showed a reduction in tumor size, the toxicities from doxorubicin, paclitaxel and docetaxel were particularly severe, which resulted in significant weight loss and deaths among the tested mice within 3 injections (Fig. 3.5B and C). Although weight loss was also observed with *nab*-paclitaxel injection, it was least severe and the mice were generally able to re-gain body weight after the last injection on Day 9. The anti-tumor effect of *nab*-paclitaxel was highly significant with considerable inhibition on tumor sizes compared to control group (P=0.0007). Moreover, more than 60% of mice survived to the end of experiments (Fig. 3.5B).

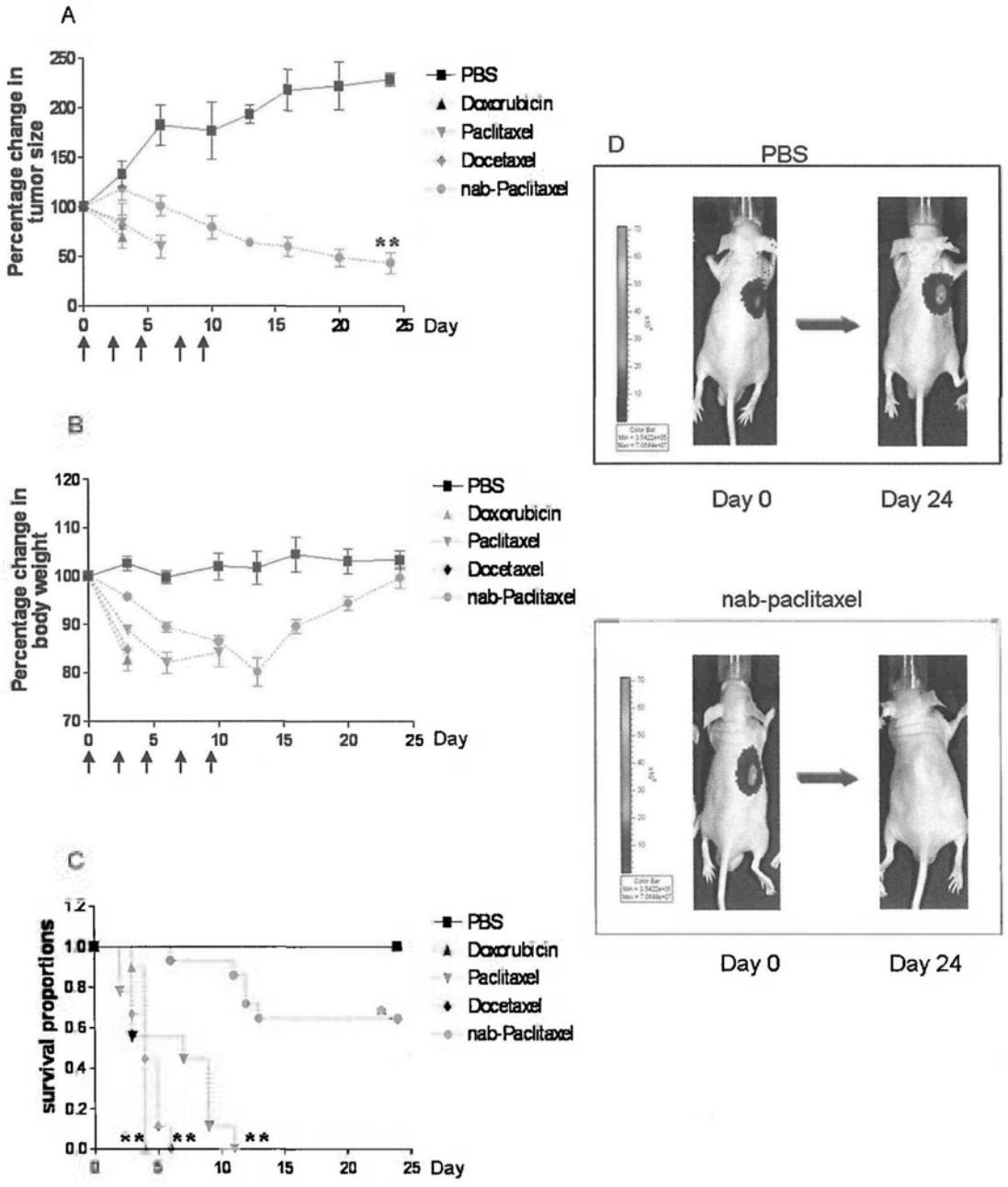

Figure 3.5 Effect of *nab*-paclitaxel on HCC tumor growth *in vivo*. SK-HEP-1/Luc+ cells (5×10^6) were injected subcutaneously into male BALB/c nude mice (PBS, n=13; *nab*-paclitaxel, n=14; paclitaxel, n=9; docetaxel, n=9; doxorubicin, n=10). Two weeks after tumor inoculation, mice received intraperitoneal injection of drugs (35mmol/kg) every two days for five times. A. Tumor growth was monitored and quantified twice weekly. A significant difference

between the vehicle group and *nab*-paclitaxel treated group was observed at the end of observation (paired t-test, $^{**}P<0.01$ vs PBS group). Animals on other treatment groups died within 3 injections. Arrows indicated time of drug injection. B. Percentage change in body weight of mice from drug treatments. C. Survival curve was plotted according to the mice status during experiments. A significant difference between the vehicle group and drug treated groups was observed (Logrank test, $^{*}P<0.05$, $^{**}P<0.01$ vs PBS group). D. IVIS images of representative mice of control and *nab*-paclitaxel treated are shown.

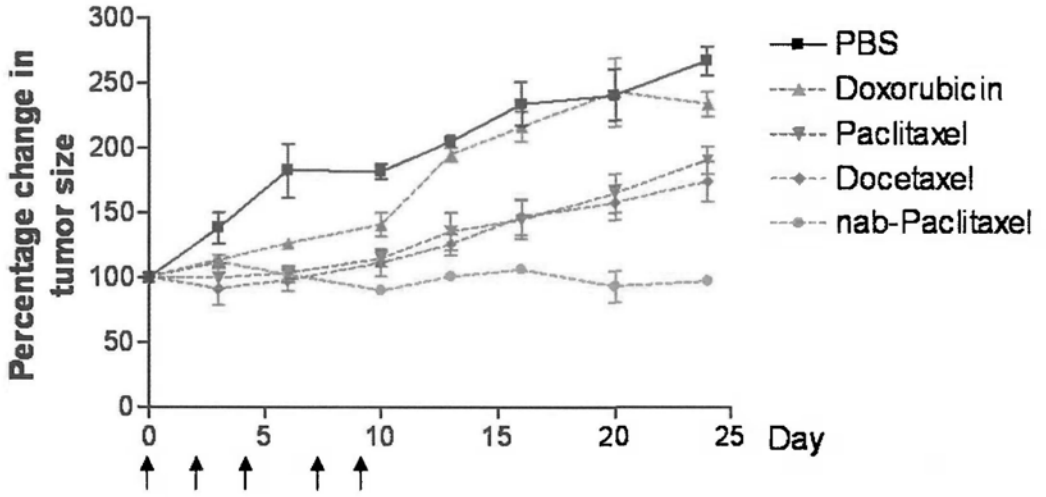

Supplementary Figure 3.1 Effect of taxanes and doxorubicin with non-toxic dosage on HCC tumor growth *in vivo*. SK-HEP-1/Luc+ cells (5×10^6) were injected subcutaneously into male BALB/c nude mice ($n = 5$ for each group). Two weeks after tumor inoculation, mice received intraperitoneal injection of drugs (12mmol/kg) every two days for five times. Tumor growth was monitored and quantified twice weekly. Arrows indicated time of drug injection.

3.3.5 STMN1 knockdown enhanced sensitivity to taxane drugs

Silencing of STMN1 has been shown to promote microtubule polymerization (219). The possible synergistic effect of STMN1 knockdown and microtubule-stabilizing drugs was hence examined in HCC. Figure 3.6A showed the STMN1 protein level in Hep3B after siRNA knockdown on day 1 and day 3. Specific STMN1 knockdown in Hep3B showed ~ 40% decrease in cell viability compared to mock on Day 3 post-transfection (Fig. 3.6B). In the combinatory study with taxanes, Hep3B transfected with siSTMN1 was 7.7-fold more sensitive to *nab*-paclitaxel (IC_{50}, 0.04±0.004nM vs 0.31±0.04nM) and 2.7-fold more sensitive to paclitaxel (IC_{50}, 1.95±0.28nM vs 5.17±0.06nM) (Fig. 3.6C). In contrast, knockdown of STMN1 had no effect on the sensitivity of doxorubicin, a drug that does not target the microtubule.

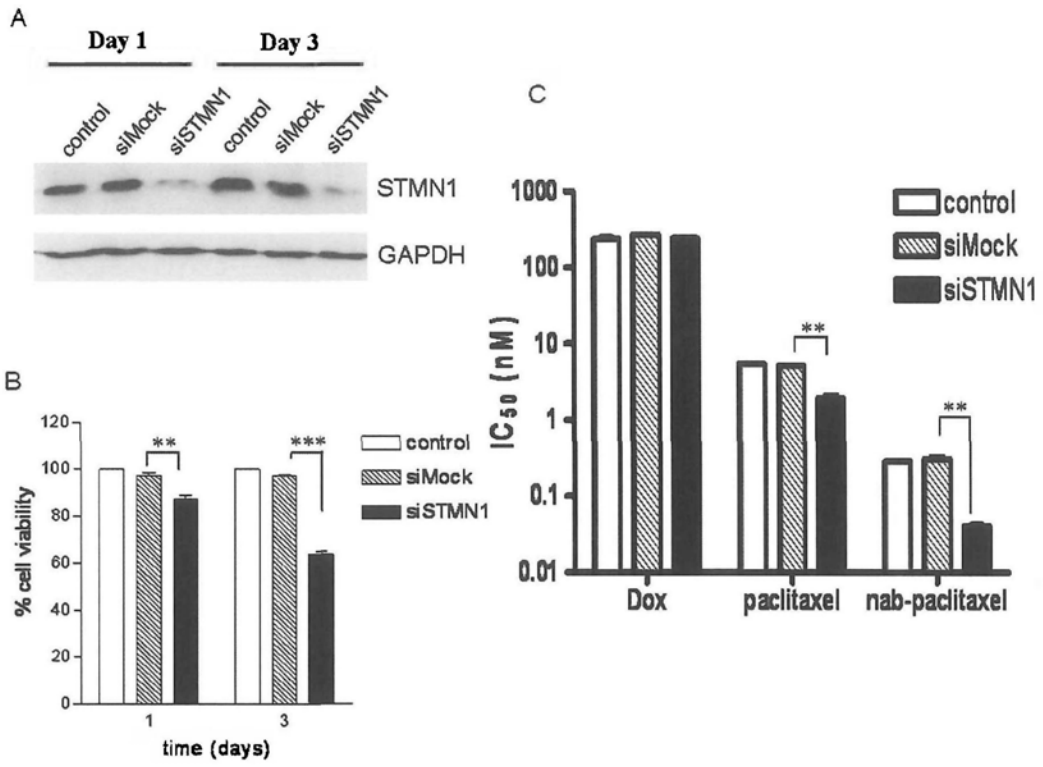

Figure 3.6 Effect on drug sensitivity following silencing of STMN1 gene expression. A. Level of STMN1 at day 1 and day 3 after siRNA knockdown. STMN1 expression was determined by western blot. Images are representative of three independent experiments. B. Silencing of STMN1 inhibited Hep3B cell viability by ~40% on day 3. Data are expressed as means ± SEM of three independent experiments (t-test, ** $P<0.01$, *** $P<0.001$ vs siMock group). C. Silencing of STMN1 expression sensitized STMN1-overexpressing cells to anti-microtubule drugs. Hep3B cells transfected with siSTMN1 were treated with doxorubicin, paclitaxel and *nab*-paclitaxel for 48 hrs. Distinct synergistic effect was suggested with *nab*-paclitaxel. Results shown represent mean ± SEM from 2 or more independent experiments (t-test, * $P<0.05$, ** $P<0.01$ vs siMock group).

3.4 Discussion

In this study, microarray profiling was performed for paired HCC tumors and adjacent non-tumoral livers in an effort to define deregulated functional ontologies that are associated with the development of HCC. Enriched differentially expressed genes obtained from SAM and Wilcoxon signed rank test were subjected to pathway analysis using IPA. Using this approach, the cellular assembly and organization through the microtubule functional networks was ranked to be the most significant cellular event in HCC. This finding is consistent with several earlier reports on expression profiling of HCC, which also suggested the microtubule-based processes and microtubule cytoskeletal organizations to be important biological and cellular components in HCC (157, 158). In line with the present finding, other profiling studies also identified the microtubule regulatory gene STMN1 to be commonly up-regulated in HCC (220, 221). Collectively, these investigations provide a rationale for targeting the microtubule in HCC. However, to my knowledge, only a few studies have reported on the use of anti-microtubule agents as a therapeutic strategy in HCC (222, 223). In this study, the effects of microtubule stabilizing taxanes in preclinical HCC models were hence examined.

Taxanes are known to bind microtubules polymers and stabilize microtubule in tumor cells, thereby arrest cells in G_2/M and promote cell death by suppressing microtubule dynamics (210, 224). Paclitaxel and docetaxel have shown significant clinical activities in various solid tumors, such as breast, ovarian, and prostate cancers; and effectiveness in preclinical study models of non-small cell lung cancer,

head and neck cancer and esophageal cancer (211-213). Because of their low aqueous solubility, organic vehicles such as polyoxyethylated castor oil (Cremophor® EL), polysorbate 80 (Tween 80) and ethanol have been used to formulate these drugs, but these solvents are also directly associated with severe toxicity and hypersensitivity reactions (163, 164). Pre-medication of steroid and anti-histamine is required to minimize the risk of hypersensitivity reaction but severe or even fatal hypersensitivity reaction may still occur (224, 225). The lyophilized formulation of *nab*-paclitaxel comprising of albumin and paclitaxel is reconstituted in 0.9% NaCl and forms a colloidal suspension during administration. Since its formulation is devoid of any solvents or ethanol (165), *nab*-paclitaxel has much less treatment-related toxicity. In comparing the effects and toxicity of paclitaxel and docetaxel with *nab*-paclitaxel, this study has shown that paclitaxel and docetaxel are more effective than doxorubicin, but *nab*-paclitaxel has exhibited the highest efficacy in inhibiting cell viability with the lowest IC_{50} consistently determined in HCC cell lines. *nab*-Paclitaxel induces G_2/M arrest through microtubule polymerization that results in apoptosis. In the *in vivo* study, an equivalent molar concentration of *nab*-paclitaxel along with paclitaxel, docetaxel and doxorubicin has been used. The present data suggests that *nab*-paclitaxel is the most effective cytotoxic agent with maximum tolerance in xenograft model.

In defining the cellular assembly network in HCC, it was also found that the microtubule regulatory gene, *STMN1*, was significantly over-expressed. STMN1 is a microtubule-destabilizing factor that plays important role in controlling cellular

proliferation by promoting microtubule depolymerization (226-229). Over-expression of STMN1 has been reported for various types of tumors such as leukemia, breast cancer, ovarian cancer and HCC (230-232). As STMN1 is a microtubule-destabilizing factor, further experiment was conducted to assess if the knockdown of STMN1 expression could provide a synergistic effect with *nab*-paclitaxel treatment in HCC. Knockdown of STMN1 expression readily reduced cell viability by about 40% in Hep3B. More significantly, suppression of STMN1 could sensitize HCC cells to *nab*-paclitaxel by ~ 8-fold. In line with this finding, Alli *et al* demonstrated that STMN1 over-expression could reduce sensitivity to paclitaxel treatment in breast cancer cell line (233). Nevertheless, knockdown of STMN1 did not seem to have altered sensitivity of HCC cells to doxorubicin, which is mainly a DNA-targeting drug. These results implied that treatment strategy targeting both microtubule and STMN1 could enhance therapeutic effects on HCC cells. In this context, the specific reduction of STMN1 expression, for example, by small molecules that inhibit STMN1 bioactivity or ribozyme-mediated knockdown approaches, may offer novel therapeutic options for HCC patients. Recently, it has been reported that STMN1 might be a molecular target of two xanthones, gambogic acid and gambogenic acid (234). The use of *nab*-paclitaxel alone or in combination treatment using gambogic acid or gambogenic acid may hold promises as novel treatment options in HCC patients and warrants for further clinical investigations.

In conclusion, the new nanoparticle conjugated form of paclitaxel, *nab*-paclitaxel,

appeared to be a safe and effective cytotoxic agent for HCC treatment. However, as mentioned above, studies have demonstrated a noticeable degree of resistance to most conventional microtubule targeting agents, including paclitaxel, docetaxel and vinblastine, for HCC treatment in clinical practice. Recent studies have suggested that activation of some signaling pathways may contribute to chemo-resistance in HCC. Among these, activation of the PI3K/Akt/mTOR pathway has been shown to contribute to resistance to many chemotherapies, including microtubule targeting agents, and this combined targeting of this pathway and the microtubule warrants for further investigation.

Chapter 4: Dual Targeting of mTOR and the Microtubule Using Temsirolimus and Vinblastine Results in Marked Anti-tumor Activity in Hepatocellular Carcinoma

4.1 Introduction

The PI3K/AKT/mTOR signaling pathway has been found to be dysregulated (or activated) in HCC (87, 88). In particular, abnormal activation of mTOR occurs in about 45% of HCC and its over-expression is associated with poor prognosis (87, 90), suggesting mTOR to be a potential therapeutic target for HCC treatment. mTOR is a key molecule in the PI3K/AKT/mTOR signaling pathway and plays a critical role in controlling cell proliferation and survival. The downstream targets of mTOR include ribosomal p70S6 kinase and the eukaryotic initiation factor eIF4E binding protein (4E-BP1), both of which are important in the control of cell cycle, cell growth and protein synthesis. Inhibition of mTOR has been shown to be effective in inhibiting tumor cell growth in various cancers, including HCC in both preclinical and clinical settings (122, 126, 235-238). One noticeable effect of mTOR inhibition has been a delayed growth of tumors (but not eradication) upon treatment (239). This is because mTOR inhibitors are cytostatic but not cytotoxic as it mainly inhibits cell proliferation by arresting cancer cell cycle progression at G_1 phase, rather than directly inducing apoptosis (239, 240). This cytostatic activity of mTOR targeting may limit its use as a single agent for anti-cancer treatment. It is anticipated that combination of an mTOR inhibitor and a cytotoxic agent may represent a more effective therapeutic regimen for anti-cancer treatment. In fact,

inhibition of mTOR has been shown to enhance the anti-tumor activity of a broad range of cytotoxic chemotherapies including cisplatin, doxorubicin, paclitaxel, carboplatin, dexamethasone, mitoxantrone and docetaxel in many types of human cancers (150-153).

Recently, gene expression profiling studies have revealed that microtubule-related cellular assembly and organization is the most crucial cellular event in HCC development (157, 158, 241), suggesting that microtubule is an important therapeutic target for HCC. Microtubule targeting agents are compounds which bind to soluble tubulin and/or directly to tubulin in the microtubules, thus affecting microtubule dynamics. These agents exert anti-mitotic activity and inhibit cell proliferation by inducing cell cycle arrest and apoptosis. The study described in Chapter 3 has demonstrated that *nab*-paclitaxel, a microtubule targeting agent, can significantly inhibit cell growth in both *in vitro* and *in vivo* models of HCC, thus supporting the crucial role of microtubule in HCC cell proliferation (241). At the same time, a few recent studies have indicated that the PI3K/Akt/mTOR signaling pathway may also be associated with resistance to taxanes and other microtubule targeting agents, in addition to its involvement in tumor cell growth/survival (27, 28).

In this study, it is postulated that combined targeting of the mTOR and the microtubule in HCC may result in better anti-tumor efficacy than single agents alone. To test this, the anti-tumor potency of temsirolimus, an mTOR inhibitor, either alone or in combination with vinblastine, a microtubule destabilizing agent, was

investigated in both *in vitro* and *in vivo* HCC models. The anti-tumor mechanism of this novel combination was also examined.

4.2 Materials and Methods

4.2.1 Drugs

Temsirolimus (CCI-779/Torisel®) was obtained from Wyeth (Monmouth Junction, NY, USA), and dissolved in DMSO at a stock concentration of 100mM and stored at -20°C. Vinblastine sulfate (DBL) was obtained from Hospira (Wellington, New Zealand), and stored at a concentration of 1mg/ml in 0.9% sodium chloride at 4°C.

4.2.2 Cell culture

HCC cell lines used in this study were Hep3B, HepG2, Huh7, PLC/PRF/5 and SNU398. They were cultured as described in Chapter 2, section 2.2.

4.2.3 Cell viability assay

Cell viability was measured by MTT Assay as described in Chapter 2, section 2.3. Cells were plated on 48-well plates at density of 8000-18000 cells per well. Next day, either vehicle (DMSO) or increasing concentrations of temsirolimus (ranging from 1nM to 100μM) was added to HCC cells for 24 hrs and 48 hrs. For combination treatment, cells were treated with increasing concentrations of temsirolimus and 1nM of vinblastine for 24 hrs.

4.2.4 Construction of expression plasmids and transfection

The full length survivin was generated by RT-PCR using total RNA extracted from Huh7 cells. An HA-tag was introduced into the N-terminal of survivin by subcloning into the pcDNA3-HA vector (provided by Dr. Eugene Chin, Brown University School of Medicine, Providence, RI, USA) as confirmed by sequencing. Both the pcDNA3-Bcl-2 plasmid and pTOPO-Mcl-1 plasmid were obtained from Addgene (Addgene Inc, Cambridge, MA, USA). Huh7, Hep3B and HepG2 cells were transfected with these expression plasmids (pcDNA3-Bcl-2, pcDNA3-HA-survivin, and pTOPO-Mcl-1) using Lipofectamine 2000 reagent (Invitrogen) according to the manufacturer's instructions. Briefly, cells plated in 6-well plates were incubated with 1μg plasmid DNA (pcDNA3-Bcl-2, pcDNA3-HA-survivin, pTOPO-Mcl-1 or pcDNA3.1). Six hours after transfection, the transfection medium was replaced with complete medium. The expression of Bcl-2, survivin, and Mcl-1 was monitored by western blot analysis.

4.2.5 Flow cytometry analysis of cell cycle

Cell cycle distribution of HCC cells was measured after exposure to temsirolimus alone or vinblastine alone or combination for 12 hrs or 16 hrs. The experimental procedures were described in Chapter 2, section 2.4.

4.2.6 Western blot analysis

Protein lysates were extracted from cells treated with temsirolimus or

temsirolimus/vinblastine combination for 24 hrs or 48 hrs. Western blot analysis was performed as described in Chapter 2, section 2.5. Primary antibodies used in this study included anti-mTOR (1:1000 dilution), anti-pi-mTOR (ser2448) (1:1000 dilution), anti-Akt (1:2000 dilution), anti-pi-Akt (ser473) (1:2000 dilution), anti-p70s6k (1:1000 dilution), anti-pi-p70S6k (Thr389) (1:1000 dilution), anti-s6 (1:1000 dilution), anti-pi-s6 (ser240/244) (1:3000 dilution), anti-4E-BP1 (1:1000 dilution), anti-pi-4E-BP1 (ser65) (1:1000 dilution), anti-cleaved PARP (1:1000 dilution), anti-survivin (1:1000 dilution) (Cell Signaling Technology), anti-Cyclin D1 (1:1000 dilution), anti-Mcl-1 (1:200 dilution) (Santa Cruz Biotechnology), anti-Bcl-2 (1:500 dilution) (Dako North America, Carpinteria, CA, USA) and anti-Actin (1:50,000 dilution) (Calbiochem, Nottingham, UK). Peroxidase conjugated secondary antibodies were applied at 1:10,000 dilution for anti-Actin, and 1:3000 for other primary antibodies (Bio-Rad).

4.2.7 Huh7 and Hep3B xenograft models and drug study

Huh7 and Hep3B xenografts were developed according to the methods described in Chapter 2, section 2.6. As IVIS imaging system was not available, luciferase gene was not transfected in the cells in this animal study. 2×10^6 Huh7 cells and 3×10^6 Hep3B cells were used for subcutaneous inoculation. Mice were randomized into four groups before treatment. Treatments were started on day 10 (for Huh7 xenografts), or day 24 (for Hep3B xenografts). Experimental groups included: (1) vehicle control, (2) temsirolimus alone (25mg/kg, 3-4 times a week, i.p.), (3)

vinblastine alone (0.4mg/kg, 1-2 times a week, i.p.), (4) a combination of temsirolimus and vinblastine (same doses and schedules as single agents alone). Tumor growth was monitored twice weekly using a digital caliper and tumor volume was calculated using the formula of [(Length × Width^2) / 2] for 6 weeks.

4.2.8 Immunohistochemistry

Formalin-fixed paraffin-embedded HCC xenograft sections were deparaffinized in xylene, rehydrated in graded alcohol and equilibrated in PBS. To inactivate endogenous peroxidase activity, the sections were incubated for 10 min with 0.1% hydrogen peroxide (H_2O_2) in methanol before blocking with 3% BSA at 37°C for 30 min. Slides were then incubated with primary antibodies overnight at 4°C. Antibodies for cleaved PARP, survivin (Cell Signaling Technology), Bcl-2 (Epitomics, Burlingame, CA, USA) and Mcl-1 (Santa Cruz Biotechnology) were used at 1: 25 dilution. After primary antibody incubation, slides were washed 3 times with PBS, and then incubated with peroxidase conjugated secondary antibody (1: 100 dilution) (Bio-Rad) for 1 hr at 37°C, followed by color development with DAB substrate (Dako North America). After dehydration in a graded series of ethanol solutions, the sections were mounted with Permount® Mounting Medium (Thermo Fisher Scientific). No antibody negative control (3% BSA) was also included. Stained slides were evaluated under light microscope at 400× magnification. The immunohistochemical score approach initiated by McCarty *et al* (242) was applied to assess both the intensity of staining and the percentage of

positive cells. The percentage of tumor cells with no staining (0), weak staining (1+), moderate staining (2+), and strong staining (3+) was recorded for each sample. This information was summarized into a single score that was the sum of the percent with a score of 1+, twice the percent 2+, and thrice the percent 3+, Maximum = 300.

4.2.9 Statistical analysis

The data was presented as mean ± SEM. Student's t-test and Mann-Whitney test analysis were performed using Graphpad Prism 4.0 software. Differences were considered statistically significant at $P<0.05$.

4.3 Results

4.3.1 Temsirolimus inhibited cell proliferation and mTOR signaling in HCC cells

To examine the effects of temsirolimus on HCC cell proliferation, five HCC cell lines (SNU398, Hep3B, HepG2, PLC/PRF/5 and Huh7) were treated with temsirolimus at increasing concentrations from 1nM to 100μM for 24 hrs and 48 hrs. Dose-dependent growth inhibition was observed in all five HCC cell lines at both 24 and 48 hrs. As early as 24 hrs upon treatment, temsirolimus was able to induce a maximal growth inhibition of about 90-95% in all HCC cell lines tested. It was noted that Huh7 was the cell line most sensitive to temsirolimus, while Hep3B was the least sensitive one. The average IC_{50} of Huh7 was 1.27±0.06μM, while SNU398, HepG2, PLC/5 and Hep3B had the IC50 values of 7.69±0.06, 8.77±0.76, 11.21±1.44

and 52.95±17.14μM at 24 hrs upon temsirolimus treatment (Fig. 4.1A).

Next, the effects of temsirolimus on mTOR signaling in HCC cells were examined. As shown in Figure 4.1B, temsirolimus (1μM) was able to inhibit the phosphorylation of mTOR (Ser2448) in Huh7, Hep3B and HepG2 cell lines as early as 24 hrs and sustained till 48 hrs. Moreover, temsirolimus induced mTOR inhibition resulted in the inhibition of its downstream effectors, including phospho-p70S6k (Thr389), phospho- S6 (Ser240/244), and phospho-4E-BP1 (Ser65) in all 3 HCC cell lines (Fig. 4.1B). These results confirmed that temsirolimus was able to inhibit mTOR activation in HCC cells. In all 3 cell lines, a consistent up-regulation of phospho-Akt at both 24 and 48 hrs was also observed (Fig. 4.1B).

A

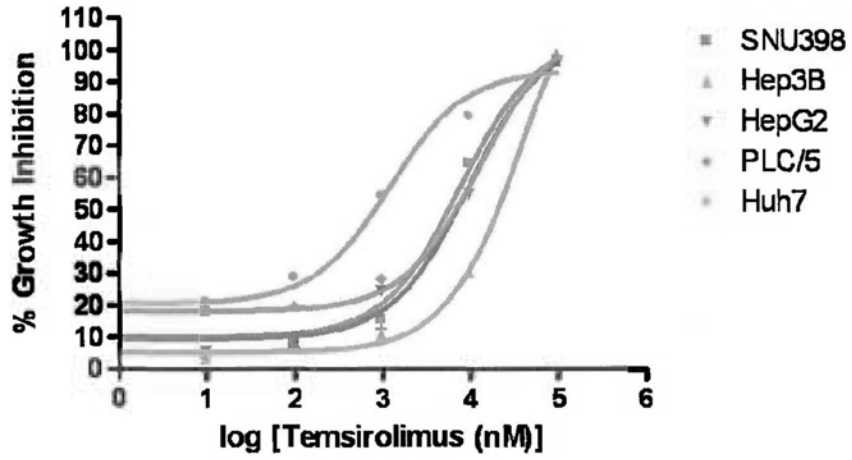

	SNU398	Hep3B	HepG2	PLC/5	Huh7
EC50	7726	40825	9637	12689	1224

B

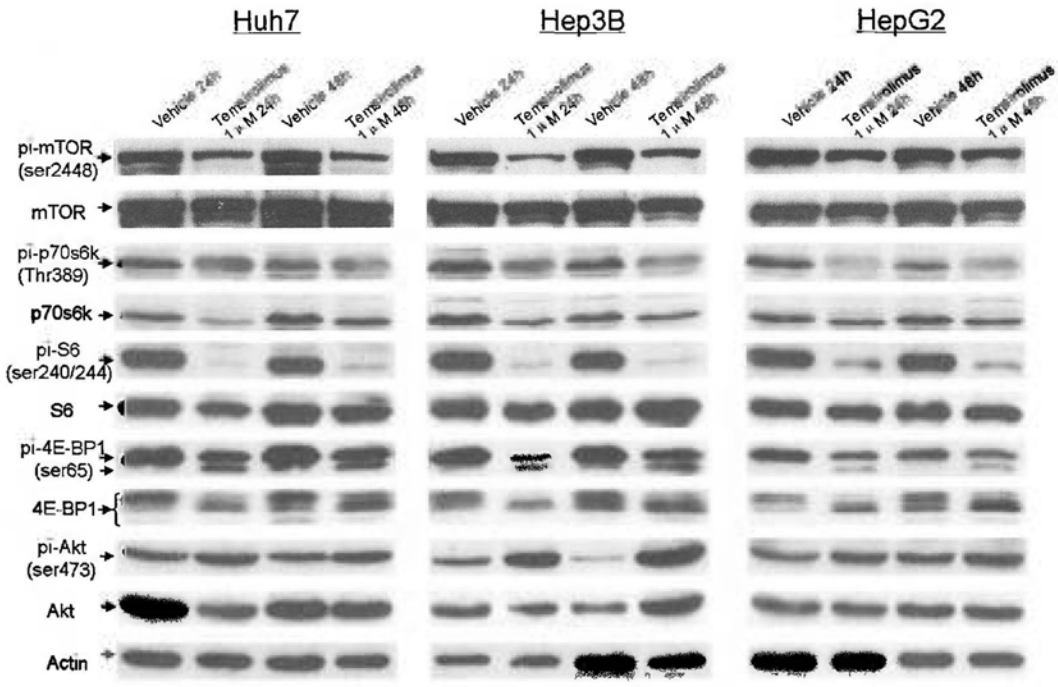

Figure 4.1 Temsirolimus inhibited cell proliferation and mTOR signaling in HCC cell lines. A. HCC cell lines Hep3B, HepG2, PLC/5, Huh7 and SNU398 were treated with increasing concentrations of temsirolimus for 24 hrs. Effect on cell viability was assessed by MTT assay. B. Temsirolimus inhibited the mTOR pathway in HCC cells. Cells were treated with 1μM temsirolimus for 24 hrs and 48 hrs.

Components of the mTOR pathway were examined by western blot analysis. Similar results were observed in 3 independent experiments.

4.3.2 Additive to synergistic anti-tumor effect by temsirolimus/vinblastine combination *in vitro*

Previous studies showed that the PI3K/Akt/mTOR signaling pathway may be associated with resistance to taxanes and other microtubule targeting agents (27, 243). Therefore, the effect of temsirolimus and vinblastine on HCC cell growth was examined in Huh7, Hep3B and HepG2 cell lines. Cell proliferation was inhibited after exposure to vinblastine alone for 24 hrs. At very low concentration (1nM), vinblastine alone only mildly inhibited HCC cell growth (~10% in Hep3B, 15% in HepG2 and 35% in Huh7 cell line). Cell proliferation was further inhibited when different doses of temsirolimus were combined with 1nM vinblastine, in Hep3B and HepG2 cells. For Huh7, the cell line most sensitive to temsirolimus, synergistic growth inhibition was observed with a much lower concentration of temsirolimus (0.01-0.1μM), with the combination regimen resulting in over 65-70% of growth inhibition (Fig. 4.2A). Similarly, in both Hep3B and HepG2 cell lines, the combination resulted in 80-90% growth inhibition at 24 hrs, indicating the therapeutic efficacy of such a combination in HCC models.

As shown in Figure 4.2B, temsirolimus alone inhibited the phosphorylation of mTOR (Ser2448), p70S6k (Thr389), ribosomal S6 (Ser240/244), and 4E-BP1 (Ser65) in all 3 HCC cell lines. Vinblastine alone did not affect mTOR signaling in all 3 HCC cell lines used and the addition of vinblastine did not resulted in further suppression of the mTOR pathway (Fig. 4.2B).

More interestingly, only the temsirolimus/vinblastine combination, but not the

single agents alone, was able to inhibit the expression of anti-apoptotic and survival proteins (including survivin, Bcl-2, Mcl-1) in all 3 HCC cell lines tested. It was noted that the expression of Cyclin D1 was not affected by combination treatment (Fig. 4.2C). These findings suggested that concerted down-regulation of several important anti-apoptotic/survival proteins may mediated the synergistic effect of the combination.

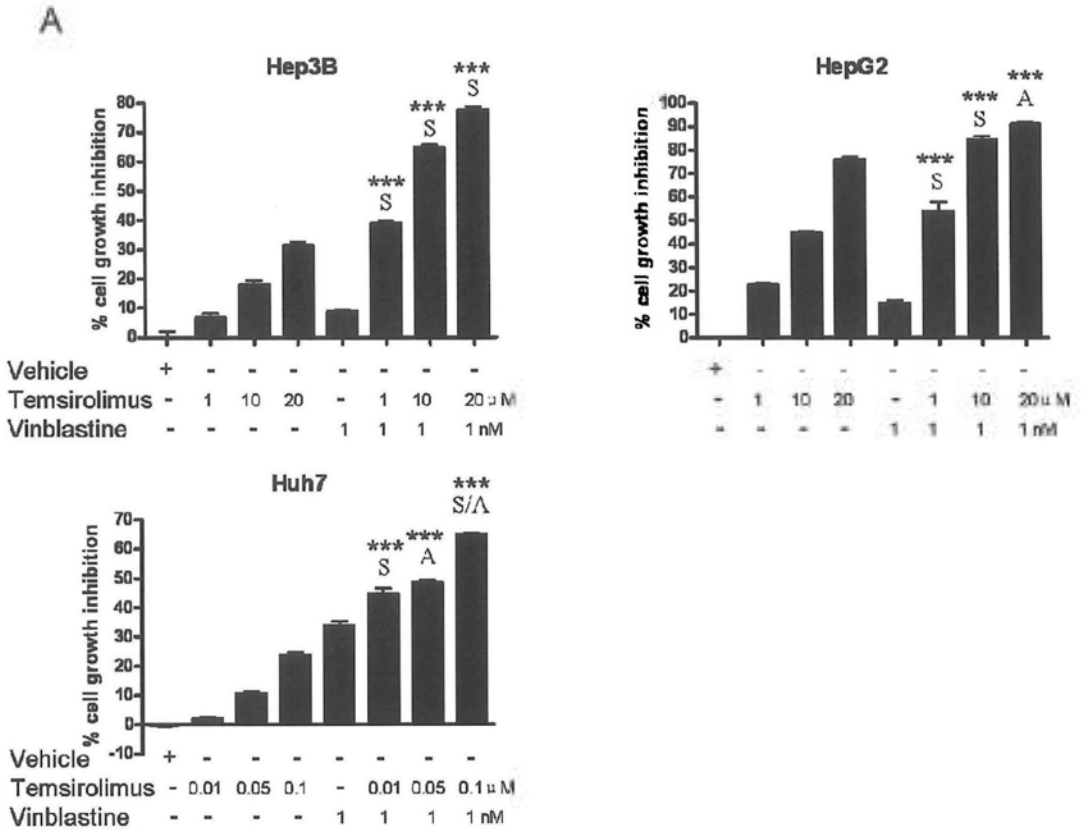
A
Hep3B
HepG2
Huh7
% cell growth inhibition
Vehicle
Temsirolimus
Vinblastine
B
Huh7
Hep3B
HepG2
pi-mTOR (ser2448)
mTOR
pi-p70s6k (Thr389)
p70s6k
pi-S6 (ser240/244)
S6
pi-4E-BP1 (ser65)
4E-BP1
Actin

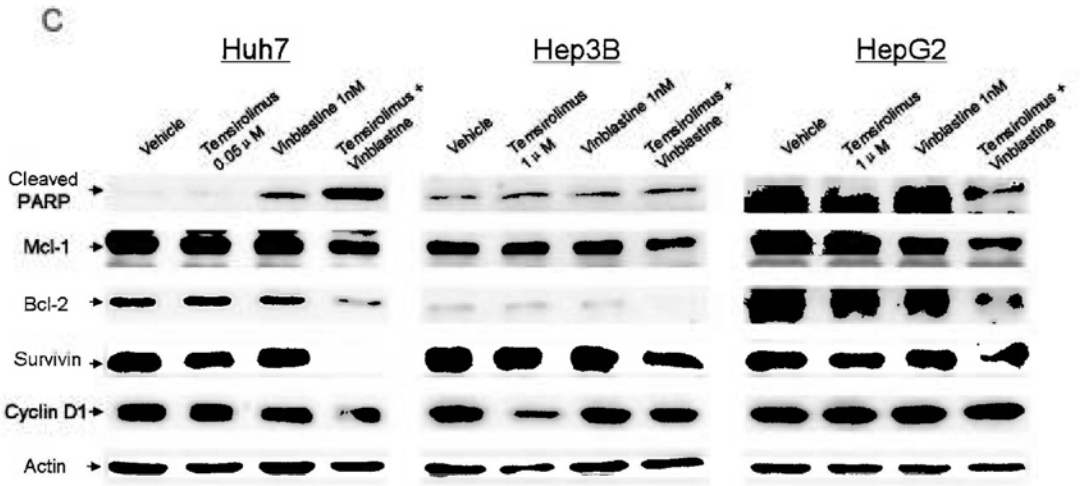

Figure 4.2 Temsirolimus exerted additive to synergistic growth inhibitory activity on HCC cells with vinblastine. A. Cells were treated with various concentrations of temsirolimus in combination with 1nM vinblastine for 24 hrs. Cell viability was assessed by MTT assay. Cumulative results from 3 independent experiments were shown as mean ± SEM (t-test, ***P<0.001 vs temsirolimus treated group) (S: synergistic effect; A: additive effect). B. mTOR pathway did not further inhibited by temsirolimus/vinblastine combination treatment. Cells were treated with temsirolimus and/or vinblastine for 24 hrs. Components of the mTOR pathway were examined by western blot analysis. C. Survivin, Bcl-2 and Mcl-1 were down-regulated by temsirolimus/vinblastine combination treatment. Cells were treated with temsirolimus and/or vinblastine for 24 hrs. The expression levels of cleaved PARP, Mcl-1, Bcl-2, survivin, Cyclin D1 and actin were assessed by western blot analysis.

4.3.3 Over-expression of survivin/Bcl-2/Mcl-1 rescued HCC cells from temsirolimus/vinblastine combination mediated growth inhibition

To confirm that down-regulation of anti-apoptotic/survival proteins, survivin, Bcl-2 and Mcl-1, is an underlying mechanism for the synergistic or enhanced anti-tumor activity of the temsirolimus/vinblastine combination, survivin, Bcl-2 or Mcl-1 was over-expressed in HCC cells by transient transfection and the effects on cell sensitivity to temsirolimus/vinblastine combination were observed. As shown in Figure 4.3, transient transfection was able to induce over-expression of survivin, Bcl-2 and Mcl-1 in all 3 HCC cell lines (Fig. 4.3A, C, E). Compared with control vector transfected cells, growth inhibition by temsirolimus/vinblastine combination was significantly reduced in survivin/Bcl-2 transfected cells and slightly reduced in Mcl-1 transfected cells (Fig. 4.3B, D, F). Whereas over-expression of survivin, Bcl-2 or Mcl-1 did not alter the growth inhibition induced by temsirolimus alone or vinblastine alone in HCC cells (Fig. 4.3B, D, F). These results suggested that down-regulation of survivin, Bcl-2 and Mcl-1 contributes directly to the observed synergistic anti-tumor activity of the temsirolimus/vinblastine combination.

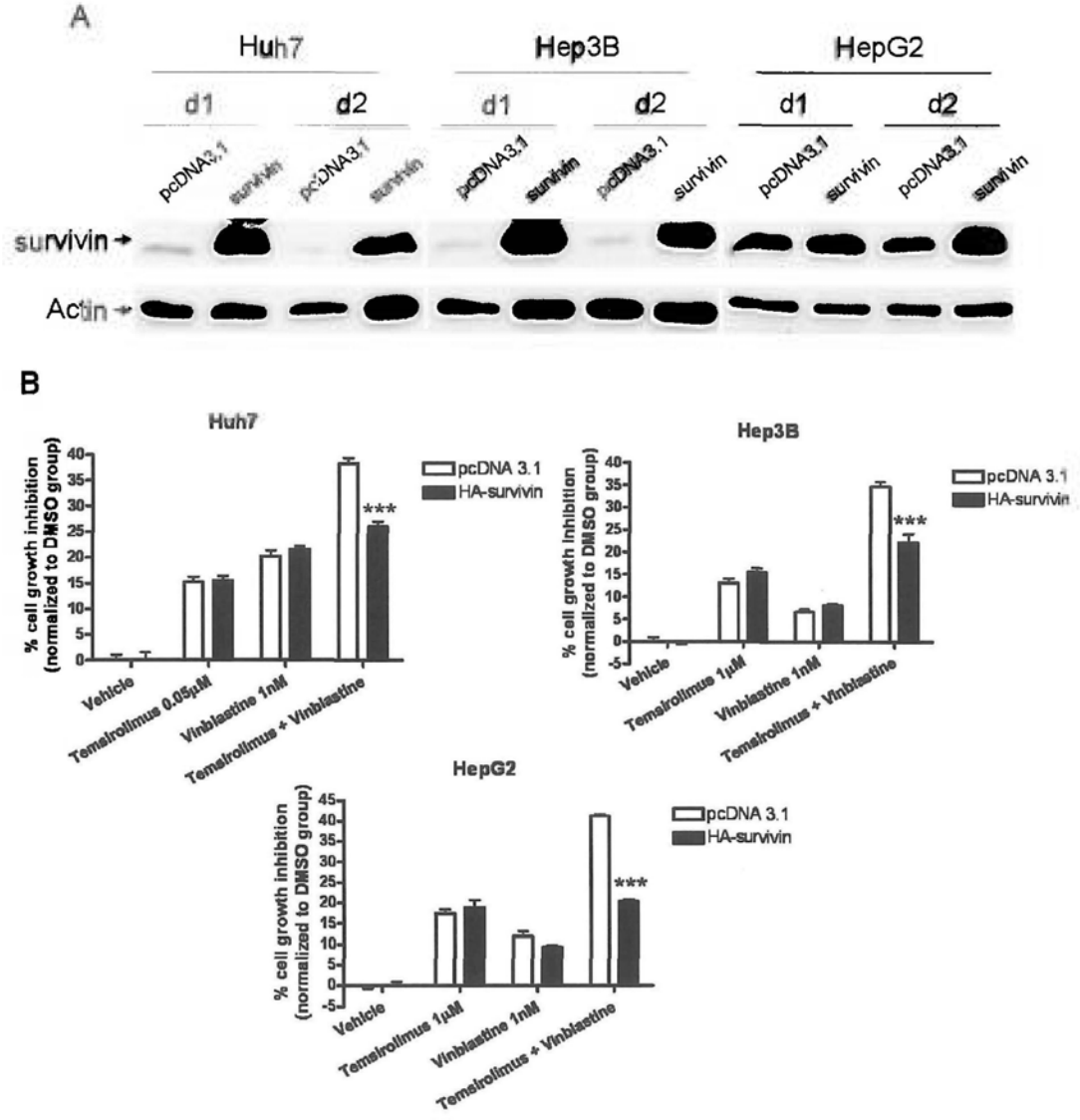
A
Huh7
Hep3B
HepG2
d1
d2
pcDNA3.1
survivin
survivin
Actin
B
Huh7
Hep3B
HepG2
% cell growth inhibition (normalized to DMSO group)
pcDNA 3.1
HA-survivin
***
Vehicle
Temsirolimus 0.05μM
Temsirolimus 1μM
Vinblastine 1nM
Temsirolimus + Vinblastine
C
Huh7
Hep3B
HepG2
d1
d2
pcDNA3.1
Bcl-2
Bcl-2
Actin

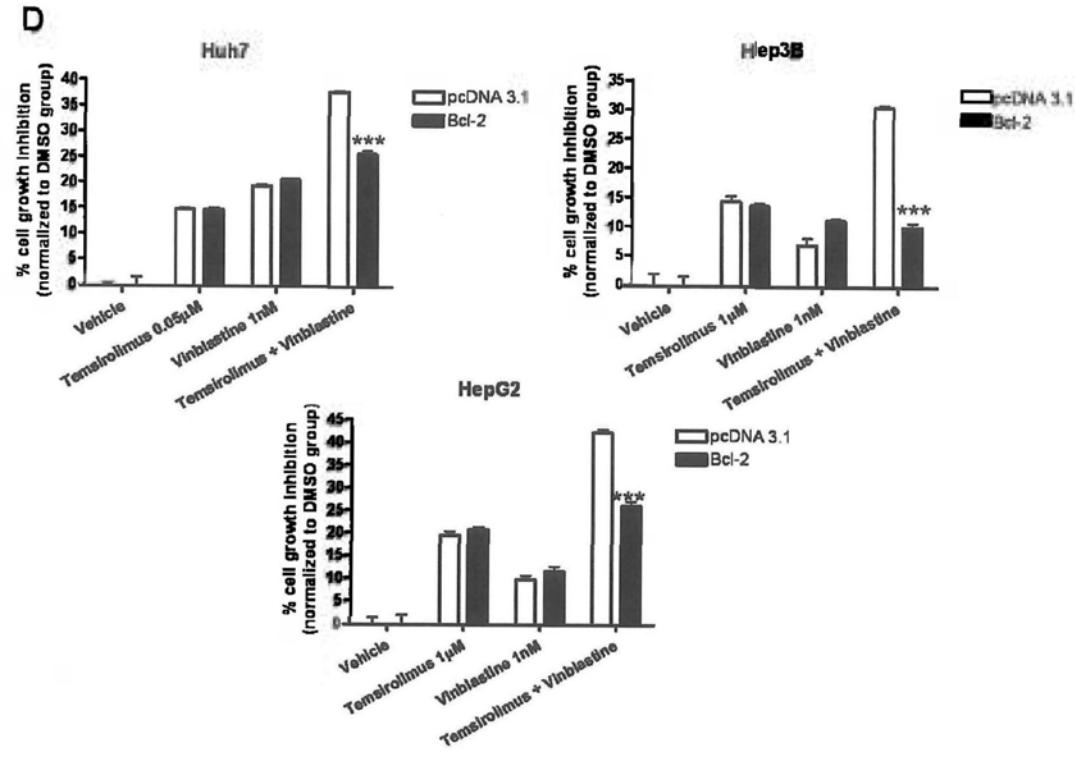
D
Huh7
Hep3B
HepG2
% cell growth inhibition (normalized to DMSO group)
pcDNA 3.1
Bcl-2
***
Vehicle
Temsirolimus 0.05μM
Temsirolimus 1μM
Vinblastine 1nM
Temsirolimus + Vinblastine

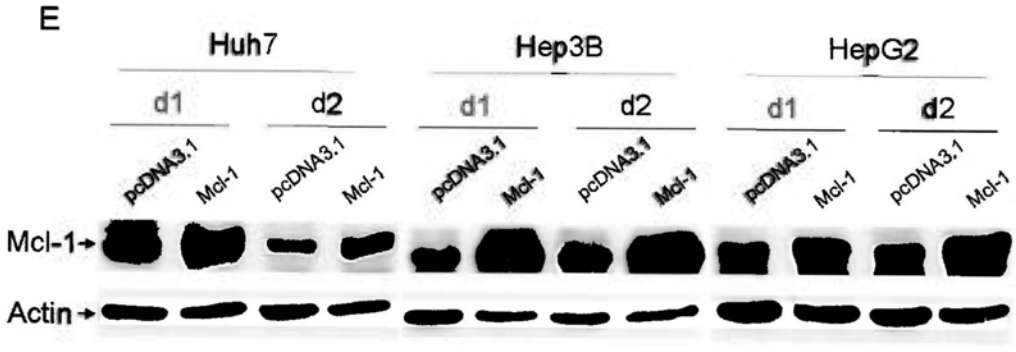
E
Huh7
Hep3B
HepG2
d1
d2
pcDNA3.1
Mcl-1
Mcl-1→
Actin→

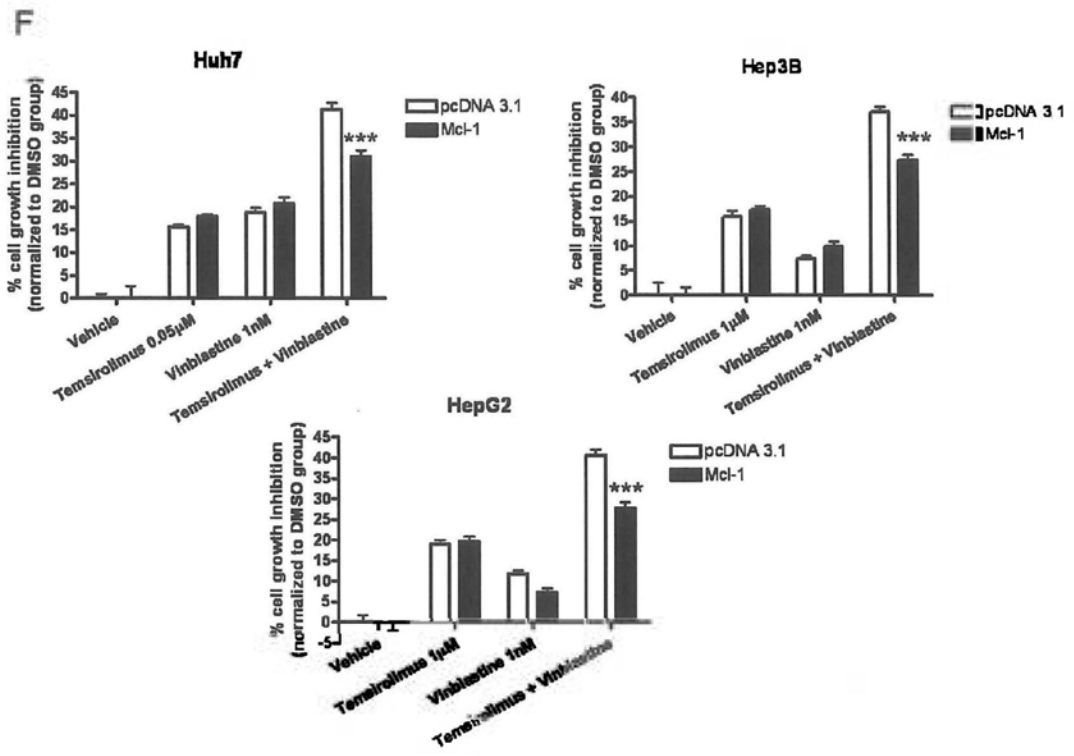

Figure 4.3 Over-expression of survivin or Bcl-2 or Mcl-1 rescued HCC cells from the growth inhibitory effect of temsirolimus/vinblastine combination. A, C, E. Expression level of survivin, Bcl-2 and Mcl-1 at day 1 and day 2 after transfection (by western blot analysis). B, D, F. Over-expression of survivin, Bcl-2, Mcl-1 partially reversed the anti-proliferative effect of temsirolimus/vinblastine combination. HCC cells transfected with survivin, Bcl-2 or Mcl-1 plasmid were treated with temsirolimus and/or vinblastine for 24 hrs. Cumulative results from 3 independent experiments were shown as mean ± SEM (t-test, ***P<0.001 vs pcDNA3.1 transfectants).

4.3.4 Temsirolimus/vinblastine combination induced cell cycle arrest

Previous studies demonstrated that mTOR inhibitors affect cell cycle progression by G_1 arrest, while vinblastine is known to induce cell cycle arrest at G_2/M phase through destabilizing microtubule polymerization (244, 245). Here, the effect of the temsirolimus/vinblastine combination on HCC cell cycle distribution was examined. In all 3 HCC cell lines tested, temsirolimus was found to induce G_1 arrest, while vinblastine induced G_2/M arrest (Fig. 4.4), which was consistent with previous reports (244, 245). With the temsirolimus/vinblastine combination, significant cell cycle arrest at both G_1 and G_2/M phases was observed, in conjunction with an obvious reduction in the S population (Fig. 4.4). These results indicated that the combination treatment was able to inhibit DNA synthesis, as well as G_1 and G_2/M cell cycle arrest in HCC cell lines.

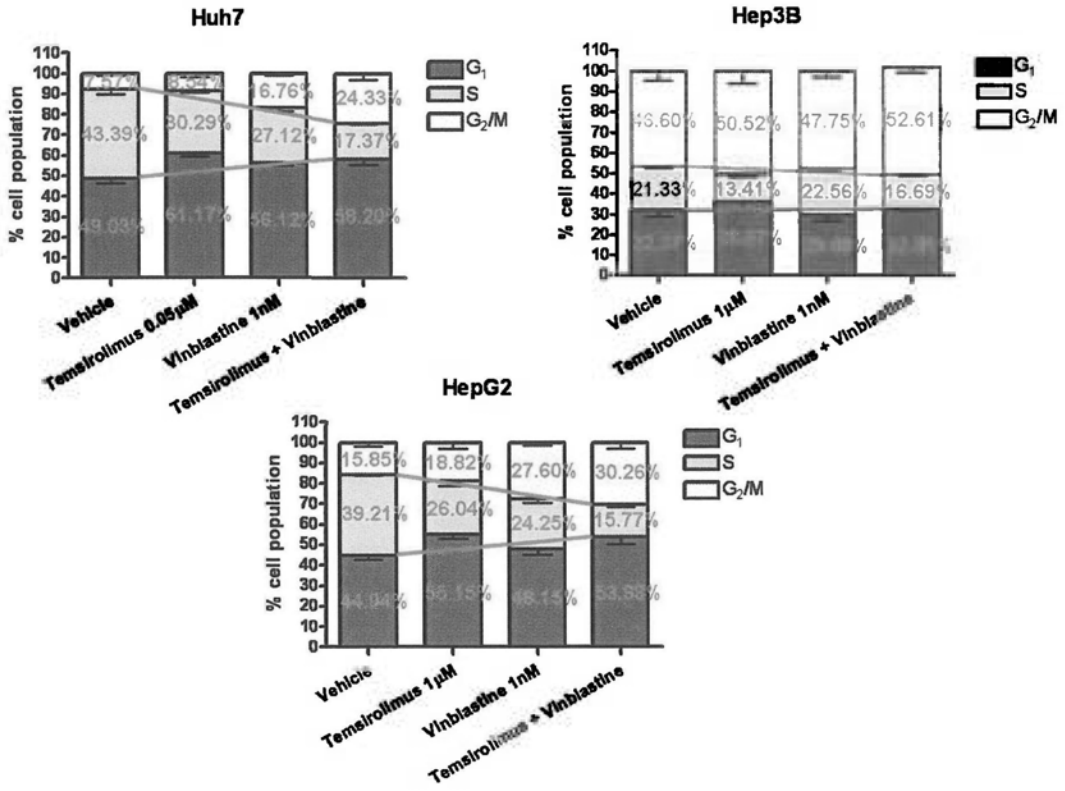

Figure 4.4 Temsirolimus/vinblastine combination resulted in both G_1 and G_2/M arrest in HCC cells. Cells treated with temsirolimus and/or vinblastine for 12 hrs or 16 hrs were harvested, stained with PI, and analyzed by flow cytometry. Cumulative results from 3 independent experiments were shown as mean ± SEM.

4.3.5 Anti-tumor effect of temsirolimus, vinblastine and the combination *in vivo*

Next, the effects of mTOR targeting, microtubule targeting and combined targeting on HCC tumor growth were examined *in vivo*. Huh7 xenografts were established by subcutaneously inoculation into BALB/c nude mice and the effects of drug treatment on tumor growth was monitored twice per week. Fractional change in tumor volume upon treatment was plotted over time (Fig. 4.5A). The vehicle control-treated group showed a gradual increase in tumor size over time. Treatment of mice with temsirolimus or vinblastine alone suppressed tumor growth ($P<0.05$). The temsirolimus/vinblastine combination was the most effective regimen when compared to either agent alone ($P<0.05$), as well as the vehicle control ($P=0.0009$). With only 2 weeks of treatment, a sustained growth inhibitory effect was observed up to 27 days post-treatment for the temsirolimus/vinblastine combination. The treatments were tolerated by all groups with no deaths observed. Initial weight loss was observed with each single agent alone and combination treatment, but the mice were able to re-gain body weight when the treatments stopped (Fig. 4.5B). Similar results were observed in Hep3B xenografts (Supplementary Fig. 4.1A and B).

4.3.6 Survivin/Bcl-2/Mcl-1 expressions were down-regulated in xenograft tumors treated with temsirolimus/vinblastine combination

Next, whether such a persistent tumor growth inhibition was due to apoptosis induction or growth suppression was examined. By immunohistochemical staining for cleaved PARP expression (a hallmark for apoptosis), no cleaved PARP

expression was observed in temsirolimus treated group, and there was not a significant increase in cleaved PARP expression in tumors from the temsirolimus/vinblastine treated group vs vinblastine alone (Fig. 4.5C and E, Supplementary Fig. 4.1C and E). This result suggested that the anti-tumor effect of the combination was likely to be due to growth suppression, but not apoptosis.

The expression of survivin, Bcl-2 and Mcl-1 proteins for all treatment groups was also examined by immunohistochemistry. Consistent with the *in vitro* results, survivin, Bcl-2 and Mcl-1 expression were markedly reduced in HCC xenografts treated with temsirolimus/vinblastine combination compared to vehicle control and single agents alone ($P<0.001$, Fig. 4.5D and E, Supplementary Fig. 4.1D and E).

A

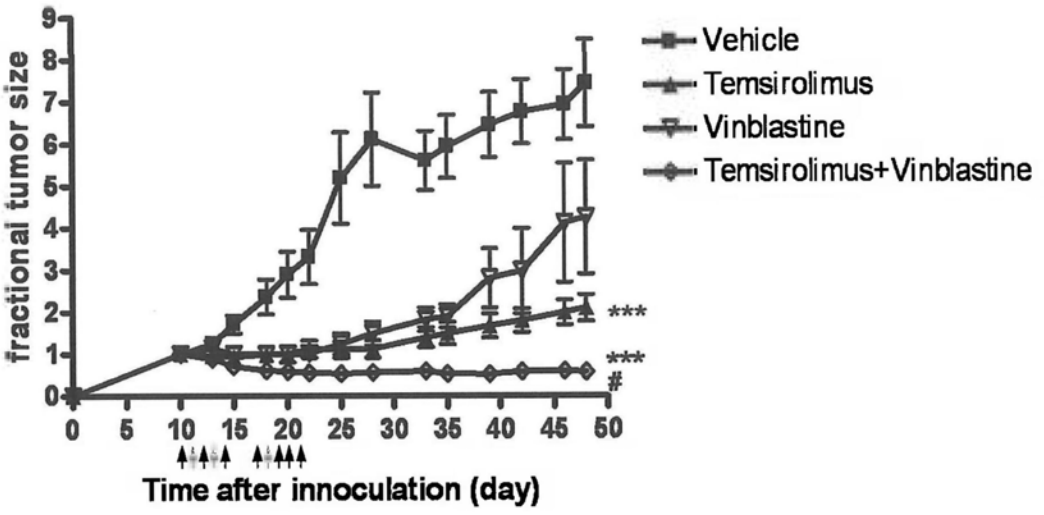
fractional tumor size
Time after innoculation (day)
Vehicle
Temsirolimus
Vinblastine
Temsirolimus+Vinblastine
***
***
#

B

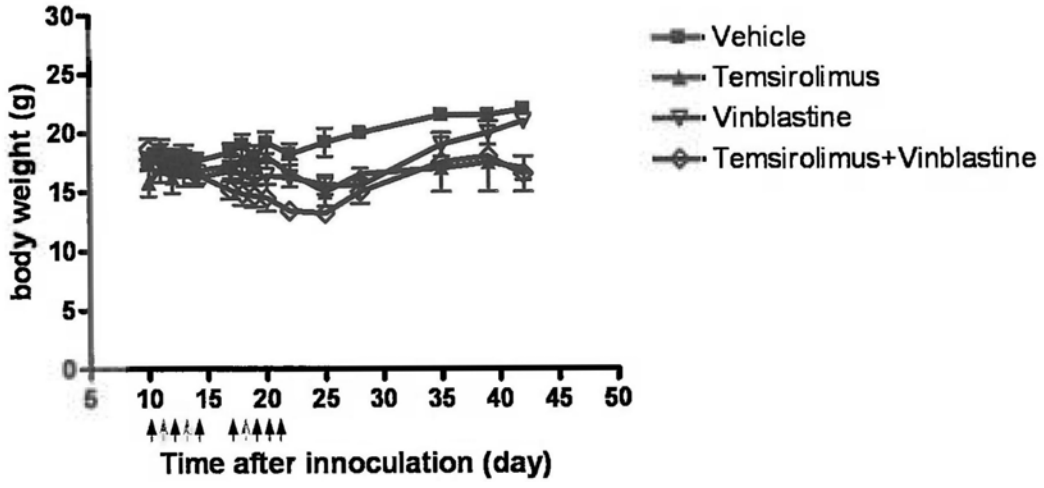
body weight (g)
Time after innoculation (day)
Vehicle
Temsirolimus
Vinblastine
Temsirolimus+Vinblastine

C

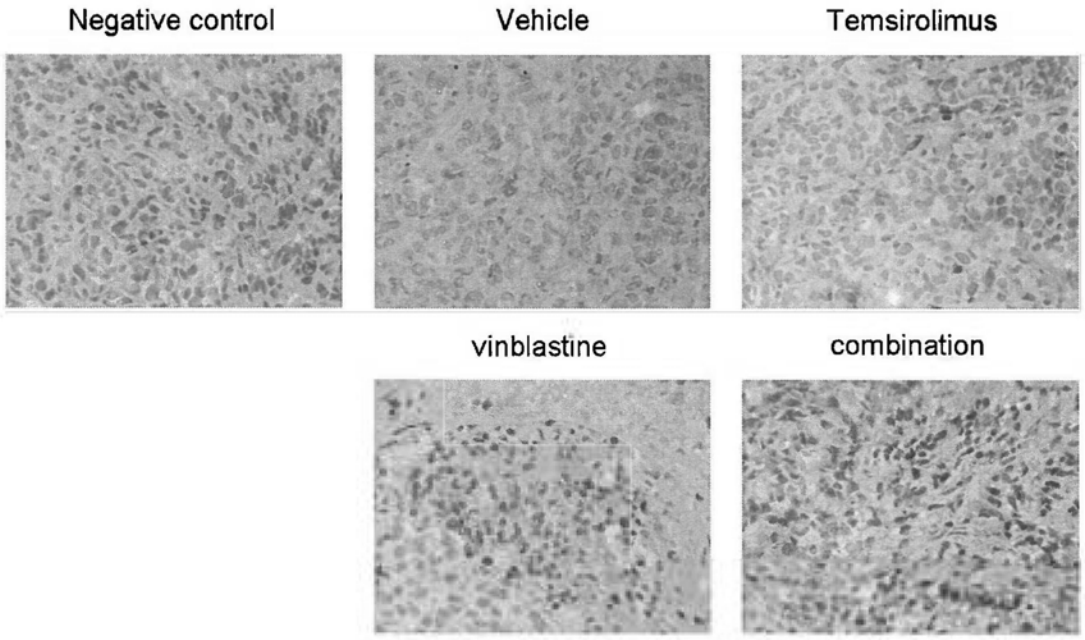
Negative control
Vehicle
Temsirolimus
vinblastine
combination

D

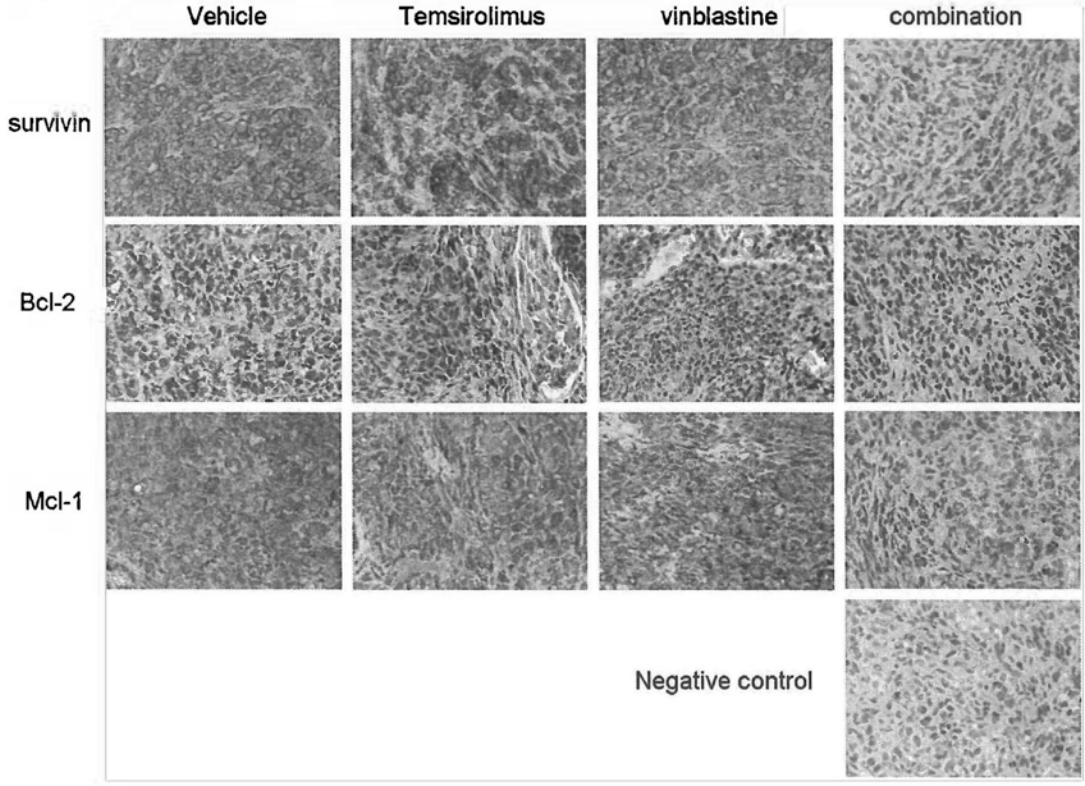
Vehicle
Temsirolimus
vinblastine
combination
survivin
Bcl-2
Mcl-1
Negative control

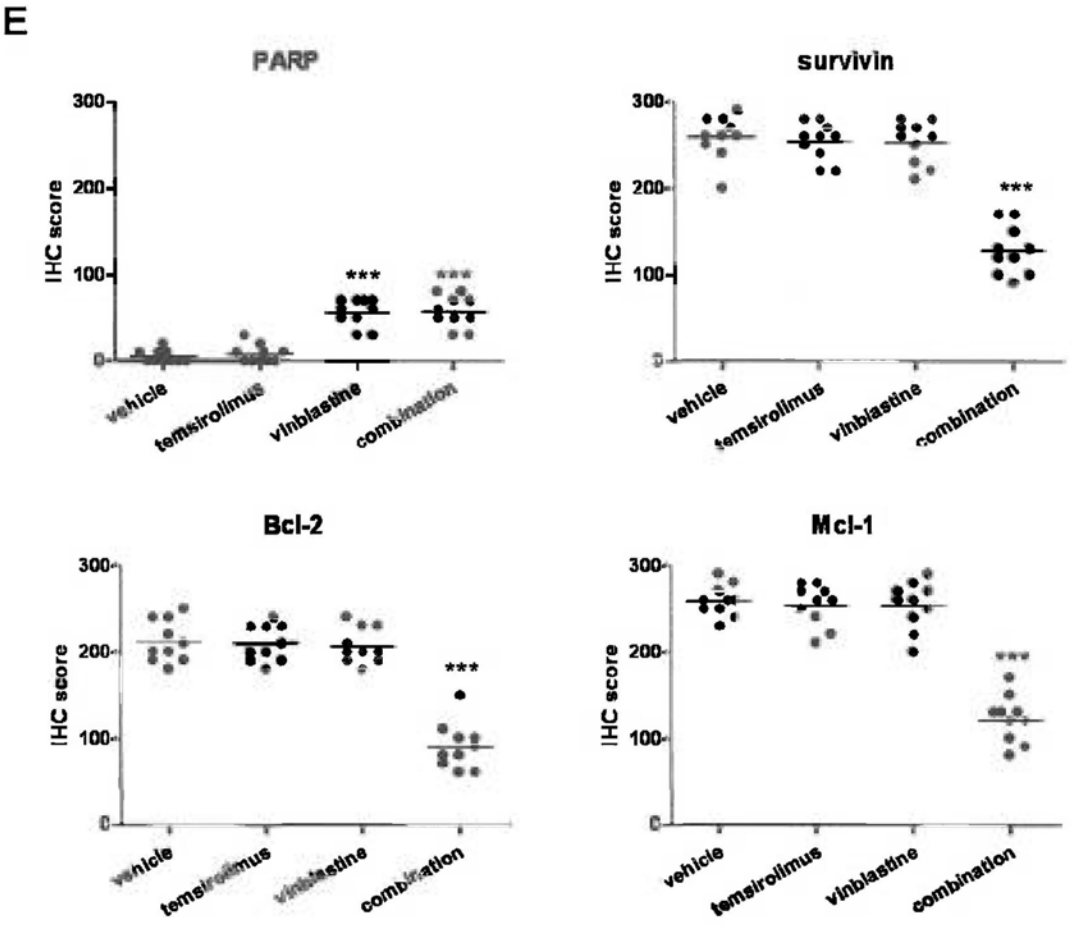

Figure 4.5 Anti-tumor effects of temsirolimus, vinblastine and the combination in Huh7 xenografts. Huh7 cells (2×10^6) were injected subcutaneously into male BALB/c nude mice. 10 days after tumor inoculation, mice received intraperitoneal injection of drugs for two weeks (black arrow: temsirolimus injection; red arrow: vinblastine injection). A. Treatment of mice with temsirolimus or vinblastine alone suppressed tumor growth. The *in vivo* anti-tumor activity of temsirolimus/vinblastine combination was more significant and sustained (up to 37 days post-treatment) (t-test, ***P<0.001 vs vehicle group, #P<0.05 vs temsirolimus or vinblastine group). Tumor growth was monitored and quantified twice weekly. Arrows indicated time of drug injection. B. Change in body weight of mice from drug treatments. C. Cell apoptosis did not increase with temsirolimus/vinblastine

combination treatment in Huh7 xenografts. Xenograft tumors were harvested, fixed, and stained for cleaved PARP by immunohistochemistry. Representative images (400× magnification) were shown. D. Survivin, Bcl-2 and Mcl-1 were down-regulated by temsirolimus/vinblastine combination treatment in Huh7 xenografts. Xenograft tumors were harvested, fixed, and stained for survivin, Bcl-2 and Mcl-1 by immunohistochemistry. Representative images (400× magnification) were shown. E. Immunohistochemistry scoring of cleaved PARP, survivin, Bcl-2 and Mcl-1 in Huh7 xenografts (n=10 per group, Mann-Whitney test, ***P<0.001 vs vehicle group).

A

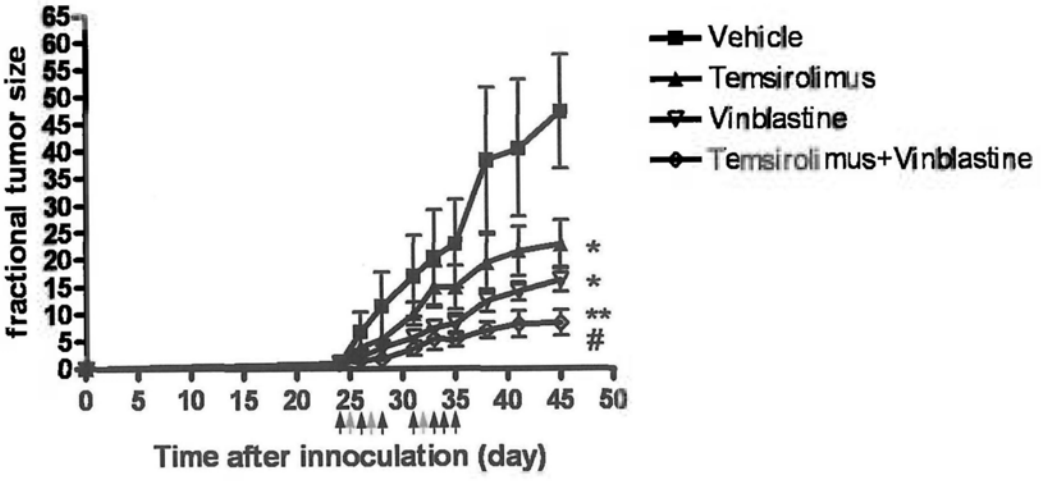
fractional tumor size
65
60
55
50
45
40
35
30
25
20
15
10
5
0
0 5 10 15 20 25 30 35 40 45 50
Time after innoculation (day)
*
*
**
#
Vehicle
Temsirolimus
Vinblastine
Temsirolimus+Vinblastine

B

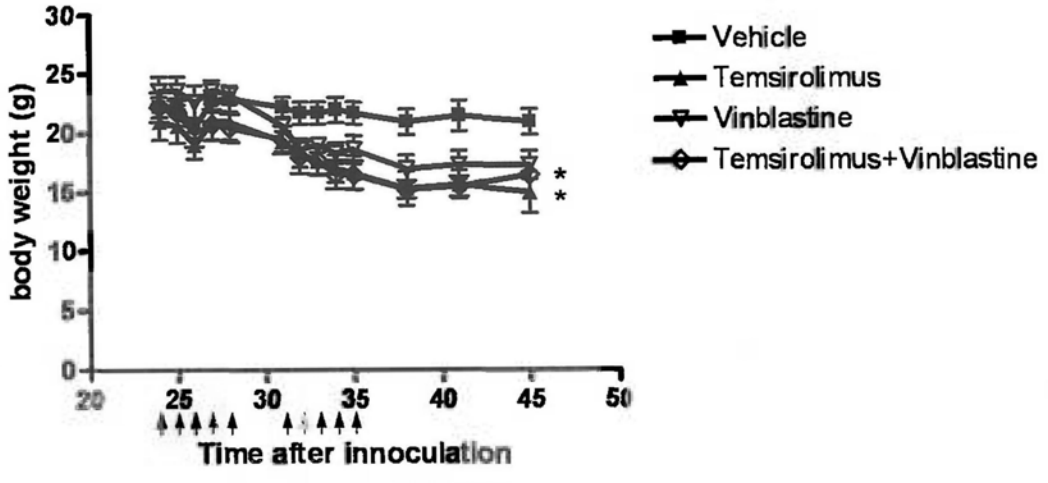
body weight (g)
30
25
20
15
10
5
0
20 25 30 35 40 45 50
Time after innoculation
*
*
Vehicle
Temsirolimus
Vinblastine
Temsirolimus+Vinblastine

C

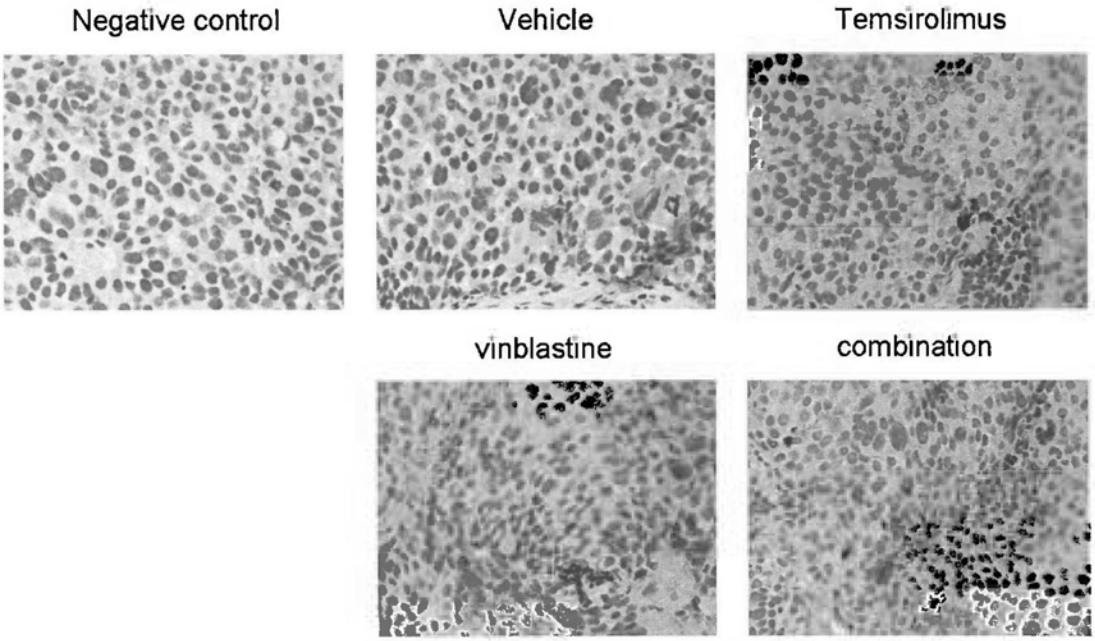
Negative control
Vehicle
Temsirolimus
vinblastine
combination

D

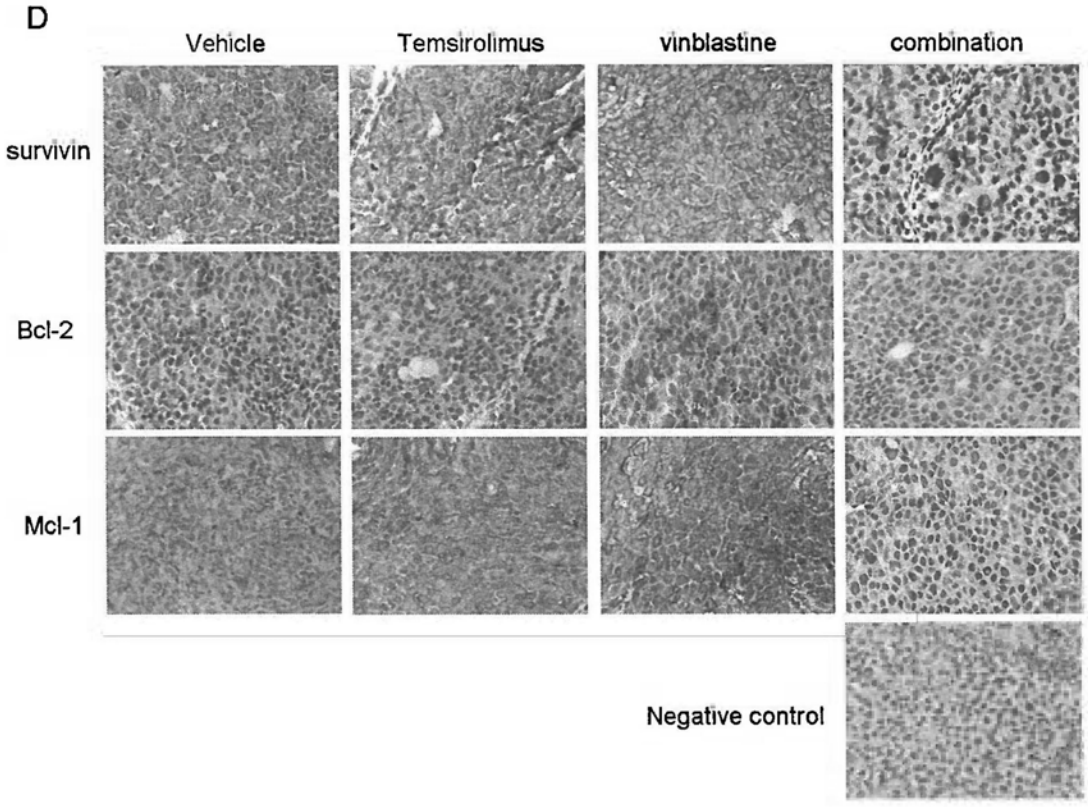
Vehicle
Temsirolimus
vinblastine
combination
survivin
Bcl-2
Mcl-1
Negative control

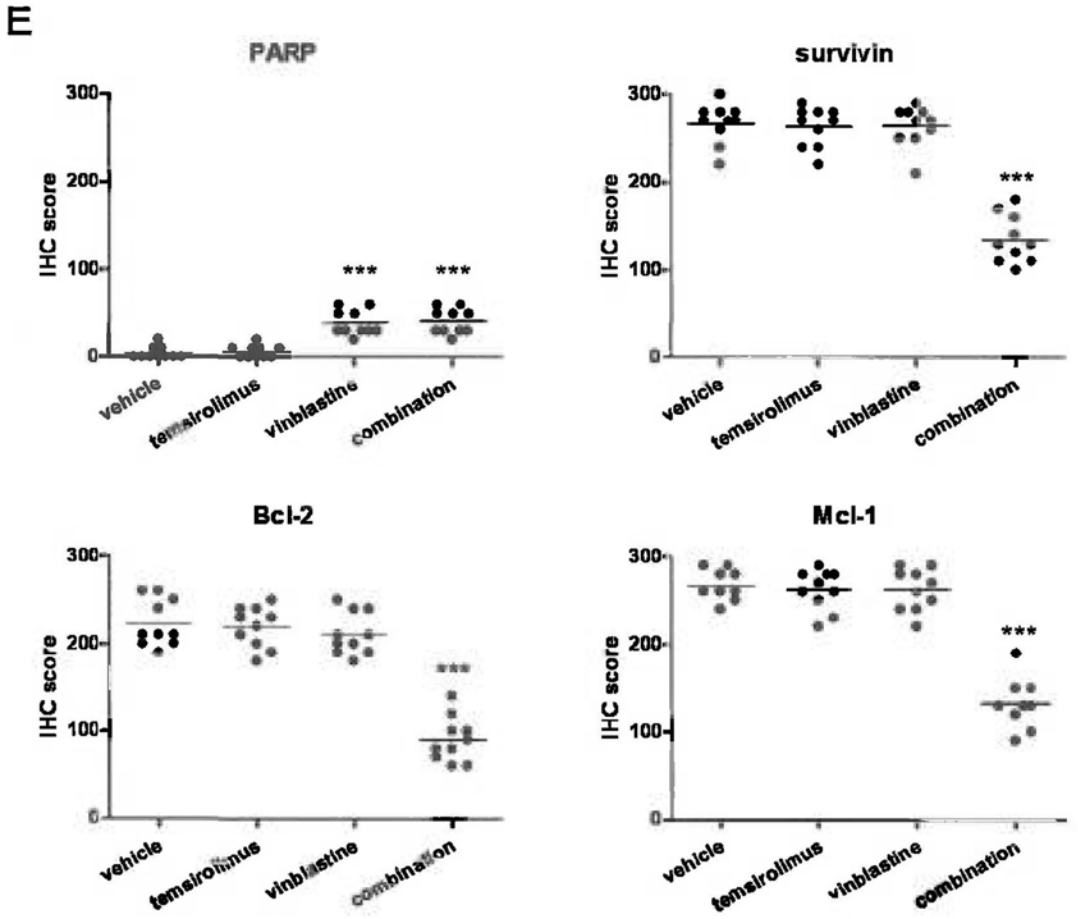

Supplementary Figure 4.1 Anti-tumor effects of temsirolimus, vinblastine and the combination in Hep3B xenografts. Hep3B cells (3×10^6) were injected subcutaneously into male BALB/c nude mice. 24 days after tumor inoculation, mice received intraperitoneal injection of drugs for two weeks (black arrow: temsirolimus injection; red arrow: vinblastine injection). A. Treatment of mice with temsirolimus or vinblastine alone suppressed tumor growth. The *in vivo* anti-tumor activity of temsirolimus/vinblastine combination was more significant and sustained (up to 10 days post-treatment) (t-test, $*P<0.05$, $**P<0.01$ vs vehicle group, $\#P<0.05$ vs temsirolimus or vinblastine group). Tumor growth was monitored and quantified twice weekly. Arrows indicated time of drug injection. B. Change in body weight of mice from drug treatments (t-test, $*P<0.05$ vs vehicle group). C. Cell apoptosis did

not increase with temsirolimus/vinblastine combination treatment in Hep3B xenografts. Xenograft tumors were harvested, fixed, and stained for cleaved PARP by immunohistochemistry. Representative images (400× magnification) were shown. D. Survivin, Bcl-2 and Mcl-1 were down-regulated by temsirolimus/vinblastine combination treatment in Hep3B xenografts. Xenograft tumors were harvested, fixed, and stained for survivin, Bcl-2 and Mcl-1 by immunohistochemistry. Representative images (400× magnification) were shown. E. Immunohistochemistry scoring of cleaved PARP, survivin, Bcl-2 and Mcl-1 in Hep3B xenografts (n=10 per group, Mann-Whitney test, ***P<0.001 vs vehicle group).

4.4 Discussion

In this study, it was demonstrated that mTOR inhibitor temsirolimus inhibited HCC cell growth *in vitro*, and combined targeting of the mTOR pathway and the microtubule using temirolimus and vinblastine elicited synergistic effect in HCC both *in vitro* and *in vivo*. The down-regulation of anti-apoptotic/survival proteins survivin, Bcl-2 and Mcl-1 may mediate the synergistic effect of the combination.

This study has shown that temsirolimus alone suppressed tumor cell proliferation in HCC cell lines and inhibited the mTOR activity accordingly. However, the growth inhibitory effects were not as good as expected, with the IC_{50} values at μM level. This is consistent with the previous view that mTOR inhibitors mainly inhibit tumor cells growth without eliciting tumoricidal activity (154, 246). Temsirolimus is a rapamycin analogue. As an mTOR inhibitor, it has two binding domains, FK506-binding protein 12 (FKBP12) binding domain and mTOR binding domain. It firstly associates with its intracellular receptor, FKBP12, and then the complex binds directly to mTOR. mTOR is also called FKBP-rapamycin associated protein (FRAP). After binding to mTOR, temsirolimus suppresses mTOR phosphorylation and mTOR-mediated phosphorylation of its downstream substrates, p70S6k and 4E-BP1 which are important for cell growth and cell cycle (122, 125). To date, no mTOR homologs that have same binding domains are identified and although mTOR inhibitors may have effect on other targets, no such targets have not been reported. When temsirolimus was combined with low dose of vinblastine (1nM), marked synergistic effect was observed in all three HCC cell lines with a maximal

achievable growth inhibition of about 80-90%. This marked growth inhibition was accompanied with cell cycle arrest at both G_1 and G_2/M phases, and PARP cleavage (a hallmark for apoptosis). In line with the present finding, an inhibitory effect on the proliferation of human endothelial cells has already been reported for the combination of rapamycin (another mTOR inhibitor) and vinblastine (168). Marimpietri *et al* also has demonstrated the combined therapeutic effects of rapamycin and vinblastine on human neuroblastoma growth, apoptosis, and angiogenesis (167). Vinblastine is a microtubule-destabilizing agent, widely used as conventional chemotherapeutic drug in the treatment of breast cancer, lung cancer, bladder cancer, and lymphoma. It binds with high affinity to tubulin and prevents the formation of cytoskeleton microtubules, and thereby causing cell cycle arrest (247). However, studies in HCC had shown inherent or acquired resistance to vinblastine as a result of high intrinsic activity of multi-drug resistance gene (MDR) in HCC (159, 160). In this study, using HCC xenograft mice model it is shown for the first time that combined temsirolimus and low dose of vinblastine (0.4mg/kg) can lead to much better tumor growth inhibition compared to single drug administration with little toxicity.

Several studies have demonstrated the linkage between mTOR and microtubule targeting agents. They have suggested that the PI3K/Akt/mTOR signaling pathway is involved in drug resistance to taxanes and other drugs acting on microtubules, including vincristine and colchicines (27, 28). VanderWeele *et al* showed that Akt activation markedly increased resistance to microtubule targeting agents, while

mTOR inhibitor rapamycin could inhibit Akt-mediated therapeutic resistance, indicating that the resistance phenotype is mTOR-dependent (28). However, the mechanisms of the synergistic effect of mTOR inhibitors and microtubule targeting agents are not fully elucidated. In this study, investigation of the molecular mechanism underlying the synergistic growth inhibitory activity of this temsirolimus/vinblastine combination on HCC, it was found that the combination significantly decreased the expression of several key anti-apoptotic and survival proteins, including survivin, Bcl-2 and Mcl-1, in HCC cells. The *in vivo* experiments for the combination vs single agents alone further confirmed the concerted down-regulation of these key anti-apoptotic and survival proteins using the combination approach. These results revealed that the concerted inhibitory effects on key survival and anti-apoptotic proteins were only induced by the combination in HCC cells and xenografts, but not single agents alone, suggesting this to be a likely mechanism contributing to the synergistic growth inhibition in HCC models. Studies have reported that survivin, Bcl-2 and Mcl-1 are important proteins in HCC (248-252). Survivin is over-expressed in about 70% cases of HCC and is significantly associated with the pathological grade of HCC, with the expression of survivin being an independent prognostic factor for HCC (248, 252). Mcl-1, an anti-apoptotic member of the Bcl-2 family, which regulates intrinsic apoptosis induction at the mitochondrial level, is over-expressed in 51% of HCC tissues (250). Bcl-2 is highly expressed in 67% of the adjacent non-tumor tissues and present only in 14-20% of HCC tissues but not in normal livers (251-253), suggesting that

expression of Bcl-2 may be partially involved in HCC development. Taken together, the concerted down-regulation of these key survival/anti-apoptotic proteins would be of clinical relevance to HCC in terms of treatment strategies. In contrast to previous findings (154), the expression of cyclin D1 was not affected either by temsirolimus alone or by combination treatment.

To further confirm the role of these three proteins, over-expression of each protein was performed. The present data showed that with over-expression of any one of these three, the growth inhibitory effect by the temsirolimus/vinblastine combination was partially rescued, which suggested that down-regulation of survivin, Bcl-2 and Mcl-1 contributed directly to the observed synergistic anti-tumor activity of the combination. Nevertheless, over-expression of any two proteins simultaneously did not further suppress the growth inhibitory effect of the combination (data not shown).

In conclusion, this study has demonstrated that mTOR inhibition by temsirolimus inhibited HCC cell growth, and more significantly, combined temsirolimus with microtubule targeting agent vinblastine had synergistic effect in HCC cells. Down-regulation of anti-apoptotic and survival proteins survivin, Bcl-2 and Mcl-1 contributes directly to the observed synergistic anti-tumor activity of the temsirolimus/vinblastine combination. These findings give new insights into potential therapeutic strategy for HCC, suggesting that combined inhibition of mTOR with microtubule targeting agents is a promising therapeutic approach for the treatment of HCC.

Chapter 5: The Role of mTOR Inhibition with Everolimus in Enhancing Chemosensitivity of Microtubule Targeting Agent Vinblastine or Patupilone in Hepatocellular Carcinoma

5.1 Introduction

In Chapter 4, it has been demonstrated that combined targeting of mTOR and the microtubule using temsirolimus and vinblastine has additive to synergistic anti-tumor effect in HCC both *in vitro* and *in vivo*. To further confirm that dual targeting of mTOR and the microtubule is a promising therapeutic strategy for HCC, the combination using other mTOR inhibitors and microtubule targeting agents is being tested.

Everolimus is another rapamycin analogue. It inhibits mTOR through the same mechanism as rapamycin, but has better pharmacological properties for clinical use in cancer. It has better solubility and can be given orally. In HCC, a phase I/II study of everolimus has been conducted in patients with advanced HCC and modest anti-tumor activity was observed including a TTP of 3.9 months and disease control rate of 44% (105). A phase III study of everolimus in HCC patients is currently ongoing.

Patupilone, a macrocyclic polyketide, is a member of the epothilone class, a group of microtubule-stabilizing agents. It binds to the β-tubulin subunit of microtubules (254, 255). *In vitro* evidence indicates that patupilone is a more potent inducer of tubulin dimerization and is more effective in stabilizing preformed

microtubules than taxanes (255, 256). In HCC cell lines, patupilone has been shown to be 4- to130-fold more potent than taxanes (222). Clinical studies of patupilone in solid tumor types including lung and ovarian cancer demonstrated high potency in its anti-cancer activity (257-259).

Here the anti-tumor effect of everolimus alone or in combination with 2 additional microtubule targeting agents, including vinblastine and patupilone, was investigated in HCC cell models. This study attempted to compare the effects of different combinations and identify the molecular mechanisms involved.

5.2 Materials and Methods

5.2.1 Drugs

Everolimus (RAD001/Afinitor®) and patipilone (Epothilone B, EPO906) were obtained from Novartis Pharma (Basel, Switzerland), and dissolved in DMSO at a stock concentration of 10mM and stored at -20°C. Vinblastine sulfate (DBL) was obtained from Hospira (Wellington, New Zealand), and stored at a concentration of 1mg/ml in 0.9% sodium chloride at 4°C.

5.2.2 Cell culture

HCC cell lines used in this study were Hep3B, HepG2, Huh7, PLC/PRF/5 and SNU398. They were cultured as described in Chapter 2, section 2.2.

5.2.3 Cell viability assay

Cell viability was measured by MTT Assay as described in Chapter 2, section 2.3. Cells were plated on 48-well plates at density of 8000-18000 cells per well. Next day, either vehicle (DMSO) or increasing concentrations of everolimus (ranging from 0.1nM to 20μM) was added to HCC cells for 48 hrs and 72 hrs. For combination treatment, cells were treated with increasing concentrations of everolimus and 0.5nM of vinblastine or patupilone for 24 hrs.

5.2.4 Flow cytometry analysis of cell cycle

Cell cycle distribution of HCC cells was measured after exposure to everolimus alone or vinblastine alone or combination for 12 hrs or 16 hrs. The experimental procedures were described in Chapter 2, section 2.4.

5.2.5 Western blot analysis

Protein lysates were extracted from cells treated with single agents alone or combinations for 24 hrs, 48 hrs or 72 hrs. Western blot analysis was performed as described in Chapter 2, section 2.5. Primary antibodies and secondary antibodies used in this study are same as described in Chapter 4, section 4.2.6.

5.2.6 Statistical analysis

The data was presented as mean ± SEM. Student's t-test was performed using Graphpad Prism 4.0 software. Differences were considered statistically significant at $P<0.05$.

5.3 Results

5.3.1 Everolimus inhibited cell proliferation and mTOR signaling in HCC cells

To examine the effects of everolimus on HCC cell proliferation, a panel of five HCC cell lines (SNU398, Hep3B, HepG2, PLC/PRF/5 and Huh7) was treated with everolimus at various concentrations for 48 hrs. Dose-dependent inhibition of cell proliferation was observed in all five HCC cell lines. When compared to temsirolimus, everolimus-induced inhibition of HCC cell proliferation was found to be similar. The IC_{50} obtained on everolimus ranged from 2.25 ± 0.35 μM to 9.21 ± 0.69 μM (Fig. 5.1A).

Western blot analysis of HCC cells exposed to vehicle (DMSO) or 10nM everolimus for 48 hrs and 72 hrs was used to investigate the molecular mechanism induced by everolimus. Everolimus inhibited the phosphorylation of mTOR (Ser2448) and three downstream effectors of mTOR, including phosphor-p70S6k (Thr389), phosphor-ribosomal S6 (Ser240/244), and phosphor-4E-BP1 (Ser65) in SNU398, Hep3B and HepG2 cells (Fig. 5.1B). Consistent with a previous report that rapamycin caused Akt activation because of the mTOR feedback loop (260), everolimus treatment was found to slightly up-regulate the phosphorylation of Akt (Fig. 5.1B). These results confirmed that mTOR activity was inhibited by everolimus.

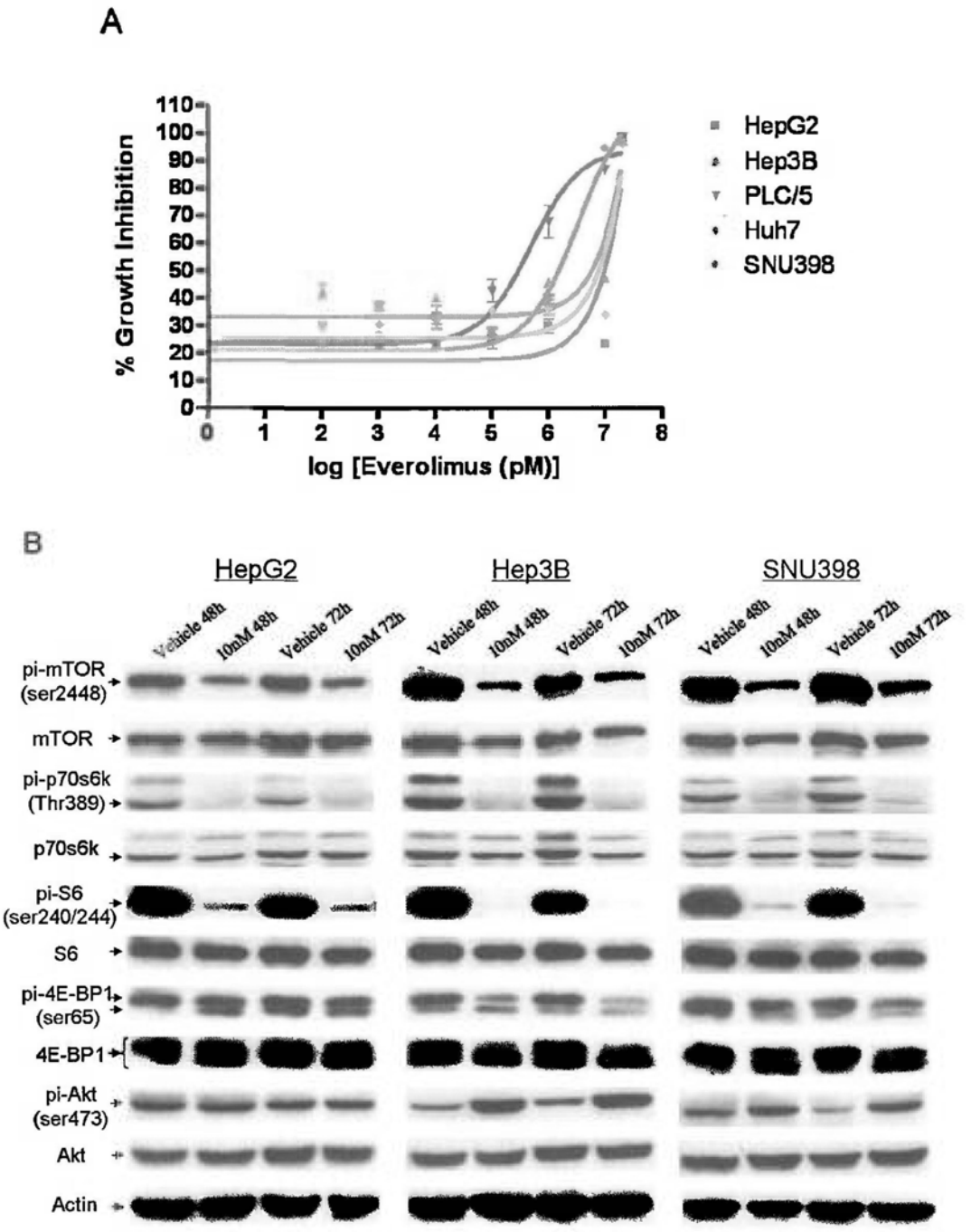

Figure 5.1 Everolimus inhibited cell proliferation and mTOR signaling in HCC cell lines. A. HCC cell lines Hep3B, HepG2, PLC/5, Huh7 and SNU398 were treated with increasing concentrations of everolimus for 48 hrs. Effect on cell viability was assessed by MTT assay. B. Everolimus inhibited the mTOR signaling in HCC cells. Cells were treated with 10nM everolimus for 48 hrs and 72 hrs. Components of the mTOR pathway were examined by western blot analysis. Similar

results were observed in 3 independent experiments.

5.3.2 Additive to Synergistic anti-tumor effect by everolimus/vinblastine combination *in vitro*

Previous studies have showed that the PI3K/Akt/mTOR signaling pathway may be associated with resistance to taxanes and other drugs acting on microtubules (27, 243). Therefore, the synergistic effect of everolimus/vinblastine on cell viability was examined in SNU398, Hep3B and HepG2 cell lines. Cell proliferation was inhibited after exposure to vinblastine alone for 24 hrs. Cell proliferation was further inhibited when different doses of everolimus were combined with 0.5nM vinblastine, in Hep3B, HepG2 and SNU398 cells (Fig. 5.2A).

Exposure to everolimus alone inhibited the phosphorylation of mTOR (Ser2448), p70S6k (Thr389), ribosomal S6 (Ser240/244), and 4E-BP1 (Ser65) in all 3 HCC cell lines. But vinblastine treatment did not affect the mTOR activity, and the inhibitory effect was not enhanced when everolimus was combined with vinblastine (Fig. 5.2B).

To further analyze the molecular mechanism of synergistic effect of everolimus and vinblastine combination, western blot analysis was used to evaluate the expression of some anti-apoptotic and survival proteins. Exposure to everolimus alone or vinblastine alone did not inhibit the expression of survivin, Bcl-2 nor Mcl-1. However, everolimus and vinblastine combination significantly decreased the expression levels of these three proteins (Fig. 5.2C). These findings suggested that concerted down-regulation of several important anti-apoptotic/survival proteins may mediate the synergistic effect of the everolimus/vinblastine combination.

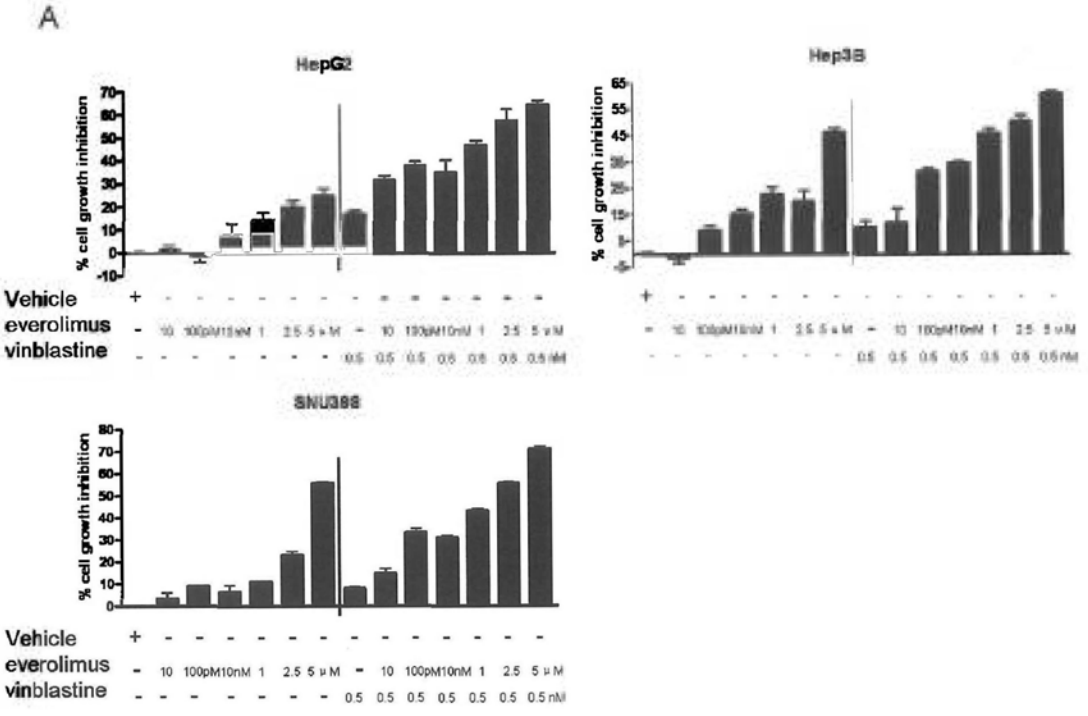
A
HepG2
Hep3B
SNU398
% cell growth inhibition
Vehicle
everolimus
vinblastine

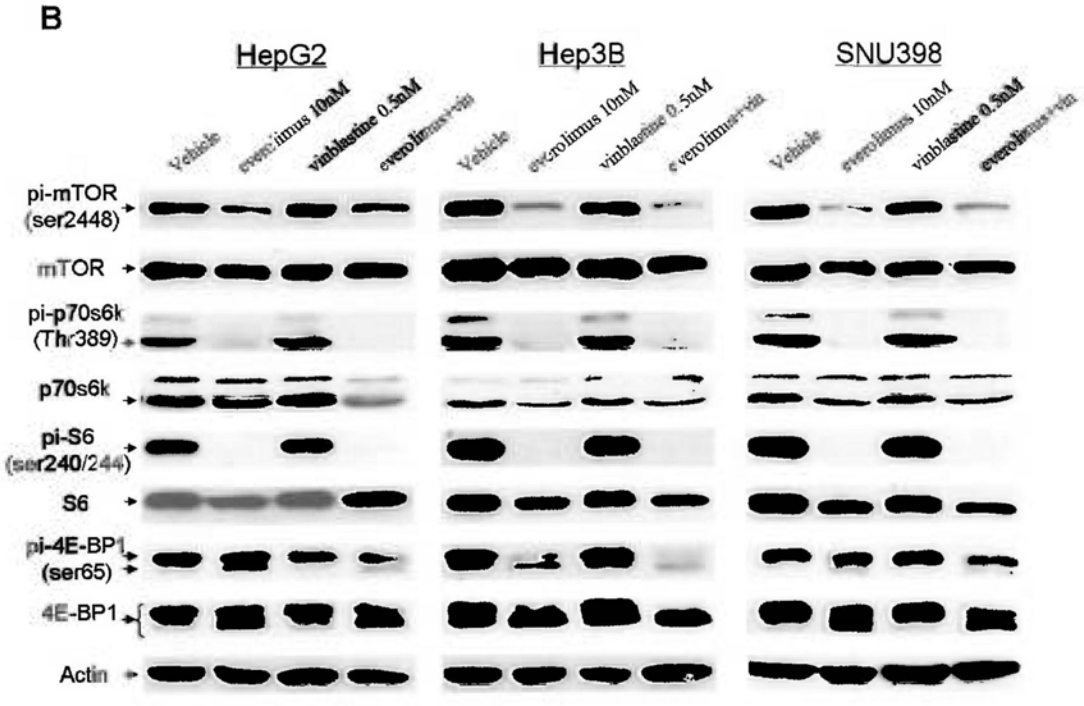
B
HepG2
Hep3B
SNU398
Vehicle
everolimus 10nM
vinblastine 0.5nM
pi-mTOR (ser2448)
mTOR
pi-p70s6k (Thr389)
p70s6k
pi-S6 (ser240/244)
S6
pi-4E-BP1 (ser65)
4E-BP1
Actin

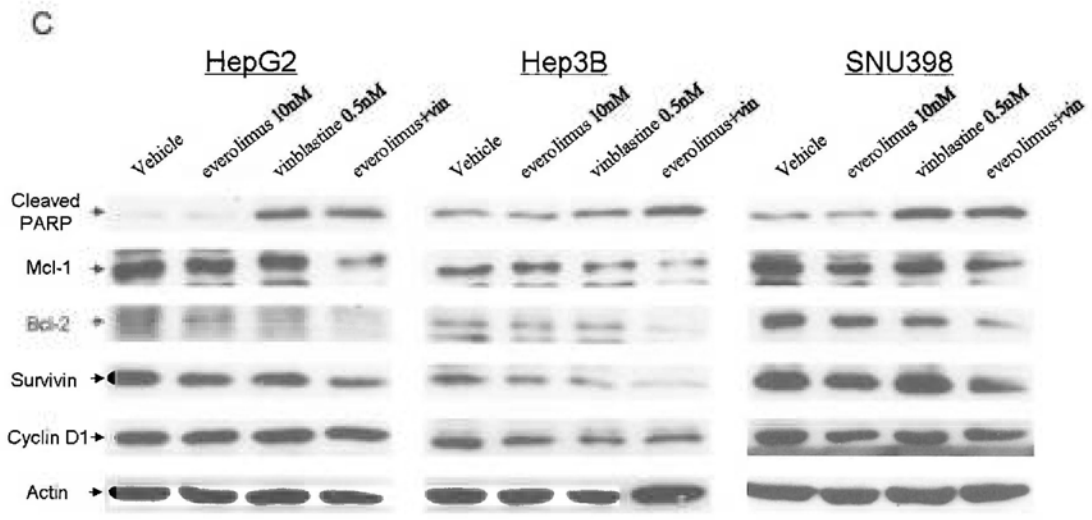

Figure 5.2 Everolimus exerted additive to synergistic growth inhibitory activity on HCC cells with vinblastine. A. Cells were treated with various concentrations of everolimus in combination with 0.5nM vinblastine for 24 hrs. Cell viability was assessed by MTT assay. Cumulative results from 3 independent experiments were shown as mean ± SEM. B. mTOR pathway did not further inhibited by everolimus/vinblastine combination treatment. Cells were treated with everolimus and/or vinblastine for 24 hrs. Components of the mTOR pathway were examined by western blot analysis. C. Survivin, Bcl-2 and Mcl-1 were down-regulated by everolimus/vinblastine combination treatment. Cells were treated with everolimus and/or vinblastine for 24 hrs. The expression levels of cleaved PARP, Mcl-1, Bcl-2, survivin, Cyclin D1 and actin were assessed by western blot analysis.

5.3.3 Everolimus moderately enhanced chemosensitivity of microtubule-stabilizing agent patupilone *in vitro*

Patupilone is 4- to 130-fold more effective than taxanes in inhibiting the growth of most HCC cell lines (222). The effect of everolimus/patupilone combination on cell viability in HCC cell lines was then examined. Dose-dependent inhibition of cell proliferation was observed in all five cell lines after exposure to patupilone alone for 24 hrs (Fig. 5.3A). However, the effect of patupilone was only mildly enhanced when combined with different doses of everolimus in SNU398, Hep3B and HepG2 cell lines (Fig. 5.3B).

In contrast to everolimus/vinblastine combination, the expression levels of the three anti-apoptotic/survival proteins (survivin, Bcl-2, Mcl-1) were not significantly affected by the everolimus/patupilone combination (Fig. 5.3C).

A

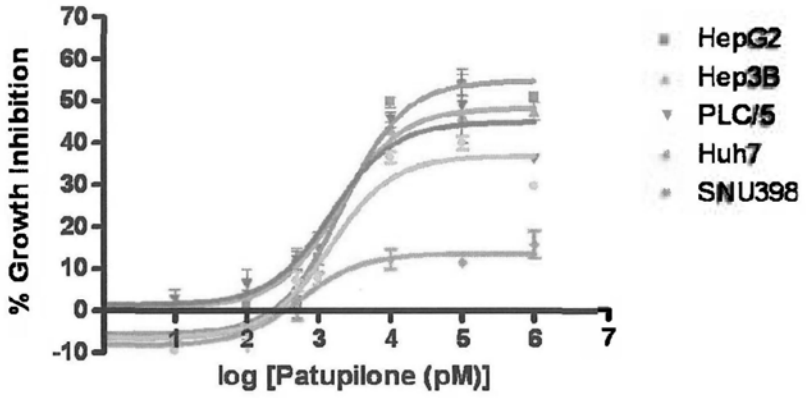
% Growth Inhibition
log [Patupilone (pM)]
HepG2
Hep3B
PLC/5
Huh7
SNU398

B

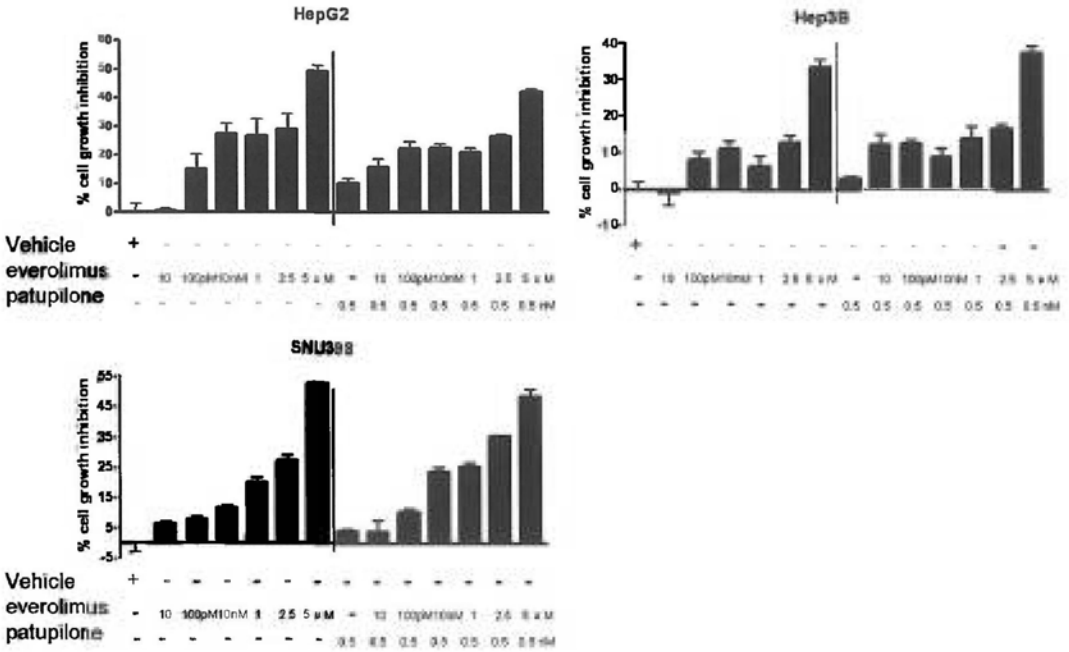
HepG2
Hep3B
SNU398
% cell growth inhibition
Vehicle
everolimus
patupilone

C

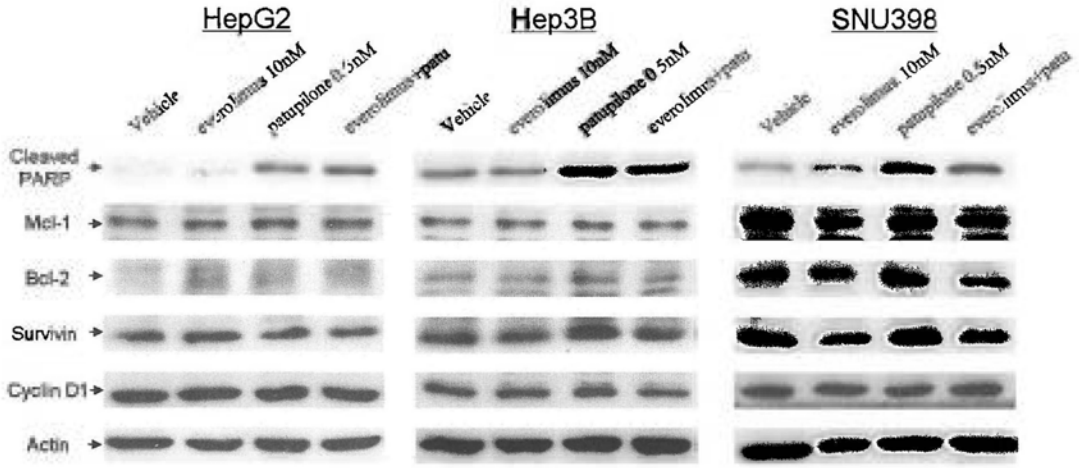
HepG2
Hep3B
SNU398
Vehicle
everolimus 10nM
patupilone 0.5nM
everolimus+patu
Cleaved PARP
Mcl-1
Bcl-2
Survivin
Cyclin D1
Actin

Figure 5.3 Everolimus moderately enhanced the effectiveness of the microtubule-stabilizing agent patupilone in HCC cells. A. Patupilone inhibited HCC cell proliferation. HCC cell lines Hep3B, HepG2, PLC/5, Huh7 and SNU398 were treated with increasing concentrations of patupilone for 24 hrs. Effect on cell viability was assessed by MTT assay. B. Cells were treated with various concentrations of everolimus in combination with 0.5nM patupilone for 24 hrs. Cell viability was assessed by MTT assay. Cumulative results from 3 independent experiments were shown as mean ± SEM. C. The expression levels of several key anti-apoptotic/survival proteins (survivin, Bcl-2, Mcl-1) were not significantly affected by the everolimus/patupilone combination. Cells were treated with everolimus and/or patupilone for 24 hrs. The expression levels of cleaved PARP, Mcl-1, Bcl-2, survivin, Cyclin D1 and actin were assessed by western blot analysis.

5.3.4 Everolimus/vinblastine combination induced cell cycle arrest

It is known that mTOR inhibitors induce cell cycle arrest at G_1 phase and vinblastine induces cell cycle arrest at G_2/M phase through destabilizing microtubule polymerization (244, 245). The effect of such an everolimus/vinblastine combination on HCC cell cycle progression was hence examined. In all 3 HCC cell lines tested, flow cytometry analysis indicated that an increase in the G_1 population was found when everolimus was applied, and an increase in the G_2/M population was found when vinblastine was applied (Fig. 5.4), which was consistent with the previous findings (245). And it was noticed that both G_1 phase and G_2/M phase arrest occurred and as a result, there was an obvious drop in the S population when the two drug combination was applied (Fig. 5.4), suggesting that the combination may cause inhibition of DNA synthesis and induces cell cycle arrest.

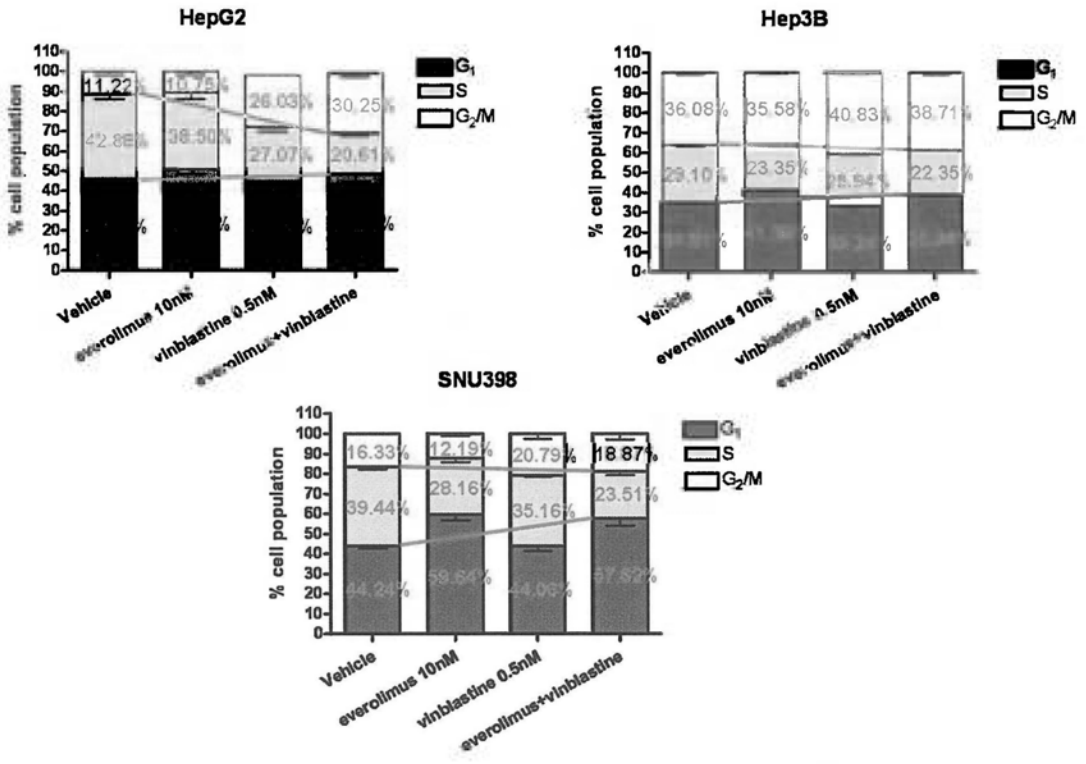

Figure 5.4 Everolimus/vinblastine combination resulted in both G_1 and G_2/M arrest in HCC cells. Cells treated with everolimus and/or vinblastine for 16 hrs were harvested, stained with PI, and analyzed by flow cytometry. Cumulative results from 3 independent experiments were shown as mean ± SEM.

5.4 Discussion

In this study, it was demonstrated that combination of everolimus and vinblastine elicited additive to synergistic anti-tumor effect in HCC cells, however, everolimus was only able to moderately enhance the efficacy of another microtubule targeting agent, patupilone.

As in the temsirolimus study, everolimus alone suppressed tumor cell proliferation in HCC cell lines and inhibited the mTOR activity accordingly. Similar to the temsirolimus/vinblastine combination, when everolimus was applied with low dose of vinblastine (0.5nM), marked synergistic effect was observed in all 3 HCC cell lines, accompanied with cell cycle arrest at both G_1 and G_2/M phases, and PARP cleavage (a hallmark for apoptosis). Further mechanistic investigation demonstrated the down-regulation of survivin, Bcl-2 and Mcl-1 expressions by everolimus/vinblastine combination as well. Recent reported studies have also demonstrated that mTOR inhibitors have synergistic effect with paclitaxel, vinblastine or vinorelbine in multiple cancers, including neuroblastoma, endometrial cancer and lymphoma (151, 167, 169-171). The results in this study are consistent with the previous reported evidences and support the role of combined targeting of mTOR and the microtubule as a promising strategy for the treatment of HCC.

However, everolimus/patupilone combination appeared to be less effective. Accordingly, marked change in survivn, Bcl-2 or Mcl-1 expressions was not observed with this combination. It was noticed that HCC cells were more sensitive to patupilone than vinblastine (maximum growth inhibition at 24 hrs was 60% vs

30% in HepG2 and Hep3B cells, data not shown). Therefore, the ability of mTOR inhibition to further enhance chenosensitivity of HCC cells to patupilone may be limited. This view is supported by a previous finding by Faried *et al* who reported that rapamycin significantly enhanced the chemosensitivity of CaSki cells (a paclitaxel resistant cell line) to paclitaxel, but did not affect the sensitivity of HeLa cells (a paclitaxel sensitive cell line) (27). Besides, pharmacokinetics and pharmacodynamics of the two compounds may also affect the combination efficacy, and this needs to be further investigated.

The findings from my studies suggested that combination of mTOR inhibitors and microtubule targeting agents may lead to diverse outcomes, e.g., less than additive, additive, or synergistic effect. Choosing the most effective combination is an important issue that can be addressed with preclinical studies. With such knowledge, selected patient population and appropriate drug combinations can be identified and clinically evaluated. Such an approach could be adopted for HCC studies.

Chapter 6: Summary

The PI3K/Akt/mTOR signaling pathway is activated in ~45% HCC, making it an important target for HCC therapy. mTOR is a druggable target for cancer treatment and increasing number of mTOR inhibitors with good pharmacologic profiles and high specificity are being developed. Cumulative evidences indicate that targeting this pathway results in good cytostatic activity both *in vitro* and *in vivo* (235-237). In this thesis, the findings in gene expression profiling of 43 paired HCC tumors and adjacent non-tumoral liver tissues revealed that microtubule-related cellular assembly is a major biological/functional process involved in the malignant transformation of HCC. Like mTOR, the microtubule is a highly druggable target and various microtubule targeting chemotherapeutic agents (e.g. taxanes) have been developed and used to treat non-HCC malignancies. Emerging evidences demonstrated the PI3K/Akt/mTOR signaling pathway also contributes to resistance to chemotherapy in several cancers including lung cancer, breast cancer and prostate cancer, besides its major role in regulating cancer cell growth and survival. This thesis hypothesizes that individually targeting of mTOR and microtubule would be effective in inhibiting HCC growth, and targeting of mTOR may enhance the activity of microtubule targeting agents in HCC models. As a proof-of-concept study, the therapeutic potential of mTOR targeting, microtubule targeting, as well as combined targeting of both mTOR and the microtubule was examined in HCC models. The *in vitro* and *in vivo* studies demonstrated that microtubule targeting agent *nab*-paclitaxel was effective in inhibiting HCC cell growth with much better

efficacy and less toxicity than other taxanes and doxorubucin; combination of mTOR inhibitor temsirolimus or everolimus, with a microtubule targeting agent vinblastine elicited additive to synergistic effect on HCC proliferation *in vitro* and *in vivo*. This may serve as a direction for future clinical studies in HCC.

Taxanes are known to bind microtubule polymers and stabilize microtubule in tumor cells, thereby arrest cells in G_2/M and promote cell death by suppressing microtubule dynamics. Recent studies have shown that drug delivery by nanoparticles can enhance therapeutic efficacy, thus reducing side effects. Therefore, the effects and toxicities of conventional paclitaxel and docetaxel were compared with *nab*-paclitaxel both *in vitro* and *in vivo*. In this study described in Chapter 3, although paclitaxel and docetaxel exhibited better therapeutic efficacy than doxorubicin, *nab*-paclitaxel was found to be the most effective microtubule targeting agent for inhibiting HCC cell growth (i.e. with the lowest IC_{50} for 3 HCC cell lines tested). *nab*-Paclitaxel induced HCC cell cycle arrest at G_2/M phase due to microtubule polymerization, resulting in apoptosis. In the *in vivo* study, *nab*-paclitaxel has a higher maximum tolerated dose compared with paclitaxel, docetaxel and doxorubicin. In the microarray data of this study, it was also found that Stathmin 1 (*STMN1*), a microtubule regulatory gene, was significantly over-expressed in HCC. The current findings also indicated that STMN1 is over-expressed in all HCC cell lines studied as well as in primary HCC tumors vs normal livers. As STMN1 is a microtubule-destabilizing factor, further experiment was conducted to assess if the knockdown of STMN1 expression could elicit

synergistic growth inhibitory effect on *nab*-paclitaxel treatment in HCC. It was observed that the knockdown of STMN1 expression reduced viability by about 40% in Hep3B. More importantly, suppression of STMN1 was able to sensitize HCC cells to *nab*-paclitaxel treatment by 7.7-fold. Therefore, *nab*-paclitaxel appeared to be a safe and effective cytotoxic agent for HCC treatment.

Meanwhile, mTOR inhibitor temsirolimus alone suppressed tumor cell proliferation in HCC cell lines and inhibited the mTOR activity accordingly, with an IC_{50} of 1.27±0.06μM (Huh7), 8.77±0.76μM (HepG2), and 52.95±17.14μM (Hep3B). When temsirolimus was applied with a low dose of another microtubule targeting agent, vinblastine (1nM), additive to synergistic effect was observed in all 3 HCC cell lines with maximum growth inhibition of 80-90%. This marked growth inhibition was accompanied by cell cycle arrest at both G_1 and G_2/M phases and PARP cleavage (a hallmark for apoptosis). It was shown for the first time that temsirolimus/vinblastine combination resulted in enhanced synergistic anti-tumor activity when compared to single drug alone in xenograft models *in vivo*. When the molecular mechanism involved in the synergistic effect of temsirolimus/vinblastine combination was further investigated, and it was found that the combination significantly decreased the expression levels of anti-apoptotic/survival proteins survivin, Bcl-2 and Mcl-1 in HCC cells. It is hypothesized that inhibition of these key anti-apoptotic/survival proteins may represent a novel mechanistic action of this highly effective temsirolimus/vinblastine combination in HCC models. Indeed, over-expression of any one of these three genes in HCC cells by transient

transfection did result in partial rescue of the growth inhibitory effect of the combination. These findings provide new insights into the treatment of HCC by combining mTOR inhibition with anti-microtubule therapy.

To further confirm that dual targeting of mTOR and the microtubule is a promising therapeutic strategy for HCC, the anti-tumor effect of another mTOR inhibitor everolimus, alone or in combination with microtubule targeting agent vinblastine or patupilone, was then investigated in HCC cells. Similar to the results obtained from the temsirolimus/vinblastine combination, everolimus/vinblastine combination resulted in an additive to synergistic effect accompanied with cell cycle arrest at both G_1 and G_2/M phases, and PARP cleavage. The combination also caused concerted down-regulation of anti-apoptotic/survival proteins (survivin, Bcl-2 and Mcl-1). However, everolimus only moderately enhanced the sensitivity of patupilone.

In conclusion, both the PI3K/Akt/mTOR pathway and the microtubule represent promising therapeutic targets for HCC treatment. As a novel nanoparticle form of paclitaxel, *nab*-paclitaxel is shown to have more enhanced efficacy with minimal toxicity in both *in vitro* and *in vivo* HCC models, suggesting *nab*-paclitaxel is a promising novel drug for HCC treatment. On the other hand, though mTOR inhibitors temsirolimus or everolimus alone did not result in cell death, combining either of these two mTOR inhibitors with conventional microtubule targeting agent vinblastine resulted in synergistic growth inhibition in HCC models. Therefore, the use of mTOR inhibitors in combination with vinblastine may hold promise as a

novel treatment option for HCC patients and warrants for further clinical investigations.

Chapter 7: Appendix chapter

7.1 Additive to synergistic anti-tumor effect by temsirolimus/*nab*-paclitaxel combination *in vitro*

Previous studies have shown that the PI3K/Akt/mTOR signaling pathway may be associated with resistance to taxanes and other drugs acting on microtubules (27, 243). Results in Chapter 3 have demonstrated that *nab*-paclitaxel had the most potent activity against HCC when compared with other taxanes. Therefore, the potential therapeutic efficacy of the temsirolimus/*nab*-paclitaxel combination was examined on HCC cell growth in a panel of HCC cell lines, including Huh7, Hep3B and HepG2. As shown in Figure 7.1A, HCC cell growth was inhibited by very low dose of *nab*-paclitaxel (1nM) as early as 24 hrs. Such a growth inhibition was further increased when *nab*-paclitaxel was combined with increasing doses of temsirolimus. In Hep3B and HepG2 cells, the temsirolimus/*nab*-paclitaxel combination was found to result in synergistic growth inhibition with maximal growth inhibition of 75-80% at 24 hrs. Whereas for Huh7, one of the most temsirolimus-sensitive cell line, temsirolimus alone already elicited very potent growth inhibitory activity and the combination with *nab*-paclitaxel resulted in additive but not synergistic growth inhibition at 24 hrs (Fig. 7.1A).

To further analyze the molecular mechanism underlying such a synergistic growth inhibitory effect of temsirolimus/*nab*-paclitaxel combination, western blot analysis was performed to evaluate the expression of several anti-apoptotic and survival proteins upon combination treatment. As shown in Figure 7.1B, exposure to

temsirolimus or *nab*-paclitaxel alone did not alter the expression of survivin, Bcl-2 or Mcl-1 at 24 hrs. However, the expressions of all these three anti-apoptotic/survival proteins were noticeably reduced by the temsirolimus/*nab*-paclitaxel combination (Fig. 7.1B). These findings suggested that concerted down-regulation of several important anti-apoptotic/survival proteins may mediate the synergistic effect of the temsirolimus/*nab*-paclitaxel combination.

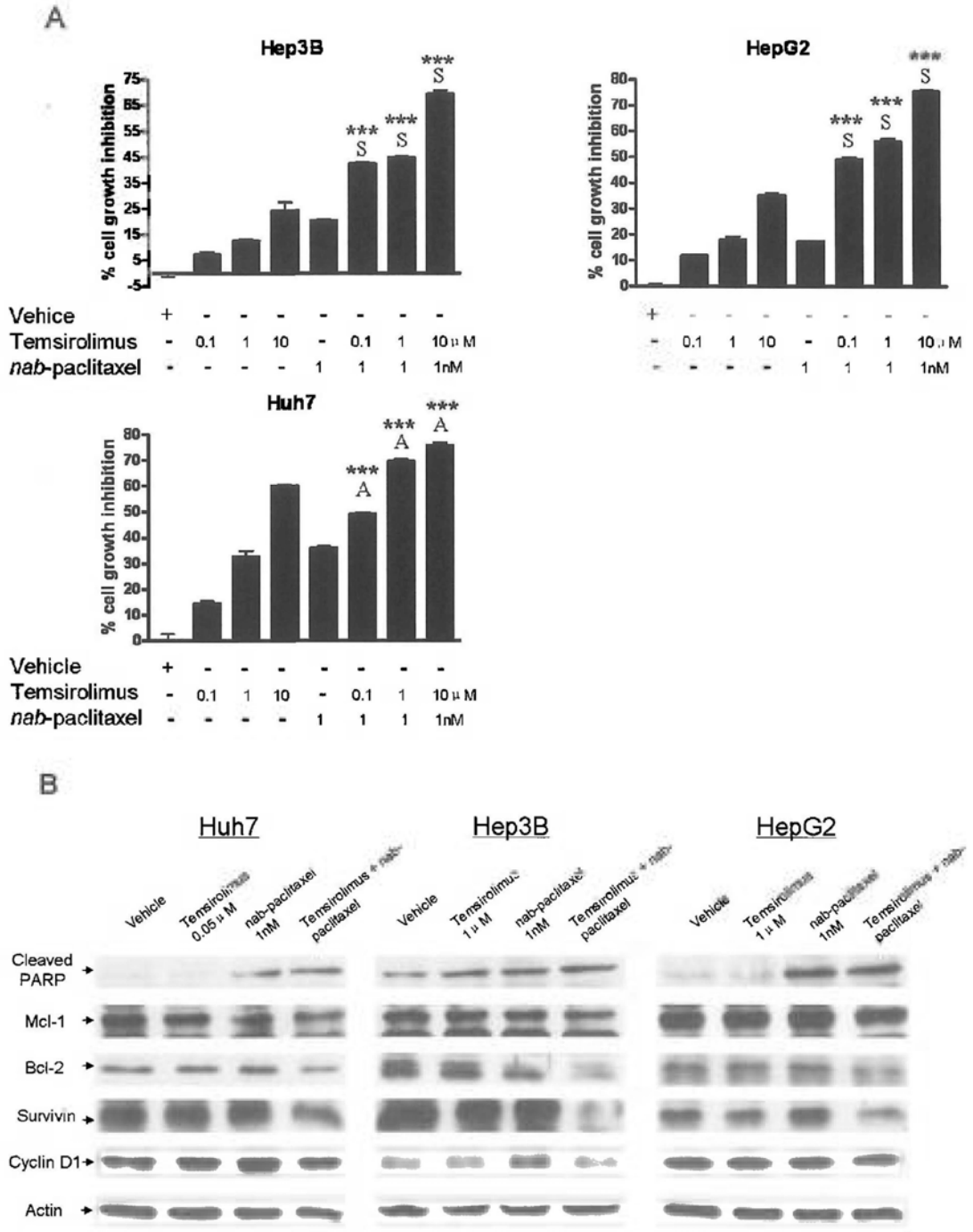

Figure 7.1 Temsirolimus exerted additive to synergistic growth inhibitory activity on HCC cells with *nab*-paclitaxel. A. Cells were treated with increasing concentrations of temsirolimus in combination with 1nM *nab*-paclitaxel for 24 hrs. Cell viability was assessed by MTT assay. Cumulative results from 3 independent experiments were shown as mean ± SEM (t-test, ***P<0.001 vs temsirolimus

treated group) (S: synergistic effect; A: additive effect). B. Survivin, Bcl-2 and Mcl-1 were down-regulated by temsirolimus/*nab*-paclitaxel combination treatment. Cells were treated with temsirolimus and/or *nab*-paclitaxel for 24 hrs. The expression levels of cleaved PARP, Mcl-1, Bcl-2, survivin, Cyclin D1 and actin were assessed by western blot analysis.

7.2 Construction of HBx, HBxΔ14 and HBxΔ35 expression vectors

pcDNA3.1-HBx, pcDNA3.1-HBxΔ14, and pcDNA3.1-HBxΔ35 were obtained from Prof. Alfred Cheng at the Department of Medicine and Therapeutics, the Chinese University of Hong Kong. An HA-HA-tag was added to each of these constructs by subcloning into the pcDNA3-HA vector (Fig. 7.2A). Simply, full lengths of HBx, HBxΔ14 (14 amino acids deletion), and HBxΔ35 (35 amino acids deletion) were amplified by PCR using the original plasmids as templates. One common forward primer and three different reverse primers were used for PCR. The primers that designed contained 4 extra nucleotides (GTAG) for forward primer, (GCTG) for reverse primers, a restriction site *Hind*III (AAGCTT) for forward primer and *Xho*I (CTCGAG) for reverse primers. The primer sequences are as follows (Table 7.1).

Each amplified DNA fragment and pcDNA3-HA vector (Fig. 7.2A) was double-digested by *Hind*III and *Xho*I (Fermentas, Burlington, Canada) in corresponding buffer and condition following the manufacturer's instructions. After heat inactivation of the digestive enzymes and purification of the amplified DNA fragments and pcDNA3-HA vector, they were ligased together using T4 ligase (Fermentas) according to the manufacturer's instructions. The sequences of the cloned fragments were then confirmed by DNA sequencing.

Several clones were picked for each construct. In order to confirm the expression of the cloned HBx genes, the DNA constructs were transfected into an HBV-negative cell line, HepG2, for 48 hrs and the expression of HBx, HBxΔ14 and HBxΔ35 were confirmed by western blot analysis (Fig. 7.2B).

A

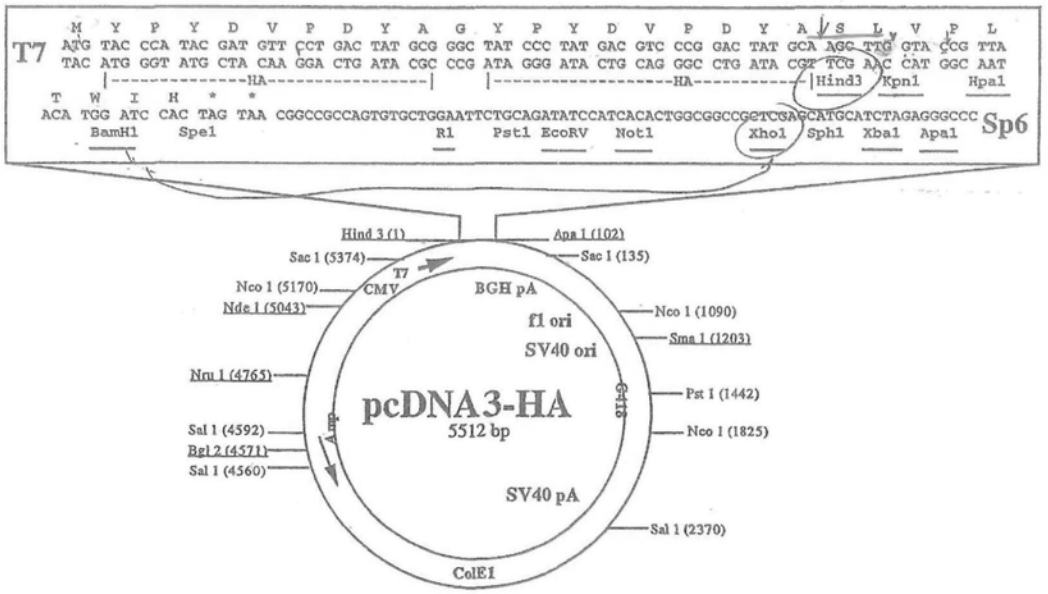

B

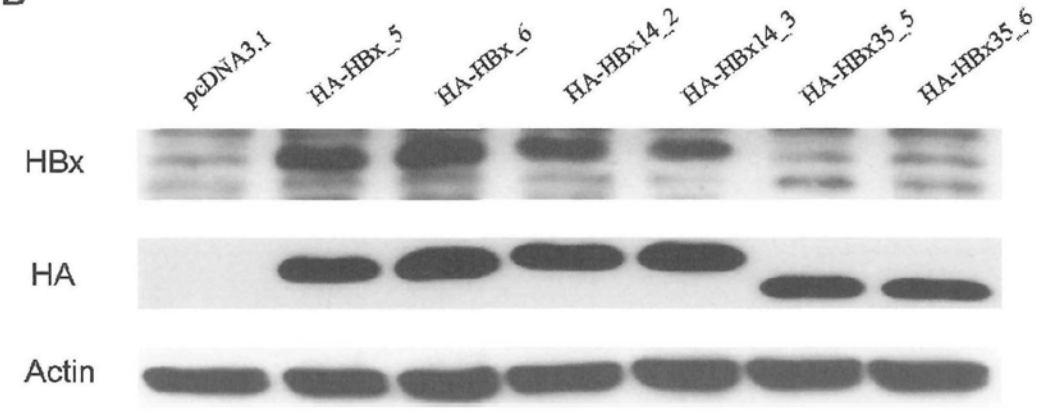

Figure 7.2 Expression of HA-HA-tagged HBx, HBxΔ14 and HBxΔ35 in HepG2 cells. A. Multi-cloning sites of the pcDNA3-HA vector was shown and the restriction digestion sites were indicated by circles. B. Expression levels of HA-HA-tagged HBx, HBxΔ14 and HBxΔ35 in HepG2 cells using different constructed clones (by western blot analysis).

Table 7.1 Primer sequences for HBx, HBxΔ14 and HBxΔ35 plasmids construction

Primer	Sequence (5'----3')	Length of PCR fragment
Forward	5'-GTAGAAGCTTGGCTGCTAGGATGTGCTG-3'	-
Reverse for HBx	5'-GCTGCTCGAGTTAGGCAGAGGTGAAAA-3'	462bp
Reverse for HBxΔ14	5'-GCTGCTCGAGTTTATGCCTACAGCCTCCT-3'	417bp
Reverse for HBxΔ35	5'-GCTGCTCGAGGTCTTTAAACACACAGTC-3'	354bp

Underlined nucleotides indicate the restriction digestion sites (*Hind*III: AAGCTT; *Xho*I: CTCGAG).

7.3 HBx did not affect HCC cell sensitivity to temsirolimus

It is well established that the majority of HCCs are related to chronic HBV or HCV infection. HBV could modulate cell proliferation through the expression of viral proteins, in particular, the X protein (HBx) (52). HBx protein is known as a multifunctional protein. It not only co-activates transcription of viral and cellular genes, but also coordinates the balance between proliferation and programmed cell death (53, 54). HBx can activate PI3K pathway and block apoptosis in a p53-independent manner (63). It is believed that high level of Akt activity may result in hyper-sensitivity to mTOR inhibitors (261). Therefore, experiments were conducted to check if HBx would affect HCC cell sensitivity to mTOR inhibitor temsirolimus in this study. HBx plasmid was kindly provided by Prof. Alfred Cheng and subsequently tagged with HA as described above. Both the HBV-negative cell line Huh7 and HepG2 cells were transfected with expression plasmid pcDNA3-HA-HBx using Lipofectamine 2000 reagent (Invitrogen). Briefly, cells were incubated with 3μg plasmid DNA. Six hours after transfection, the transfection medium was replaced by complete medium. The expression of HBx was assessed by western blot analysis. As shown in Figure 7.3A, the expression of HA-HA-HBx was observed up to 48 hrs after transfection. Similar to the previous report by Lee *et al* (63), expression of HBx only resulted in moderate activation of Akt (Fig. 7.3A). Figure 7.3B shows that HBx transfection slightly stimulated the HCC cell growth. However, at both 1μM and 10μM concentrations (drug was given 1 day post-transfection), temsirolimus elicited a very similar degree of HCC cell growth

inhibition at 24 hrs as assayed by MTT (P>0.05) (Fig. 7.3C).

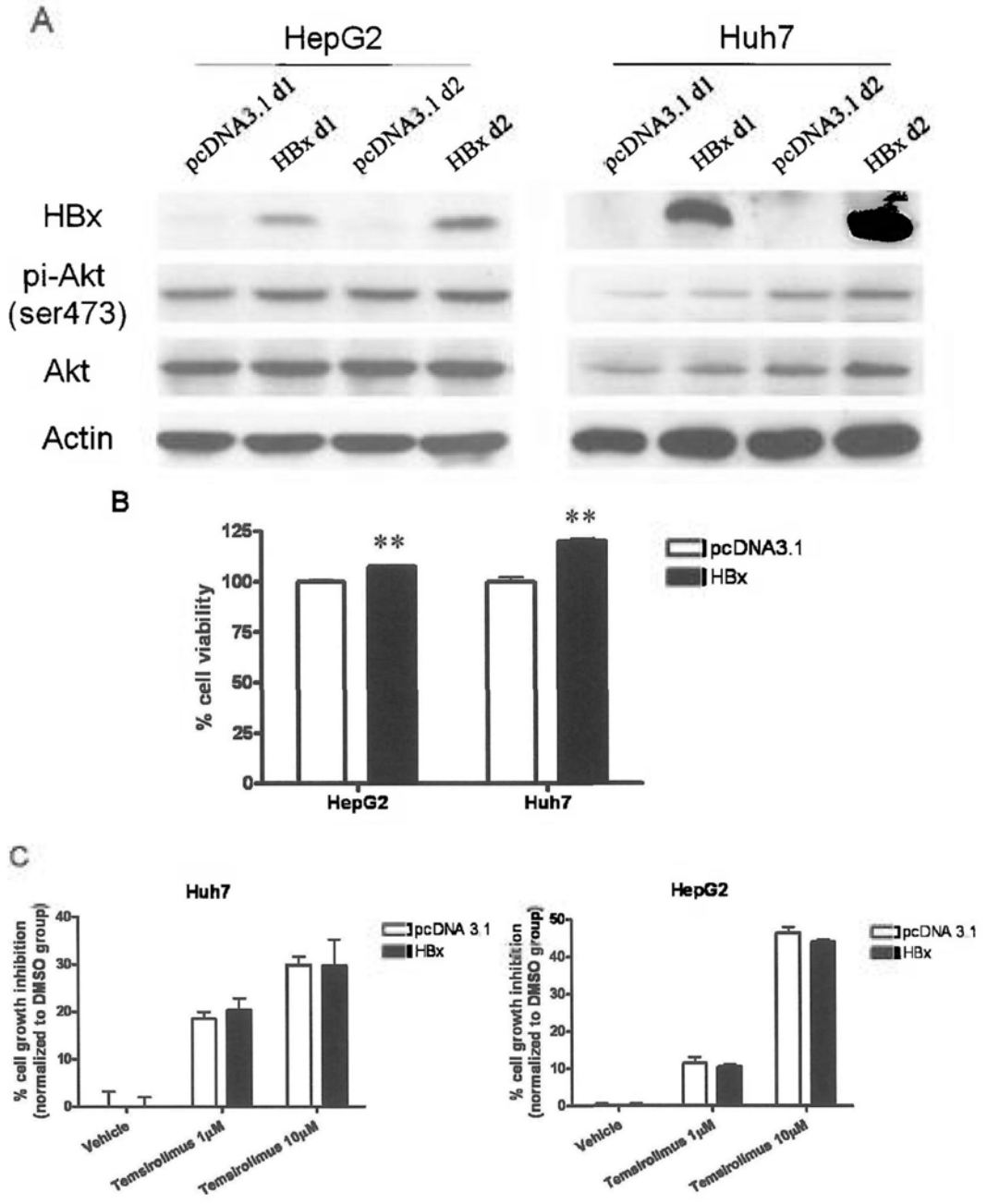

Figure 7.3 HBx did not affect HCC cell sensitivity to temsirolimus. A. Expression levels of HBx, pi-Akt (ser473) and Akt at day 1 and day 2 after HBx plasmid transfection in the HBV-negative cell lines HepG2 and Huh7 (by western blot analysis). B. HBx moderately stimulated HCC cell growth. HCC cells were transfected with HBx plasmid for 48 hrs. Cell viability was assessed by MTT assay. Cumulative results from 3 independent experiments were shown as mean ± SEM

(t-test, **P<0.01 vs pcDNA3.1 transfectants). C. Expression of HBx did not affect HCC cell sensitivity to temsirolimus. HCC cells transfected with HBx plasmid were treated with temsirolimus for 24 hrs. Cumulative results from 3 independent experiments were shown as mean ± SEM (t-test, P>0.05 vs pcDNA3.1 transfectants).

Chapter 8: Future direction

1. In Chapter 3, it was demonstrated the *in vitro* and *in vivo* anti-tumor activity of *nab*-paclitaxel and the synergistic effect of *nab*-paclitaxel/siSTMN1 combination *in vitro*. I would propose to investigate the *in vivo* anti-tumor activity of *nab*-paclitaxel/siSTMN1 combination in HCC xenograft models. Firstly, STMN1 shRNA SK-HEP-1 or Hep3B stable clone and mock shRNA SK-HEP-1 or Hep3B stable clone will be established. Then HCC xenografts will be established by inoculating SK-HEP-1 or Hep3B stable cells subcutaneously into nude mice. When the tumors reach the size of ~3 × 3mm^2, *nab*-paclitaxel or vehicle control (PBS) will be administrated by intraperitoneal injection (i.p.) every 2 days for 5 times, at a dose of 35mmol/kg. Tumor size will be carefully monitored and measured using a digital caliper once every 2 days. Tumor volume from the vehicle, *nab*-paclitaxel treated plus mock shRNA and *nab*-paclitaxel treated plus STMN1 shRNA groups will be compared.

Results from *in vivo* experiments will serve as a proof-of-principal study for combined targeting of microtubule and STMN1 in HCC.

2. In Chapter 4 and Chapter 5, it was demonstrated that combined targeting of mTOR and the microtubule elicited marked anti-tumor effect in HCC both *in vitro* and *in vivo*. However, it was noticed that different drug combinations may have different effects; temsirolimus/vinblastine and everolimus/vinblastine combinations had synergistic effect, but everolimus only moderately enhanced the sensitivity of

patupilone. To choose the most appropriate drug combination, I propose a screening study of more drug combinations in order to determine the best synergistic activity in HCC models. For mTOR inhibitors, rapamycin, everolimus, temsirolimus, ridaforolimus, and dual inhibitors such as AZD8055 (an mTORC1/2 inhibitor) and BEZ235 (a dual PI3K-mTOR inhibitor) will be included; while for microtubule targeting drugs, drugs that have been studied and reported in part within this thesis (paclitaxel, docetaxel, *nab*-paclitaxel, vinblastine, vinorelbine and patupilone), and newer anti-microtubule agents, halichondrins (such as eribulin) will be included. Growth inhibitory effects of various drug combinations will be evaluated in multiple HCC cell lines by MTT assay. The results will reveal specific drug combination that could potentially be the most clinically relevant therapeutic option in HCC.

References

1. Bosch FX, Ribes J, Diaz M, Cleries R. Primary liver cancer: Worldwide incidence and trends. Gastroenterology 2004;127:S5-S16.

2. Yang L, Parkin DM, Ferlay J, Li LA, Chen YD. Estimates of cancer incidence in China for 2000 and projections for 2005. Cancer Epidemiology Biomarkers & Prevention 2005;14:243-250.

3. Schafer DF, Sorrell MF. Hepatocellular carcinoma. Lancet 1999;353:1253-1257.

4. Gomaa AI, Khan SA, Toledano MB, Waked I, Taylor-Robinson SD. Hepatocellular carcinoma: Epidemiology, risk factors and pathogenesis. World Journal of Gastroenterology 2008;14:4300-4308.

5. Di Bisceglie AM. Epidemiology and clinical presentation of hepatocellular carcinoma. Journal of Vascular and Interventional Radiology 2002;13:S169-S171.

6. Block TM, Mehta AS, Fimmel CJ, Jordan R. Molecular viral oncology of hepatocellular carcinoma. Oncogene 2003;22:5093-5107.

7. Gao JD, Shao YF, Xu Y, Ming LH, Wu ZY, Liu GT, Wang XH, Gao WH, Sun YT, Feng XL, Liang LM, Zhang YH, Sun ZT Tight association of hepatocellular carcinoma with HBV infection in North China. Hepatobiliary & Pancreatic Diseases International 2005;4:46-49.

8. De Mitri MS, Cassini R, Morsica G, Bagaglio S, Andreone P, Loggi E, Muratori P, et al. Virological analysis, genotypes and mutational patterns of the HBV precore/core gene in HBV/HCV-related hepatocellular carcinoma. Journal of Viral Hepatitis 2006;13:574-581.

9. Benvegnu L, Fattovich G, Noventa F, Tremolada F, Chemello L, Cecchetto A, Alberti A. Concurrent Hepatitis-B and Hepatitis-C Virus-Infection and Risk of Hepatocellular-Carcinoma in Cirrhosis - a Prospective-Study. Cancer 1994;74:2442-2448.

10. Sezaki H, Kobayashi M, Hosaka T, Someya T, Akuta N, Suzuki F, Tsubota A, et al. Hepatocellular carcinoma in noncirrhotic young adult patients with chronic hepatitis B viral infection. Journal of Gastroenterology 2004;39:550-556.

11. ElRefaie A, Savage K, Bhattacharya S, Khakoo S, Harrison TJ, ElBatanony M, Soliman ES, et al. HCV-associated hepatocellular carcinoma without cirrhosis. Journal of Hepatology 1996;24:277-285.

12. Fargion S, Fracanzani AL, Piperno A, Braga M, Dalba R, Ronchi G, Fiorelli G. Prognostic Factors for Hepatocellular-Carcinoma in Genetic Hemochromatosis. Hepatology 1994;20:1426-1431.

13. Caballeria L, Pares A, Castells A, Gines A, Bru C, Rodes J. Hepatocellular carcinoma in primary biliary cirrhosis: Similar incidence to that in hepatitis C virus-related cirrhosis. American Journal of Gastroenterology 2001;96:1160-1163.

14. Davila JA, Morgan RO, Shaib Y, McGlynn KA, El-Serag HB. Hepatitis C infection and the increasing incidence of hepatocellular carcinoma: A population-based study. Gastroenterology 2004;127:1372-1380.

15. Herath NI, Leggett BA, Macdonald GA. Review of genetic and epigenetic alterations in hepatocarcinogenesis. Journal of Gastroenterology and Hepatology 2006;21:15-21.

16. Yoo HY, Patt CH, Geschwind JF, Thuluvath PJ. The outcome of liver transplantation in patients with hepatocellular carcinoma in the united states between 1987 and 2001: 5-year survival has improved significantly with time. Journal of Clinical Oncology 2003;21:4329-4335.

17. Vilana R, Bruix J, Bru C, Ayuso C, Sole M, Rodes J. Tumor Size Determines the Efficacy of Percutaneous Ethanol Injection for the Treatment of Small Hepatocellular-Carcinoma. Hepatology

1992;16:353-357.

18. Llovet JM, Real MI, Montana X, Planas R, Coll S, Aponte J, Ayuso C, et al. Arterial embolisation or chemoembolisation versus symptomatic treatment in patients with unresectable hepatocellular carcinoma: a randomised controlled trial. Lancet 2002;359:1734-1739.

19. Lo CM, Ngan H, Tso WK, Liu CL, Lam CM, Poon RTP, Fan ST, et al. Randomized controlled trial of transarterial lipiodol chemoembolization for unresectable hepatocellular carcinoma. Hepatology 2002;35:1164-1171.

20. Gish RG, Porta C, Lazar L, Ruff P, Feld R, Croitoru A, Feun L, et al. Phase III randomized controlled trial comparing the survival of patients with unresectable hepatocellular carcinoma treated with nolatrexed or doxorubicin (vol 25, pg 3069, 2007). Journal of Clinical Oncology 2007;25:4512-4512.

21. O'Dwyer PJ, Giantonio BJ, Levy DE, Kauh JS, Fitzgerald DB, Benson AB. Gefitinib in advanced unresectable hepatocellular carcinoma: Results from the Eastern Cooperative Oncology Group's Study E1203. Journal of Clinical Oncology 2006;24:4143.

22. Ramanathan RK, Belani CP, Singh DA, Tanaka M, Lenz HJ, Yen Y, Kindler HL, et al. Phase II study of lapatinib, a dual inhibitor of epidermal growth factor receptor (EGFR) tyrosine kinase 1 and 2 (Her2/Neu) in patients (pts) with advanced biliary tree cancer (BTC) or hepatocellular cancer (HCC). A California Consortium (CCC-P) Trial. Journal of Clinical Oncology 2006;24:4010.

23. Yeo W, Mok TS, Zee B, Leung TWT, Lai PBS, Lau WY, Koh J, et al. A randomized phase iii study of doxorubicin versus cisplatin/interferon alpha-2b/doxorubicin/fluorouracil (PIAF) combination chemotherapy for unresectable hepatocellular carcinoma. Journal of the National Cancer Institute 2005;97:1532-1538.

24. Endicott JA, Ling V. The Biochemistry of P-Glycoprotein-Mediated Multidrug Resistance. Annual Review of Biochemistry 1989;58:137-171.

25. Ng IOL, Liu CL, Fan ST, Ng M. Expression of P-glycoprotein in hepatocellular carcinoma - A determinant of chemotherapy response. American Journal of Clinical Pathology 2000;113:355-363.

26. Park JG, Lee SK, Hong IG, Kim HS, Lim KH, Choe KJ, Kim WH, et al. Mdr1 Gene-Expression - Its Effect on Drug-Resistance to Doxorubicin in Human Hepatocellular-Carcinoma Cell-Lines. Journal of the National Cancer Institute 1994;86:700-705.

27. Faried LS, Faried A, Kanuma T, Nakazato T, Tamura T, Kuwano H, Minegishi T. Inhibition of the mammalian target of rapamycin (mTOR) by rapamycin increases chemosensitivity of CaSki cells to paclitaxel. European Journal of Cancer 2006;42:934-947.

28. VanderWeele DJ, Zhou RX, Rudin CM. Akt up-regulation increases resistance to microtubule-directed chemotherapeutic agents through mammalian target of rapamycin. Molecular Cancer Therapeutics 2004;3:1605-1613.

29. Llovet JM, Ricci S, Mazzaferro V, Hilgard P, Gane E, Blanc JF, de Oliveira AC, et al. Sorafenib in advanced hepatocellular carcinoma. New England Journal of Medicine 2008;359:378-390.

30. Cheng AL, Kang YK, Chen ZD, Tsao CJ, Qin SK, Kim JS, Luo RC, et al. Efficacy and safety of sorafenib in patients in the Asia-Pacific region with advanced hepatocellular carcinoma: a phase III randomised, double-blind, placebo-controlled trial. Lancet Oncology 2009;10:25-34.

31. Aguilar F, Harris CC, Sun T, Hollstein M, Cerutti P. Geographic-Variation of P53 Mutational Profile in Nonmalignant Human Liver. Science 1994;264:1317-1319.

32. Hosono S, Chou MJ, Lee CS, Shih C. Infrequent Mutation of P53 Gene in Hepatitis-B Virus

Positive Primary Hepatocellular Carcinomas. Oncogene 1993;8:491-496.

33. Minouchi K, Kaneko S, Kobayashi K. Mutation of p53 gene in regenerative nodules in cirrhotic liver. Journal of Hepatology 2002;37:231-239.

34. Nose H, Imazeki F, Ohto M, Omata M. P53 Gene-Mutations and 17p Allelic Deletions in Hepatocellular-Carcinoma from Japan. Cancer 1993;72:355-360.

35. Edamoto Y, Hara A, Biernat W, Terracciano L, Cathomas G, Riehle HM, Matsuda M, et al. Alterations of RB1, p53 and Wnt pathways in hepatocellular carcinomas associated with hepatitis C, hepatitis B and alcoholic liver cirrhosis. International Journal of Cancer 2003;106:334-341.

36. Ishizaki Y, Ikeda S, Fujimori M, Shimizu Y, Kurihara T, Itamoto T, Kikuchi A, et al. Immunohistochemical analysis and mutational analyses of beta-catenin, Axin family and APC genes in hepatocellular carcinomas. International Journal of Oncology 2004;24:1077-1083.

37. Ito Y, Takeda T, Sakon M, Tsujimoto M, Higashiyama S, Noda K, Miyoshi E, et al. Expression and clinical significance of erb-B receptor family in hepatocellular carcinoma. British Journal of Cancer 2001;84:1377-1383.

38. Santoni-Rugiu E, Jensen MR, Factor VM, Thorgeirsson SS. Acceleration of c-myc-induced hepatocarcinogenesis by co-expression of transforming growth factor (TGF)-alpha in transgenic mice is associated with TGF-beta 1 signaling disruption. American Journal of Pathology 1999;154:1693-1700.

39. Daveau M, Scotte M, Francois A, Coulouarn C, Ros G, Tallet Y, Hiron M, et al. Hepatocyte growth factor, transforming growth factor alpha, and their receptors as combined markers of prognosis in hepatocellular carcinoma. Molecular Carcinogenesis 2003;36:130-141.

40. Wang R, Ferrell DL, Faouzi S, Maher JJ, Bishop JM. Activation of the Met receptor by cell attachment induces and sustains hepatocellular carcinomas in transgenic mice. Journal of Cell Biology 2001;153:1023-1033.

41. Feitelson MA, Sun B, Tufan NLS, Liu J, Pan JB, Lian ZR. Genetic mechanisms of hepatocarcinogenesis. Oncogene 2002;21:2593-2604.

42. Kubo T, Yamamoto J, Shikauchi Y, Niwa Y, Matsubara K, Yoshikawa H. Apoptotic speck protein-like, a highly homologous protein to apoptotic speck protein in the pyrin domain, is silenced by DNA methylation and induces apoptosis in human hepatocellular carcinoma. Cancer Research 2004;64:5172-5177.

43. Maeta Y, Shiota G, Okano J, Murawaki Y. Effect of promoter methylation of the p16 gene on phosphorylation of retinoblastoma gene product and growth of hepatocellular carcinoma cells. Tumor Biology 2005;26:300-305.

44. Matsuda Y, Ichida T, Matsuzawa J, Sugimura K, Asakura H. p16(INK4) is inactivated by extensive CpG methylation in human hepatocellular carcinoma. Gastroenterology 1999;116:394-400.

45. Murata H, Tsuji S, Tsujii M, Sakaguchi Y, Fu HY, Kawano S, Hori M. Promoter hypermethylation silences cyclooxygenase-2 (Cox-2) and regulates growth of human hepatocellular carcinoma cells. Laboratory Investigation 2004;84:1050-1059.

46. Wong CM, Lee JMF, Ching YP, Jin DY, Ng IOL. Genetic and epigenetic alterations of DLC-1 gene in hepatocellular carcinoma. Cancer Research 2003;63:7646-7651.

47. Wong IHN, Lo YMD, Zhang J, Liew CT, Ng MHL, Wong N, Lai PBS, et al. Detection of aberrant p16 methylation in the plasma and serum of liver cancer patients. Cancer Research 1999;59:71-73.

48. Brechot C, Pourcel C, Louise A, Rain B, Tiollais P. Presence of Integrated Hepatitis-B

Virus-DNA Sequences in Cellular DNA of Human Hepatocellular-Carcinoma. Nature 1980;286:533-535.

49. Murakami Y, Saigo K, Takashima H, Minami M, Okanoue T, Brechot C, Paterlini-Brechot P. Large scaled analysis of hepatitis B virus (HBV) DNA integration in HBV related hepatocellular carcinomas. Gut 2005;54:1162-1168.

50. Minami M, Daimon Y, Mori K, Takashima H, Nakajima T, Itoh Y, Okanoue T. Hepatitis B virus-related insertional mutagenesis in chronic hepatitis B patients as an early drastic genetic change leading to hepatocarcinogenesis. Oncogene 2005;24:4340-4348.

51. Wang J, Chenivesse X, Henglein B, Brechot C. Hepatitis-B Virus Integration in a Cyclin-a Gene in a Hepatocellular-Carcinoma. Nature 1990;343:555-557.

52. Feitelson MA, Duan LX. Hepatitis B virus x antigen in the pathogenesis of chronic infections and the development of hepatocellular carcinoma. American Journal of Pathology 1997;150:1141-1157.

53. Klein NP, Schneider RJ. Activation of Src family kinases by hepatitis B virus HBx protein and coupled signaling to Ras. Molecular and Cellular Biology 1997;17:6427-6436.

54. Shih WL, Kuo ML, Chuang SE, Cheng AL, Doong SL. Hepatitis B virus X protein inhibits transforming growth factor-beta-induced apoptosis through the activation of phosphatidylinositol 3-kinase pathway. Journal of Biological Chemistry 2000;275:25858-25864.

55. Balsano C, Avantaggiati ML, Natoli G, Demarzio E, Will H, Perricaudet M, Levrero M. Full-Length and Truncated Versions of the Hepatitis-B Virus (Hbv) X-Protein (Px) Transactivate the Cmyc Protooncogene at the Transcriptional Level. Biochemical and Biophysical Research Communications 1991;176:985-992.

56. Twu JS, Lai MY, Chen DS, Robinson WS. Activation of Protooncogene C-Jun by the X-Protein of Hepatitis-B Virus. Virology 1993;192:346-350.

57. Chirillo P, Falco M, Puri PL, Artini M, Balsano C, Levrero M, Natoli G. Hepatitis B virus pX activates NF-kappa B-dependent transcription through a Raf-independent pathway. Journal of Virology 1996;70:641-646.

58. Seto E, Mitchell PJ, Yen TSB. Transactivation by the Hepatitis-B Virus-X Protein Depends on Ap-2 and Other Transcription Factors. Nature 1990;344:72-74.

59. Lee YH, Yun YD. HBx protein of hepatitis B virus activates Jak1-STAT signaling. Journal of Biological Chemistry 1998;273:25510-25515.

60. Benn J, Schneider RJ. Hepatitis-B Virus Hbx Protein Activates Ras-Gtp Complex-Formation and Establishes a Ras, Raf, Map Kinase Signaling Cascade. Proceedings of the National Academy of Sciences of the United States of America 1994;91:10350-10354.

61. Park US, Park SK, Lee YI, Park JG, Lee YI. Hepatitis B virus-X protein upregulates the expression of p21(waf1/cip1) and prolongs G1 -> S transition via a p53-independent pathway in human hepatoma cells. Oncogene 2000;19:3384-3394.

62. Cha MY, Kim CM, Park YM, Ryu WS. Hepatitis B virus X protein is essential for the activation of Wnt/beta-catenin signaling in hepatoma cells. Hepatology 2004;39:1683-1693.

63. Lee YI, Kang-Park S, Do SI, Lee YI. The hepatitis B virus-X protein activates a phosphatidylinositol 3-kinase-dependent survival signaling cascade. Journal of Biological Chemistry 2001;276:16969-16977.

64. Pang RWC, Poon RTP. From molecular biology to targeted therapies for hepatocellular carcinoma: The future is now. Oncology 2007;72:30-44.

65. Llovet JM, Bruix J. Molecular targeted therapies in hepatocellular carcinoma. Hepatology 2008;48:1312-1327.

66. Tanaka S, Arii S. Molecular targeted therapy for hepatocellular carcinoma in the current and potential next strategies Journal of Gastroenterology 2011;46:289-296.

67. Bader AG, Kang SY, Zhao L, Vogt PK. Oncogenic PI3K deregulates transcription and translation. Nature Reviews Cancer 2005;5:921-929.

68. Engelman JA, Luo J, Cantley LC. The evolution of phosphatidylinositol 3-kinases as regulators of growth and metabolism. Nature Reviews Genetics 2006;7:606-619.

69. Vivanco I, Sawyers CL. The phosphatidylinositol 3-kinase-AKT pathway in human cancer. Nature Reviews Cancer 2002;2:489-501.

70. Yap TA, Garrett MD, Walton MI, Raynaud F, de Bono JS, Workman P. Targeting the PI3K-AKT-mTOR pathway: progress, pitfalls, and promises. Current Opinion in Pharmacology 2008;8:393-412.

71. Dunlop EA, Tee AR. Mammalian target of rapamycin complex 1: Signalling inputs, substrates and feedback mechanisms. Cellular Signalling 2009;21:827-835.

72. Mamane Y, Petroulakis E, LeBacquer O, Sonenberg N. MTOR, translation initiation and cancer. Oncogene 2006;25:6416-6422.

73. Ding L, Getz G, Wheeler DA, Mardis ER, McLellan MD, Cibulskis K, Sougnez C, et al. Somatic mutations affect key pathways in lung adenocarcinoma. Nature 2008;455:1069-1075.

74. Samuels Y, Wang ZH, Bardelli A, Silliman N, Ptak J, Szabo S, Yan H, et al. High frequency of mutations of the PIK3CA gene in human cancers. Science 2004;304:554-554.

75. Thomas RK, Baker AC, DeBiasi RM, Winckler W, LaFramboise T, Lin WM, Wang M, et al. High-throughput oncogene mutation profiling in human cancer. Nature Genetics 2007;39:347-351.

76. Wood LD, Parsons DW, Jones S, Lin J, Sjoblom T, Leary RJ, Shen D, et al. The genomic landscapes of human breast and colorectal cancers. Science 2007;318:1108-1113.

77. Benistant C, Chapuis H, Roche S. A specific function for phosphatidylinositol 3-kinase alpha (p85 alpha-p110 alpha) in cell survival and for phosphatidylinositol 3-kinase beta (p85 alpha-p110 beta) in de novo DNA synthesis of human colon carcinoma cells. Oncogene 2000;19:5083-5090.

78. Brugge J, Hung MC, Mills GB. A new mutational aktivation in the PI3K pathway. Cancer Cell 2007;12:104-107.

79. Li Y, Tian Z, Fu B, Xin Y. LOH on 10023.3 and mutation of tumor suppressor gene PTEN in gastric cancer and precancerous lesions. Annals of Oncology 2008;19:43-43.

80. Cully M, You H, Levine AJ, Mak TW. Beyond PTEN mutations: the PI3K pathway as an integrator of multiple inputs during tumorigenesis. Nature Reviews Cancer 2006;6:184-192.

81. Feilotter HE, Coulon V, McVeigh JL, Boag AH, Dorion-Bonnet F, Duboue B, Latham WCW, et al. Analysis of the 10q23 chromosomal region and the PTEN gene in human sporadic breast carcinoma. British Journal of Cancer 1999;79:718-723.

82. Gray IC, Stewart LMD, Phillips SMA, Hamilton JA, Gray NE, Watson GJ, Spurr NK, et al. Mutation and expression analysis of the putative prostate tumour-suppressor gene PTEN. British Journal of Cancer 1998;78:1296-1300.

83. Bellacosa A, Defeo D, Godwin AK, Bell DW, Cheng JQ, Altomare DA, Wan MH, et al. Molecular Alterations of the Akt2 Oncogene in Ovarian and Breast Carcinomas. International Journal of Cancer 1995;64:280-285.

84. Bleeker FE, Felicioni L, Buttitta F, Lamba S, Cardone L, Rodolfo M, Scarpa A, et al. AKT1(E17K)

in human solid tumours. Oncogene 2008;27:5648-5650.

85. Malanga D, Scrima M, De Marco C, Fabiani F, De Rosa N, De Gisi S, Malara N, et al. Activating E17K mutation in the gene encoding the protein kinase AKT1 in a subset of squamous cell carcinoma of the lung. Cell Cycle 2008;7:665-669.

86. Martelli AM, Chiarini F, Evangelisti C, Grimaldi C, Ognibene A, Manzoli L, Billi AM, et al. The phosphatidylinositol 3-kinase/AKT/mammalian target of rapamycin signaling network and the control of normal myelopoiesis. Histology and Histopathology 2010;25:669-680.

87. Sahin F, Kannangai R, Adegbola O, Wang JZ, Su G, Torbenson M. mTOR and P70S6 kinase expression in primary liver neoplasms. Clinical Cancer Research 2004;10:8421-8425.

88. Villanueva A, Chiang DY, Newell P, Peix J, Thung S, Alsinet C, Tovar V, et al. Pivotal Role of mTOR Signaling in Hepatocellular Carcinoma. Gastroenterology 2008;135:1972-1983.

89. Sieghart W, Fuereder T, Schmid K, Cejka D, Werzowa J, Wrba F, Wang X, et al. Mammalian target of rapamycin pathway activity in hepatocellular carcinomas of patients undergoing liver transplantation. Transplantation 2007;83:425-432.

90. Zhou LD, Huang Y, Li JD, Wang ZM. The mTOR pathway is associated with the poor prognosis of human hepatocellular carcinoma. Medical Oncology 2010;27:255-261.

91. Tavian D, De Petro G, Benetti A, Portolani N, Giulini SM, Barlati S. u-PA and c-MET mRNA expression is co-ordinately enhanced while hepatocyte growth factor mRNA is down-regulated in human hepatocellular carcinoma. International Journal of Cancer 2000;87:644-649.

92. Sakata H, Takayama H, Sharp R, Rubin JS, Merlino G, LaRochelle WJ. Hepatocyte growth factor scatter factor overexpression induces growth, abnormal development, and tumor formation in transgenic mouse livers. Cell Growth & Differentiation 1996;7:1513-1523.

93. Tovar V, Alsinet C, Villanueva A, Hoshida Y, Chiang DY, Sole M, Thung S, et al. IGF activation in a molecular subclass of hepatocellular carcinoma and pre-clinical efficacy of IGF-1R blockage. Journal of Hepatology;52:550-559.

94. Mannova P, Beretta L. Activation of the N-Ras-PI3K-Akt-mTOR pathway by hepatitis C virus: Control of cell survival and viral replication. Journal of Virology 2005;79:8742-8749.

95. Neef M, Ledermann M, Saegesser H, Schneider V, Reichen J. Low-dose oral rapamycin treatment reduces fibrogenesis, improves liver function, and prolongs survival in rats with established liver cirrhosis. Journal of Hepatology 2006;45:786-796.

96. Bader AG, Kang SY, Vogt PK. Cancer-specific mutations in PIK3CA are oncogenic in vivo. Proceedings of the National Academy of Sciences of the United States of America 2006;103:1475-1479.

97. Samuels Y, Diaz LA, Schmidt-Kittler O, Cummins JM, DeLong L, Cheong I, Rago C, et al. Mutant PIK3CA promotes cell growth and invasion of human cancer cells. Cancer Cell 2005;7:561-573.

98. Zhao JJ, Liu ZN, Wang L, Shin E, Loda MF, Roberts TM. The oncogenic properties of mutant p110 alpha and p110 beta phosphatidylinositol 3-kinases in human mammary epithelial cells. Proceedings of the National Academy of Sciences of the United States of America 2005;102:18443-18448.

99. Liu PX, Cheng HL, Roberts TM, Zhao JJ. Targeting the phosphoinositide 3-kinase pathway in cancer. Nature Reviews Drug Discovery 2009;8:627-644.

100. Buontempo F, Ersahin T, S. M, Senturk S, Etro D, Ozturk M, Capitani S, et al. Inhibition of Akt signaling in hepatoma cells induces apoptotic cell death independent of Akt activation status.

Investigational New Drugs 2010:Epub ahead of print.

101. Ladu S, Calvisi DF, Conner EA, Farina M, Factor VM, Thorgeirsson SS. E2F1 inhibits c-Myc-driven apoptosis via PIK3CA/Akt/mTOR and COX-2 in a mouse model of human liver cancer. Gastroenterology 2008;135:1322-1332.

102. Campos LT, Nemunaitis J, Stephenson J, Richards D, Barve M, Gardner L, Niecestro R, et al. Phase II study of single agent perifosine in patients with hepatocellular carcinoma (HCC). Journal of Clinical Oncology 2009;27:e15505.

103. Chen KF, Chen HL, Tai WT, Feng WC, Hsu CH, Chen PJ, and Cheng AL. Activation of PI3K/Akt signaling pathway mediates acquired resistance to sorafenib in hepatocellular carcinoma cells Journal of Pharmacology and Experimental Therapeutics 2011:Epub ahead of print.

104. Schoniger-Hekele M, Muller C. Pilot study: rapamycin in advanced hepatocellular carcinoma. Alimentary Pharmacology & Therapeutics 2010;32:763-768.

105. Blaszkowsky LS, Abrams TA, Miksad RA, Zheng H, Meyerhardt JA, Schrag D, Kwak EL, et al. Phase I/II study of everolimus in patients with advanced hepatocellular carcinoma (HCC). . In: ASCO Annual Meeting; 2010: Journal of Clinical Oncology; 2010. p. e14542.

106. Kelley RK, Nimeiri HS, Vergo MT, Bergsland EK, Ko AH, Munster PN, Reinert A, et al. A phase I trial of the combination of temsirolimus (TEM) and sorafenib (SOR) in advanced hepatocellular carcinoma (HCC). In: gastrointestinal Cancer Symposium; 2011: Journal of Clinical Oncology; 2011. p. TPS213.

107. Buchbinder EI, Cohen MB, Jung DE, Panka DJ, Atkins MB, Mier JWaC, D. C. . In vitro efficacy of the dual PI3-kinase/mTOR inhibitor NVP-BEZ235 in hepatocellular carcinoma In: Molecular Cancer Therapeutics; 2009; 2009. p. C60.

108. Lemke LE, Paine-Murrieta GD, Taylor CW, Powis G. Wortmannin inhibits the growth of mammary tumors despite the existence of a novel wortmannin-insensitive phosphatidylinositol-3-kinase. Cancer Chemotherapy and Pharmacology 1999;44:491-497.

109. Hu LM, Zaloudek C, Mills GB, Gray J, Jaffe RB. In vivo and in vitro ovarian carcinoma growth inhibition by a phosphatidylinositol 3-kinase inhibitor (LY294002). Clinical Cancer Research 2000;6:880-886.

110. Amaravadi R, Thompson CB. The survival kinases Akt and Pim as potential pharmacological targets. Journal of Clinical Investigation 2005;115:2618-2624.

111. Knight ZA, Gonzalez B, Feldman ME, Zunder ER, Goldenberg DD, Williams O, Loewith R, et al. A pharmacological map of the PI3-K family defines a role for p110 alpha in insulin signaling. Cell 2006;125:733-747.

112. Marone R, Cmijanovic V, Giese B, Wymann MP. Targeting phosphoinositide 3-kinase - Moving towards therapy. Biochimica Et Biophysica Acta-Proteins and Proteomics 2008;1784:159-185.

113. Fan QW, Knight ZA, Goldenberg DD, Yu W, Mostov KE, Stokoe D, Shokat KM, et al. A dual PI3 kinase/mTOR inhibitor reveals emergent efficacy in glioma. Cancer Cell 2006;9:341-349.

114. Flinn IW, Byrd JC, Furman RR, Brown JR, Lin TS, Bello C, Giese NA, et al. Preliminary evidence of clinical activity in a phase I study of CAL-101, a selective inhibitor of the p1108 isoform of phosphatidylinositol 3-kinase (P13K), in patients with select hematologic malignancies. Journal of Clinical Oncology 2009;27:3543.

115. Jimeno A, Hong DS, Hecker S, Clement R, Kurzrock R, Pestano LA, Hiscox A, et al. Phase I trial of PX-866, a novel phosphoinositide-3-kinase (PI-3K) inhibitor. Journal of Clinical Oncology

2009;27:3542.

116. Wagner AJ, Von Hoff DH, LoRusso PM, Tibes R, Mazina KE, Ware JA, Yan Y, et al. A first-in-human phase I study to evaluate the pan-PI3K inhibitor GDC-0941 administered QD or BID in patients with advanced solid tumors. Journal of Clinical Oncology 2009;27:3501.

117. Hilgard P, Klenner T, Stekar J, Nossner G, Kutscher B, Engel J. D-21266, a new heterocyclic alkylphospholipid with antitumour activity. European Journal of Cancer 1997;33:442-446.

118. Van Ummersen L, Binger K, Volkman J, Marnocha R, Tutsch K, Kolesar J, Arzoomanian R, et al. A phase I trial of perifosine (NSC 639966) on a loading dose/maintenance dose schedule in patients with advanced cancer. Clinical Cancer Research 2004;10:7450-7456.

119. Tolcher AW, Yap TA, Fearen I, Taylor A, Carpenter C, Brunetto AT, Beeram M, et al. A phase I study of MK-2206, an oral potent allosteric Akt inhibitor (Akti), in patients (pts) with advanced solid tumor (ST). Journal of Clinical Oncology 2009;27:3503.

120. Vezina C, Kudelski A, Sehgal SN. Rapamycin (Ay-22,989), a New Antifungal Antibiotic .1. Taxonomy of Producing Streptomycete and Isolation of Active Principle. Journal of Antibiotics 1975;28:721-726.

121. Yatscoff RW, Legatt DF, Kneteman NM. Therapeutic Monitoring of Rapamycin - a New Immunosuppressive Drug. Therapeutic Drug Monitoring 1993;15:478-482.

122. Faivre S, Kroemer G, Raymond E. Current development of mTOR inhibitors as anticancer agents. Nature Reviews Drug Discovery 2006;5:671-688.

123. Guertin DA, Sabatini DM. Defining the role of mTOR in cancer. Cancer Cell 2007;12:9-22.

124. Hay N. The Akt-mTOR tango and its relevance to cancer. Cancer Cell 2005;8:179-183.

125. Sabatini DM. mTOR and cancer: insights into a complex relationship. Nature Reviews Cancer 2006;6:729-734.

126. Atkins MB, Hidalgo M, Stadler WM, Logan TF, Dutcher JP, Hudes GR, Park Y, et al. Randomized phase II study of multiple dose levels of CCI-779, a novel mammalian target of rapamycin kinase inhibitor, in patients with advanced refractory renal cell carcinoma. Journal of Clinical Oncology 2004;22:909-918.

127. Campsen J, Zimmerman MA, Mandell S, Kaplan M, Kam I. A Decade of Experience Using mTor Inhibitors in Liver Transplantation. Journal of Transplantation 2011;Epub 2011 Mar 15.

128. Levy G, Schmidli H, Punch J, Tuttle-Newhall E, Mayer D, Neuhaus P, Samuel D, et al. Safety, tolerability, and efficacy of everolimus in de novo liver transplant recipients: 12-and 36-month results. Liver Transplantation 2006;12:1640-+.

129. Roberts RJ, Wells AC, Unitt E, Griffiths M, Tasker AD, Allison MED, Bradley JA, et al. Sirolimus-induced pneumonitis following liver transplantation. Liver Transplantation 2007;13:853-856.

130. Montalbano M, Neff GW, Yamashiki N, Meyer D, Bettiol M, Slapak-Green G, Ruiz P, et al. A retrospective review of liver transplant patients treated with sirolimus from a single center: An analysis of sirolimus-related complications. Transplantation 2004;78:264-268.

131. Toso C, Meeberg GA, Bigam DL, Oberholzer J, Shapiro AMJ, Gutfreund K, Ma MM, et al. De novo sirolimus-based immunosuppression after liver transplantation for hepatocellular carcinoma: Long-term outcomes and side effects. Transplantation 2007;83:1162-1168.

132. Kneteman NM, Oberholzer J, Al Saghier M, Meeberg GA, Blitz M, Ma MM, Wong WWS, et al. Sirolimus-based immunosuppression for liver transplantation in the presence of extended criteria for hepatocellular carcinoma. Liver Transplantation 2004;10:1301-1311.

133. Schnitzbauer AA, Zuelke C, Graeb C, Rochon J, Bilbao I, Burra P, de Jong KP, et al. A prospective randomised, open-labeled, trial comparing sirolimus-containing versus mTOR-inhibitor-free immunosuppression in patients undergoing liver transplantation for hepatocellular carcinoma. Bmc Cancer 2010;10:190.

134. Sarbassov DD, Guertin DA, Ali SM, Sabatini DM. Phosphorylation and regulation of Akt/PKB by the rictor-mTOR complex. Science 2005;307:1098-1101.

135. Shah OJ, Wang ZY, Hunter T. Inappropriate activation of the TSC/Rheb/mTOR/S6K cassette induces IRS1/2 depletion, insulin resistance, and cell survival deficiencies. Current Biology 2004;14:1650-1656.

136. Feldman ME, Apsel B, Uotila A, Loewith R, Knight ZA, Ruggero D, Shokat KM. Active-Site Inhibitors of mTOR Target Rapamycin-Resistant Outputs of mTORC1 and mTORC2. Plos Biology 2009;7:371-383.

137. Thoreen CC, Kang SA, Chang JW, Liu QS, Zhang JM, Gao Y, Reichling LJ, et al. An ATP-competitive Mammalian Target of Rapamycin Inhibitor Reveals Rapamycin-resistant Functions of mTORC1. Journal of Biological Chemistry 2009;284:8023-8032.

138. Chresta CM, Davies BR, Hickson I, Harding T, Cosulich S, Critchlow SE, Vincent JP, et al. AZD8055 Is a Potent, Selective, and Orally Bioavailable ATP-Competitive Mammalian Target of Rapamycin Kinase Inhibitor with In vitro and In vivo Antitumor Activity. Cancer Research 2010;70:288-298.

139. Zhao JJ, Cheng HL, Jia SD, Wang L, Gjoerup OV, Mikami A, Roberts TM. The p110 alpha isoform of PI3K is essential for proper growth factor signaling and oncogenic transformation. Proceedings of the National Academy of Sciences of the United States of America 2006;103:16296-16300.

140. Guillermet-Guibert J, Bjorklof K, Salpekar A, Gonella C, Ramadani F, Bilancio A, Meek S, et al. The p110 beta isoform of phosphoinositide 3-kinase signals downstream of G protein-coupled receptors and is functionally redundant with p110 gamma. Proceedings of the National Academy of Sciences of the United States of America 2008;105:8292-8297.

141. O'Reilly KE, Rojo F, She QB, Solit D, Mills GB, Smith D, Lane H, et al. mTOR inhibition induces upstream receptor tyrosine kinase signaling and activates Akt. Cancer Research 2006;66:1500-1508.

142. Cloughesy TF, Yoshimoto K, Nghiemphu P, Brown K, Dang J, Zhu SJ, Hsueh T, et al. Antitumor activity of rapamycin in a phase I trial for patients with recurrent PTEN-Deficient glioblastoma. Plos Medicine 2008;5:139-151.

143. Maira SM, Stauffer F, Brueggen J, Furet P, Schnell C, Fritsch C, Brachmann S, et al. Identification and characterization of NVP-BEZ235, a new orally available dual phosphatidylinositol 3-kinase/mammalian target of rapamycin inhibitor with potent in vivo antitumor activity. Molecular Cancer Therapeutics 2008;7:1851-1863.

144. Serra V, Markman B, Scaltriti M, Eichhorn PJA, Valero V, Guzman M, Botero ML, et al. NVP-BEZ235, a dual PI3K/mTOR inhibitor, prevents PI3K signaling and inhibits the growth of cancer cells with activating PI3K mutations. Cancer Research 2008;68:8022-8030.

145. Ma WW, Adjei AA. Novel Agents on the Horizon for Cancer Therapy. Ca-a Cancer Journal for Clinicians 2009;59:111-137.

146. Chiorean EG, Mahadevan D, Harris WB, Von Hoff DD, Younger AE, Rensvold DM, Shelton CF, et al. Phase I evaluation of SF1126, a vascular targeted PI3K inhibitor, administered twice weekly

IV in patients with refractory solid tumors. Journal of Clinical Oncology 2009;27:2558.

147. Moelling K, Schad K, Bosse M, Zimmermann S, Schweneker M. Regulation of Raf-Akt cross-talk. Journal of Biological Chemistry 2002;277:31099-31106.

148. Carracedo A, Ma L, Teruya-Feldstein J, Rojo F, Salmena L, Alimonti A, Egia A, et al. Inhibition of mTORC1 leads to MAPK pathway activation through a PI3K-dependent feedback loop in human cancer. Journal of Clinical Investigation 2008;118:3065-3074.

149. Raynaud FI, Eccles S, Clarke PA, Hayes A, Nutley B, Alix S, Henley A, et al. Pharmacologic characterization of a potent inhibitor of class I phosphatidylinositide 3-kinases. Cancer Research 2007;67:5840-5850.

150. Beuvink I, Boulay A, Fumagalli S, Zilbermann F, Ruetz S, O'Reilly T, Natt F, et al. The mTOR inhibitor RAD001 sensitizes tumor cells to DNA-damaged induced apoptosis through inhibition of p21 translation. Cell 2005;120:747-759.

151. Mondesire WH, Jian WG, Zhang HX, Ensor J, Hung MC, Mills GB, Meric-Bernstam F. Targeting mammalian target of rapamycin synergistically enhances chemotherapy-induced cytotoxicity in breast cancer cells. Clinical Cancer Research 2004;10:7031-7042.

152. Wu LC, Birle DC, Tannock IF. Effects of the mammalian target of rapamycin inhibitor CCI-779 used alone or with chemotherapy on human prostate cancer cells and xenografts. Cancer Research 2005;65:2825-2831.

153. Yan HJ, Frost P, Shi YJ, Hoang B, Sharma S, Fisher M, Gera J, et al. Mechanism by which mammalian target of rapamycin inhibitors sensitize multiple myeloma cells to dexamethasone-induced apoptosis. Cancer Research 2006;66:2305-2313.

154. Tam KH, Yang ZF, Lau CK, Lam CT, Pang RWC, Poon RTP. Inhibition of mTOR enhances chemosensitivity in hepatocellular carcinoma. Cancer Letters 2009;273:201-209.

155. Piguet AC, Semela D, Keogh A, Wilkens L, Stroka D, Stoupis C, St-Pierre MV, et al. Inhibition of mTOR in combination with doxorubicin in an experimental model of hepatocellular carcinoma. Journal of Hepatology 2008;49:78-87.

156. Bu XX, Le C, Jia FQ, Guo XL, Zhang L, Zhang BH, Wu MC, et al. Synergistic effect of mTOR inhibitor rapamycin and fluorouracil in inducing apoptosis and cell senescence in hepatocarcinoma cells. Cancer Biology & Therapy 2008;7:392-396.

157. Patil MA, Chua MS, Pan KH, Lin R, Lih CJ, Cheung ST, Ho C, et al. An integrated data analysis approach to characterize genes highly expressed in hepatocellular carcinoma. Oncogene 2005;24:3737-3747.

158. Tung CY, Jen CH, Hsu MT, Wang HW, Lin CH. A novel regulatory event-based gene set analysis method for exploring global functional changes in heterogeneous genomic data sets. Bmc Genomics 2009;10.

159. Nowak AK, Chow PKH, Findlay M. Systemic therapy for advanced hepatocellular carcinoma: a review. European Journal of Cancer 2004;40:1474-1484.

160. Nies AT, Konig J, Pfannschmidt M, Klar E, Hofmann WJ, Keppler D. Expression of the multidrug resistance proteins MRP2 and MRP3 in human hepatocellular carcinoma. International Journal of Cancer 2001;94:492-499.

161. Chao Y, Chan WK, Birkhofer MJ, Hu OYP, Wang SS, Huang YS, Liu M, et al. Phase II and pharmacokinetic study of paclitaxel therapy for unresectable hepatocellular carcinoma patients. British Journal of Cancer 1998;78:34-39.

162. Hebbar M, Ernst O, Cattan S, Dominguez S, Oprea C, Mathurin P, Triboulet JP, et al. Phase II

trial of docetaxel therapy in patients with advanced hepatocellular carcinoma. Oncology 2006;70:154-158.

163. Szebeni J, Alving CR, Savay S, Barenholz Y, Priev A, Danino D, Talmon Y. Formation of complement-activating particles in aqueous solutions of Taxol: possible role in hypersensitivity reactions. International Immunopharmacology 2001;1:721-735.

164. Gelderblom H, Verweij J, Nooter K, Sparreboom A. Cremophor EL: the drawbacks and advantages of vehicle selection for drug formulation. European Journal of Cancer 2001;37:1590-1598.

165. Green MR, Manikhas GM, Orlov S, Afanasyev B, Makhson AM, Bhar P, Hawkins MJ. Abraxane((R)), a novel Cremophor((R))-free, albumin-bound particle form of paclitaxel for the treatment of advanced non-small-cell lung cancer. Annals of Oncology 2006;17:1263-1268.

166. Blum JL, Savin MA, Edelman G, Pippen JE, Robert NJ, Geister BV, Kirby RL, et al. Phase II study of weekly albumin-bound paclitaxel for patients with metastatic breast cancer heavily pretreated with taxanes. Clinical Breast Cancer 2007;7:850-856.

167. Marimpietri D, Brignole C, Nico B, Pastorino F, Pezzolo A, Piccardi F, Cilli M, et al. Combined therapeutic effects of vinblastine and rapamycin on human neuroblastoma growth, apoptosis, and angiogenesis. Clinical Cancer Research 2007;13:3977-3988.

168. Campostrini N, Marimpietri D, Totolo A, Mancone C, Fimia GM, Ponzoni M, Righetti PG. Proteomic analysis of anti-angiogenic effects by a combined treatment with vinblastine and rapamycin in an endothelial cell line. Proteomics 2006;6:4420-4431.

169. Shafer A, Zhou CX, Gehrig PA, Boggess JF, Bae-Jump VL. Rapamycin potentiates the effects of paclitaxel in endometrial cancer cells through inhibition of cell proliferation and induction of apoptosis. International Journal of Cancer 2010;126:1144-1154.

170. Haritunians T, Mori A, O'Kelly J, T Luong Q, Giles FJ, Koeffler HP. Antiproliferative activity of RAD001 (everolimus) as a single agent and combined with other agents in mantle cell lymphoma. Leukemia 2007;21:333-339.

171. Sessa C, Tosi D, Vigano L, Albanell J, Hess D, Maur M, Cresta S, et al. Phase Ib study of weekly mammalian target of rapamycin inhibitor ridaforolimus (AP23573; MK-8669) with weekly paclitaxel. Annals of Oncology 2010;21:1315-1322.

172. Ribatti D, Nico B, Mangieri D, Longo V, Sansonno D, Vacca A, Dammacco F. In vivo inhibition of human hepatocellular carcinoma related angiogenesis by vinblastine and rapamycin. Histology and Histopathology 2007;22:285-289.

173. Na GC, Timasheff SN. Thermodynamic Linkage between Tubulin Self-Association and the Binding of Vinblastine. Biochemistry 1980;19:1355-1365.

174. Plosker GL, Figgitt DP. Rituximab - A review of its use in non-Hodgkin's lymphoma and chronic lymphocytic leukaemia. Drugs 2003;63:803-843.

175. Sandler AB. Chemotherapy for small cell lung cancer. Seminars in Oncology 2003;30:9-25.

176. Jassem J, Kosmidis P, Ramlau R, Zarogoulidis K, Novakova L, Breton J, Etienne PL, et al. Oral vinorelbine in combination with cisplatin: a novel active regimen in advanced non-small-cell lung cancer. Annals of Oncology 2003;14:1634-1639.

177. Seidman AD. Monotherapy options in the management of metastatic breast cancer. *Seminars in Oncology* 2003;30:6-10.

178. Okouneva T, Hill BT, Wilson L, Jordan MA. The effects of vinflunine, vinorelbine, and vinblastine on centromere dynamics. Molecular Cancer Therapeutics 2003;2:427-436.

179. Panda D, Ananthnarayan V, Larson G, Shih C, Jordan MA, Wilson L. Interaction of the antitumor compound cryptophycin-52 with tubulin. Biochemistry 2000;39:14121-14127.
180. Towle MJ, Salvato KA, Budrow J, Wels BF, Kuznetsov G, Aalfs KK, Welsh S, et al. In vitro and in vivo anticancer activities of synthetic macrocyclic ketone analogues of halichondrin B. Cancer Research 2001;61:1013-1021.
181. Loganzo F, Discafani CM, Annable T, Beyer C, Musto S, Hari M, Tan XZ, et al. HTI-286, a synthetic analogue of the tripeptide hemiasterlin, is a potent antimicrotubule agent that circumvents P-glycoprotein-mediated resistance in vitro and in vivo. Cancer Research 2003;63:1838-1845.
182. Hamel E. Natural-Products Which Interact with Tubulin in the Vinca Domain - Maytansine, Rhizoxin, Phomopsin-a, Dolastatin-10 and Dolastatin-15 and Halichondrin-B. Pharmacology & Therapeutics 1992;55:31-51.
183. Manfredi JJ, Parness J, Horwitz SB. Taxol Binds to Cellular Microtubules. Journal of Cell Biology 1982;94:688-696.
184. Belani CP, Langer C. First-line chemotherapy for NSCLC: an overview of relevant trials. Lung Cancer 2002;38:S13-S19.
185. Bollag DM, McQueney PA, Zhu J, Hensens O, Koupal L, Liesch J, Goetz M, et al. Epothilones, a New Class of Microtubule-Stabilizing Agents with a Taxol-Like Mechanism of Action. Cancer Research 1995;55:2325-2333.
186. Honore S, Kamath K, Braguer D, Wilson L, Briand C, Jordan MA. Suppression of microtubule dynamics by discodermolide by a novel mechanism is associated with mitotic arrest and inhibition of tumor cell proliferation. Molecular Cancer Therapeutics 2003;2:1303-1311.
187. Skoufias DA, Wilson L. Mechanism of Inhibition of Microtubule Polymerization by Colchicine - Inhibitory Potencies of Unliganded Colchicine and Tubulin Colchicine Complexes. Biochemistry 1992;31:738-746.
188. Tozer GM, Kanthou C, Parkins CS, Hill SA. The biology of the combretastatins as tumour vascular targeting agents. International Journal of Experimental Pathology 2002;83:21-38.
189. Lakhani NJ, Sarkar MA, Venitz J, Figg WD. 2-methoxyestradiol, a promising anticancer agent. Pharmacotherapy 2003;23:165-172.
190. Yoshimatsu K, Yamaguchi A, Yoshino H, Koyanagi N, Kitoh K. Mechanism of action of E7010, an orally active sulfonamide antitumor agent: Inhibition of mitosis by binding to the colchicine site of tubulin. Cancer Research 1997;57:3208-3213.
191. Panda D, Miller HP, Islam K, Wilson L. Stabilization of microtubule dynamics by estramustine by binding to a novel site in tubulin: A possible mechanistic basis for its antitumor action. Proceedings of the National Academy of Sciences of the United States of America 1997;94:10560-10564.
192. Jordan MA, Wilson L. Microtubules as a target for anticancer drugs. Nature Reviews Cancer 2004;4:253-265.
193. Yu K, Toral-Barza L, Shi C, Zhang WG, Zask A. Response and determinants of cancer cell susceptibility to PI3K inhibitors. Cancer Biology & Therapy 2008;7:307-315.
194. Ito Y, Sasaki Y, Harimoto M, Wada S, Ito T, Tanaka Y, Kasahara A, et al. Activation of mitogen-activated protein kinase extracellular signal-regulated protein kinase in human hepatocellular carcinoma. Hepatology 1997;26:1002-1002.
195. Schmidt CM, McKillop IH, Cahill PA, Sitzmann JV. Increased MAPK expression and activity in

primary human hepatocellular carcinoma. Biochemical and Biophysical Research Communications 1997;236:54-58.

196. Saini KS, and Piccart-Gebhart MJ. Dual Targeting of the PI3K and MAPK Pathways in Breast Cancer. Asia-Pacific Journal of Oncology & Hematology 2010.

197. Kinkade CW, Castillo-Martin M, Puzio-Kuter A, Yan J, Foster TH, Gao H, Sun Y, et al. Targeting AKT/mTOR and ERK MAPK signaling inhibits hormone-refractory prostate cancer in a preclinical mouse model. Journal of Clinical Investigation 2008;118:3051-3064.

198. Lasithiotakis KG, Sinnberg TW, Schittek B, Flaherty KT, Kulms D, Maczey E, Garbe C, et al. Combined inhibition of MAPK and mTOR signaling inhibits growth, induces cell death, and abrogates invasive growth of melanoma cells. Journal of Investigative Dermatology 2008;128:2013-2023.

199. Liu L, Cao YC, Chen C, Zhang XM, McNabola A, Wilkie D, Wilhelm S, et al. Sorafenib blocks the RAF/MEK/ERK pathway, inhibits tumor angiogenesis, and induces tumor cell apoptosis in hepatocellular carcinoma model PLC/PRF/5. Cancer Research 2006;66:11851-11858.

200. Wang Z, Zhou J, Fan J, Qiu SJ, Yu Y, Huang XW, Tang ZY. Effect of rapamycin alone and in combination with sorafenib in an orthotopic model of human hepatocellular carcinoma. Clinical Cancer Research 2008;14:5124-5130.

201. Shinohara ET, Cao C, Niermann K, Mu Y, Zeng FH, Hallahan DE, Lu B. Enhanced radiation damage of tumor vasculature by mTOR inhibitors. Oncogene 2005;24:5414-5422.

202. Albert JM, Kim KW, Cao C, Lu B. Targeting the Akt/mammalian target of rapamycin pathway for radiosensitization of breast cancer. Molecular Cancer Therapeutics 2006;5:1183-1189.

203. Manegold PC, Paringer C, Kulka U, Krimmel K, Eichhorn ME, Wilkowski R, Jauch KW, et al. Antiangiogenic therapy with mammalian target of rapamycin inhibitor RAD001 (Everolimus) increases radiosensitivity in solid cancer. Clinical Cancer Research 2008;14:892-900.

204. Chan KYY, Lai PBS, Squire JA, Beheshti B, Wong NLY, Sy SMH, Wong N. Positional expression profiling indicates candidate genes in deletion hotspots of hepatocellular carcinoma. Modern Pathology 2006;19:1546-1554.

205. Yokoe T, Tanaka F, Mimori K, Inoue H, Ohmachi T, Kusunoki M, Mori M. Efficient identification of a novel cancer/testis antigen for immunotherapy using three-step microarray analysis. Cancer Research 2008;68:1074-1082.

206. Bergamaschi A, Hjortland GO, Triulzi T, Sorlie T, Johnsen H, Ree AH, Russnes HG, et al. Molecular profiling and characterization of luminal-like and basal-like in vivo breast cancer xenograft models. Molecular Oncology 2009;3:469-482.

207. Zagani R, Hamzaoui N, Cacheux W, De Reynies A, Terris B, Chaussade S, Romagnolo B, et al. Cyclooxygenase-2 Inhibitors Down-regulate Osteopontin and Nr4a2-New Therapeutic Targets for Colorectal Cancers. Gastroenterology 2009;137:1358-1366.

208. Goto Y, Matsuzaki Y, Kurihara S, Shimizu A, Okada T, Yamamoto K, Murata H, et al. A new melanoma antigen fatty acid-binding protein 7, involved in proliferation and invasion, is a potential target for immunotherapy and molecular target therapy. Cancer Research 2006;66:4443-4449.

209. Scrideli CA, Carlotti CG, Okamoto OK, Andrade VS, Cortez MAA, Motta FJN, Lucio-Eterovic AK, et al. Gene expression profile analysis of primary glioblastomas and non-neoplastic brain tissue: identification of potential target genes by oligonucleotide microarray and real-time quantitative PCR. Journal of Neuro-Oncology 2008;88:281-291.

210. Nogales E, Wolf SG, Downing KH. Structure of the alpha beta tubulin dimer by electron crystallography. Nature 1998;391:199-203.

211. Rowinsky EK. The development and clinical utility of the taxane class of antimicrotubule chemotherapy agents. Annual Review of Medicine 1997;48:353-374.

212. Gan YB, Wientjes MG, Schuller DE, Au JLS. Pharmacodynamics of taxol in human head and neck tumors. Cancer Research 1996;56:2086-2093.

213. Yen WC, Wientjes MG, Au JLS. Differential effect of taxol in rat primary and metastatic prostate tumors: Site-dependent pharmacodynamics. Pharmaceutical Research 1996;13:1305-1312.

214. Desai N, Trieu V, Yao ZW, Louie L, Ci S, Yang A, Tao CL, et al. Increased antitumor activity, intratumor paclitaxel concentrations, and endothelial cell transport of Cremophor-free, albumin-bound paclitaxel, ABI-007, compared with Cremophor-based paclitaxel. Clinical Cancer Research 2006;12:1317-1324.

215. Desai NP, Trieu V, Hwang LY, Wu RJ, Soon-Shiong P, Gradishar WJ. Improved effectiveness of nanoparticle albumin-bound (nab) paclitaxel versus polysorbate-based docetaxel in multiple xenografts as a function of HER2 and SPARC status. Anti-Cancer Drugs 2008;19:899-909.

216. Wong N, Chan KYY, Macgregor PF, Lai PBS, Squire JA, Beheshti B, Albert M, et al. Transcriptional profiling identifies gene expression changes associated with IFN-alpha tolerance in hepatitis C-related hepatocellular carcinoma cells. Clinical Cancer Research 2005;11:1319-1326.

217. Milross CG, Mason KA, Hunter NR, Chung WK, Peters LJ, Milas L. Relationship of mitotic arrest and apoptosis to antitumor effect of paclitaxel. Journal of the National Cancer Institute 1996;88:1308-1314.

218. Fan WM. Possible mechanisms of paclitaxel-induced apoptosis. Biochemical Pharmacology 1999;57:1215-1221.

219. Alli E, Yang JM, Hait WN. Silencing of stathmin induces tumor-suppressor function in breast cancer cell lines harboring mutant p53. Oncogene 2007;26:1003-1012.

220. Breuhahn K, Vreden S, Haddad R, Beckebaum S, Stippel D, Flemming P, Nussbaum T, et al. Molecular profiling of human hepatocellular carcinoma defines mutually exclusive interferon regulation and insulin-like growth factor II overexpression. Cancer Research 2004;64:6058-6064.

221. Wang W, Peng JX, Yang JQ, Yang LY. Identification of Gene Expression Profiling in Hepatocellular Carcinoma Using cDNA Microarrays. Digestive Diseases and Sciences 2009;54:2729-2735.

222. Mok TSK, Choi E, Yau D, Johri A, Yeo W, Chan ATC, Wong C. Effects of patupilone (epothilone B; EPO906), a novel chemotherapeutic agent, in hepatocellular carcinoma: An in vitro study. Oncology 2006;71:292-296.

223. Nimeiri HS, Singh DA, Kasza K, Taber DA, Ansari RH, Vokes EE, Kindler HL. The epothilone B analogue ixabepilone in patients with advanced hepatobiliary cancers: a trial of the University of Chicago Phase II Consortium. Investigational New Drugs 2010;28:854-858.

224. Schiff PB, Horwitz SB. Taxol Stabilizes Microtubules in Mouse Fibroblast Cells. Proceedings of the National Academy of Sciences of the United States of America-Biological Sciences 1980;77:1561-1565.

225. Kloover JS, den Bakker MA, Gelderblom H, van Meerbeeck JP. Fatal outcome of a hypersensitivity reaction to paclitaxel: a critical review of premedication regimens. British Journal of Cancer 2004;90:304-305.

226. Belmont LD, Mitchison TJ. Identification of a protein that interacts with tubulin dimers and increases the catastrophe rate of microtubules. Cell 1996;84:623-631.

227. Mistry SJ, Atweh GF. Stathmin inhibition enhances okadaic acid-induced mitotic arrest - A potential role for stathmin in mitotic exit. Journal of Biological Chemistry 2001;276:31209-31215.

228. Marklund U, Larsson N, Gradin HM, Brattsand G, Gullberg M. Oncoprotein 18 is a phosphorylation-responsive regulator of microtubule dynamics. Embo Journal 1996;15:5290-5298.

229. Mistry SJ, Li HC, Atweh GF. Role for protein phosphatases in the cell-cycle-regulated phosphorylation of stathmin. Biochemical Journal 1998;334:23-29.

230. Price DK, Ball JR, Bahrani-Mostafavi Z, Vachris JC, Kaufman JS, Naumann RW, Higgins RV, et al. The phosphoprotein Op18/stathmin is differentially expressed in ovarian cancer. Cancer Investigation 2000;18:722-730.

231. Bieche I, Lachkar S, Becette V, Cifuentes-Diaz C, Sobel A, Lidereau R, Curmi PA. Overexpression of the stathmin gene in a subset of human breast cancer. British Journal of Cancer 1998;78:701-709.

232. Daibata M, Matsuo Y, Machida H, Taguchi T, Ohtsuki Y, Taguchi H. Differential gene-expression profiling in the leukemia cell lines derived from indolent and aggressive phases of CD56(+) T-cell large granular lymphocyte leukemia. International Journal of Cancer 2004;108:845-851.

233. Alli E, Bash-Babula J, Yang JM, Hait WN. Effect of stathmin on the sensitivity to antimicrotubule drugs in human breast cancer. Cancer Research 2002;62:6864-6869.

234. Wang X, Chen YC, Han QB, Chan CY, Wang H, Liu Z, Cheng CHK, et al. Proteomic identification of molecular targets of gambogic acid: Role of stathmin in hepatocellular carcinoma. Proteomics 2009;9:242-253.

235. Phung TL, Ziv K, Dabydeen D, Eyiah-Mensch G, Riveros M, Perruzzi C, Sun J, et al. Pathological angiogenesis is induced by sustained Akt signaling and inhibited by rapamycin. Cancer Cell 2006;10:159-170.

236. Ito D, Fujimoto K, Mori T, Kami K, Koizumi M, Toyoda E, Kawaguchi Y, et al. In vivo antitumor effect of the mTOR inhibitor CCI-779 and gemcitabine in xenograft models of human pancreatic cancer. International Journal of Cancer 2006;118:2337-2343.

237. Lang SA, Gaumann A, Koehl GE, Seidel U, Bataille F, Klein D, Ellis LM, et al. Mammalian target of rapamycin is activated in human gastric cancer and serves as a target for therapy in an experimental model. International Journal of Cancer 2007;120:1803-1810.

238. Witzig TE, Geyer SM, Ghobrial I, Inwards DJ, Fonseca R, Kurtin P, Ansell SM, et al. Phase II trial of single-agent temsirolimus (CCI-779) for relapsed mantle cell lymphoma. Journal of Clinical Oncology 2005;23:5347-5356.

239. Mabuchi S, Altomare DA, Connolly DC, Klein-Szanto A, Litwin S, Hoelzle MK, Hensley HH, et al. RAD001 (everolimus) delays tumor onset and progression in a transgenic mouse model of ovarian cancer. Cancer Research 2007;67:2408-2413.

240. Wu CJ, Wangpaichitr M, Feun L, Kuo MT, Robles C, Lampidis T, Savaraj N. Overcoming cisplatin resistance by mTOR inhibitor in lung cancer. Molecular Cancer 2005;4.

241. Zhou Q, Ching AK, Leung WK, Szeto CY, Ho SM, Chan PK, Yuan YF, et al. Novel therapeutic potential in targeting microtubules by nanoparticle albumin-bound paclitaxel in hepatocellular carcinoma. International Journal of Oncology 2011;38:721-731.

242. McCarty KS, Miller LS, Cox EB, Konrath J, McCarty KS. Estrogen-Receptor Analyses - Correlation of Biochemical and Immunohistochemical Methods Using Monoclonal Antireceptor Antibodies. Archives of Pathology & Laboratory Medicine 1985;109:716-721.

243. Hu LM, Hofmann J, Lu YL, Mills GB, Jaffe RB. Inhibition of phosphatidylinositol 3 '-kinase increases efficacy of paclitaxel in in vitro and in vivo ovarian cancer models. Cancer Research 2002;62:1087-1092.

244. Hosoi H, Dilling MB, Shikata T, Liu LN, Shu L, Ashmun RA, Germain GS, et al. Rapamycin causes poorly reversible inhibition of mTOR and induces p53-independent apoptosis in human rhabdomyosarcoma cells. Cancer Research 1999;59:886-894.

245. Baker WJ, Maenpaa JU, Wurz GT, Koester SK, Seymour RC, Emshoff VD, Wiebe VJ, et al. Toremifene Enhances Cell-Cycle Block and Growth-Inhibition by Vinblastine in Multidrug-Resistant Human Breast-Cancer Cells. Oncology Research 1993;5:207-212.

246. Wang L, Shi WY, Wu ZY, Varna M, Wang AH, Zhou L, Chen L, et al. Cytostatic and anti-angiogenic effects of temsirolimus in refractory mantle cell lymphoma. Journal of Hematology & Oncology 2010;3.

247. Vacca A, Iurlaro M, Ribatti D, Minischetti M, Nico B, Ria R, Pellegrino A, et al. Antiangiogenesis is produced by nontoxic doses of vinblastine. Blood 1999;94:4143-4155.

248. Chau GY, Lee AFY, Tsay SH, Ke YR, Kao HL, Wong FH, Tsou AP, et al. Clinicopathological significance of survivin expression in patients with hepatocellular carcinoma. Histopathology 2007;51:204-218.

249. Fleischer B, Schulze-Bergkamen H, Schuchmann M, Weber A, Biesterfeld S, Muller M, Krammer PH, et al. Mcl-1 is an anti-apoptotic factor for human hepatocellular carcinoma. International Journal of Oncology 2006;28:25-32.

250. Sieghart W, Losert D, Strommer S, Cejka D, Schmid K, Rasoul-Rockenschaub S, Bodingbauer M, et al. Mcl-1 overexpression in hepatocellular carcinoma: A potential target for antisense therapy. Journal of Hepatology 2006;44:151-157.

251. Yildiz L, Baris S, Aydin O, Kefeli M, Kandemir B. Bcl-2 Positivity in B and C Hepatitis and Hepatocellular Carcinomas. Hepato-Gastroenterology 2008;55:2207-2210.

252. Yang Y, Zhu J, Gou H, Cao D, Jiang M, Hou M. Clinical significance of Cox-2, Survivin and Bcl-2 expression in hepatocellular carcinoma (HCC). Medical Oncology 2010:Epub ahead of print.

253. Pizem J, Marolt VF, Luzar B, Cor A. Proliferative and apoptotic activity in hepatocellular carcinoma and surrounding non-neoplastic liver tissue. Pflugers Archiv-European Journal of Physiology 2001;442:R174-R176.

254. Nettles JH, Li HL, Cornett B, Krahn JM, Snyder JP, Downing KH. The binding mode of epothilone A on alpha,beta-tubulin by electron crystallography. Science 2004;305:866-869.

255. Altmann KH, Bold G, Caravatti G, End N, Florsheimer A, Guagnano V, O'Reilly T, et al. Epothilones and their analogs - Potential new weapons in the fight against cancer. Chimia 2000;54:612-621.

256. Kowalski RJ, Giannakakou P, Hamel E. Activities of the microtubule-stabilizing agents epothilones A and B with purified tubulin and in cells resistant to paclitaxel (Taxol(R)). Journal of Biological Chemistry 1997;272:2534-2541.

257. Rubin EH, Rothermel J, Tesfaye F, Chen TL, Hubert M, Ho YY, Hsu CH, et al. Phase I dose-finding study of weekly single-agent patupilone in patients with advanced solid tumors. Journal of Clinical Oncology 2005;23:9120-9129.

258. Osterlind K, Sanchez JM, Zatloukal P, Hamm J, Belani CP, Kim E, Felip E, et al. Phase I/II dose escalation trial of patupilone every 3 weeks in patients with non-small cell lung cancer. Journal of Clinical Oncology 2005;23:647S-647S.

259. Smit WM, Sufliarsky J, Spanik S, Wagnerova M, Kaye S, Oza AM, Gore M, et al. Phase I/II dose-escalation trial of patupilone every 3 weeks in patients with resistant/refractory ovarian cancer. Ejc Supplements 2005;3:261-262.

260. Sekulic A, Hudson CC, Homme JL, Yin P, Otterness DM, Karnitz LM, Abraham RT. A direct linkage between the phosphoinositide 3-Kinase-AKT signaling pathway and the mammalian target of rapamycin in mitogen-stimulated and transformed cells. Cancer Research 2000;60:3504-3513.

261. Neshat MS, Mellinghoff IK, Tran C, Stiles B, Thomas G, Petersen R, Frost P, et al. Enhanced sensitivity of PTEN-deficient tumors to inhibition of FRAP/mTOR. Proceedings of the National Academy of Sciences of the United States of America 2001;98:10314-10319.